THE
PHYSICAL REVIEW
A Journal of Experimental and Theoretical Physics Established by E. L. Nichols in 1893
VOL. 51, NO. 3 FEBRUARY 1, 1937 SECOND SERIES

Intensities of X-Ray Reflections from Bismuth Crystals Between 25° and 530° Abs.[1]

ALEXANDER GOETZ AND ROBERT B. JACOBS*
Cryogenic Laboratory, California Institute of Technology, Pasadena, California
(Received October 15, 1936)

The temperature variation of the "integrated intensities" of reflections of Mo $K\alpha$ radiation from Bi crystals on (111) are reported over a range from near the boiling point of hydrogen to the melting point of the crystal. A modified Bragg spectrometer with stationary ionization chamber was used. The cryostat in which the crystal is mounted for observations at low temperatures is described as well as the thermostatic arrangement used for high temperatures. The observations were taken for the second, third and fifth order. The relative values of the integrated intensities (J_T/J_N) were found to follow the Debye-Waller relation:

$$J_T = J_0 \cdot e^{-2M \cdot \sin^2 \vartheta}$$

for $\Theta \gtrless T$ within the range of the experimental error. Also the $\sin^2 \vartheta$-relation was found to hold well for the three orders used, thus the reduction $\ln (J_T/J_0)/\sin^2 \vartheta = f(T)$ could serve to determine the Debye factor in first approximation. As $f(T)$ is almost linear, M'/T (the slope of the line) was determined to be $1.15 \cdot 10^{-2}$. By an approximation method the characteristic temperatures of Bi were calculated without (Θ) and with (Θ^*) consideration of the zero-point energy. The values obtained are: $\Theta = 92.5°$ and $\Theta^* = 95.9°$ (abs.). Although the scattering of the observations is of nearly the same order of magnitude as the difference between the Debye function with and without zero-point energy, the deviations from the former are smaller and our measurements thus support the assumption of the zero point energy.

No indication of a discontinuity of (J_T/J_0) was found in the region of the pseudoallotropic transformation point at 75°C.

However, a deviation from the relation begins 50° to 80° before the melting point in the direction of an absolute increase of M which finally even becomes positive. Although $(J_T/J_0) = f(T)$ is reversible for $dT/dt \gtrless 0$, a hysteresis of the function over this temperature region indicates a dependence upon the thermal history of the crystal which may be attributed to a temperature dependence of the secondary extinction.

INTRODUCTION

THE purpose of this paper is to describe measurements of the temperature dependence of the intensity of x-rays reflected from Bi crystals over a temperature range extending from the melting point of bismuth down to the neighborhood of the boiling point of hydrogen (25° abs).[2, 3]

The reasons for undertaking this type of investigation are several:

First: previous investigations[4–6] made it probable to assume a process of "decrystallization" beginning 50°–100° before the melting point, that is, a process in which certain parts of the crystal, not arrayed in the perfect lattice configuration (e.g., intermosaic boundary regions, loci of plastic deformation or regions distorted by the segregation of impurities), which can thus be considered to approach an "amorphous"

[1] Partly contained in R. B. Jacobs, Thesis, Cal. Inst. (1934).
[*] Now at Harvard University.
[2] R. B. Jacobs and A. Goetz, Phys. Rev. **47**, 94 (1935).
[3] R. B. Jacobs and A. Goetz, Phys. Rev. **47**, 257 (1935).
[4] A. Goetz and R. C. Hergenrother, Phys. Rev. **38**, 2075 (1931).
[5] A. Goetz and R. C. Hergenrother, Phys. Rev. **39**, 548 (1932).
[6] A. Goetz and R. C. Hergenrother, Phys. Rev. **40**, 643 (1932).

state, begin to yield. Such an assumption seems to be natural in view of the fact that distorted lattice sections in contradistinction to regions of perfect array cannot have a sharp melting point. This process of decrystallization, which was previously suggested for the interpretation of the divergence between the thermal macroscopic and the lattice expansion in the neighborhood of the melting point should be revealed in the temperature variation of the integrated intensities of Bragg reflections of the crystal in the temperature range mentioned above; in other words, such a process would prove to be the cause of a temperature dependence of the secondary extinction.

Second: It is of considerable interest to check the validity of the Debye-Waller relation between integrated intensities (J) and temperature (T), over as large a temperature range as possible. This holds particularly for low temperatures where $T<\Theta$ (characteristic temperature) since the relation[7, 8]

$$J_T = J_0 \cdot e^{-2M \cdot \sin^2\vartheta} \tag{1}$$

defines

$$M = \frac{6h^2}{m \cdot k \cdot \Theta \cdot \lambda^2} \cdot \left[\frac{\varphi(\Theta/T)}{\Theta/T} + 0.25 \right], \tag{2}$$

where $\varphi(\Theta/T)$ is the Debye function and $\frac{1}{4}$ is a correction for the zero-point energy. As $\varphi(\Theta/T)$ shows only small variation for values of Θ/T between 0 and 1, the temperature variation of the [ ] term approaches linearity ($\sim T$), thus M/T can be considered within the range of experimental error to be invariant with temperature for $T>\Theta$. It is obvious that $M(T)$ can only be checked experimentally if temperature independence of other extinguishing factors can safely be assumed. This assumption seems justified (as far as the causes of the secondary extinction are concerned) in temperature ranges sufficiently far removed from the melting point of the crystal.

Third: Whereas the theories had originally been restricted to elastically isotropic crystals (cubic systems) they have recently been extended by Zener and Jauncey[9] to anisotropic systems assuming the same $M(T)$ function to be valid. As the temperature function of crystals belonging to such systems have not been measured previously, the use of Bi (rhombohedral) served this purpose as well as previous considerations. With regard to the latter point, it seemed advisable to measure the intensities of as many as possible orders from the same plane for the test of the validity of the $\sin^2\vartheta$—relation for the case of an irregular system.

Fourth: A number of authors[10, 11] have described the occurrence of discontinuous changes of certain physical and chemical[12] properties of Bi crystals in the region of 75°C whereas others[13, 14] could not find such changes in properties generally known to accompany an allotropic transformation. Since it has been shown[6] that the atomic distances along [111] do not change discontinuously in this region, one is forced to ascribe the alleged change to a case of pseudo-allotropy. Thus the determination of the temperature function of the x-ray reflections in this particular region was another aim of this investigation.

Experimental work done previously in the line of the temperature variation of reflections is described in numerous papers.[15–18] It is, however, almost entirely restricted to crystals of the cubic system of nonmetallic substances and also to temperatures above the boiling point of liquid air, that is $T \geq \Theta$.

In the high temperature range, the melting point of the crystal was in no case approached within a few degrees. The latter fact is easily explained by the predominant use of rocksalt crystals for these experiments, the vapor pressure of which is so large near its point of fusion that the evaporation changes the crystal surfaces sufficiently to cause changes of intensity.

---

[7] P. Debye, Ann. d. Physik **43**, 49 (1914).
[8] I. Waller, Zeits. f. Physik **17**, 398 (1923).
[9] C. Zener and G. E. M. Jauncey, Phys. Rev. **49**, 17, 122 (1936).
[10] For a bibliography before 1930 see A. Goetz and M. F. Hasler, Phys. Rev. **36**, 1777 (1930).
[11] A. Goetz and A. B. Focke, Phys. Rev. **45**, 170 (1934).
[12] J. A. Hedvall, R. Hedin, E. Anderson, Zeits. f. anorg. allgem. Chemie **212**, 84 (1933).
[13] A. Schulze, Zeits. f. tech. Physik **11**, 16 (1930).
[14] S. Aoyama and G. Monna, Rep. Tohoku Un. **23**, 52 (1934).
[15] W. H. Bragg, Phil. Mag. **27**, 881 (1914).
[16] I. Backhurst, Proc. Roy. Soc. **102**, 340 (1922).
[17] I. Waller and R. W. James, Phil. Mag. **49**, 585, 885 (1925).
[18] F. C. Blake, Rev. Mod. Phys. **5**, 169 (1933).

2. Method

For a Bragg spectrometer an instrument with stationary ionization chamber previously described by Hergenrother[19] was used in a modified form. In order to make the whole assembly safe for the application of liquid hydrogen in cooling the crystal, it was mounted in a station of the Cryogenic Laboratory, the construction of which has been described elsewhere.[20]

All measurements described in this paper were performed with Mo-$K\alpha$ radiation. The procedure for obtaining the integrated intensity values was as follows: after the crystal was adjusted by means described below, the x-ray tube (Müller) was swung to the proper angle with respect to the ionization chamber for the particular order under observation. The cryostat, and with it the crystal, was then turned by means of an electrometer *once* through an angle $\Delta\vartheta$ larger than the rocking angle with a velocity $v \sim d\vartheta/dt = \text{const}$. The total charge Q_t collected by the electrometer during the time interval t consists of:

$$Q_t \sim \int_0^t (Q_s + Q_r)dt \sim \int_\vartheta^{\vartheta+\Delta\vartheta} (Q_s + Q_r)d\vartheta \cdots$$

as $dt \sim d\vartheta$, where Q_s and Q_r represent the scattered (background) and reflected intensity components respectively. The $\int_0^t Q_s dt$ is determined by a control exposure of the ionization chamber for the length of t in the neighborhood, though in safe distance from the reflection.

3. Apparatus

The greatest technical difficulty lay in the construction of the cryostat for the crystal. A semischematic vertical cut through it is shown in Fig. 1: The outer circumference of the apparatus is formed by a cylindrical brass tube three inches in diameter (1). Two large windows are cut into its base in order to make the crystal holder accessible (1*a*). The container for liquid air or liquid hydrogen (3) is mounted concentrically inside of (1). It is suspended adiabatically in (1) by means of the thin-walled German silver tube (3*a*). The upper lid of (3) carries isothermically mounted the protective shield (2) which extends over and beyond the whole length of (3).

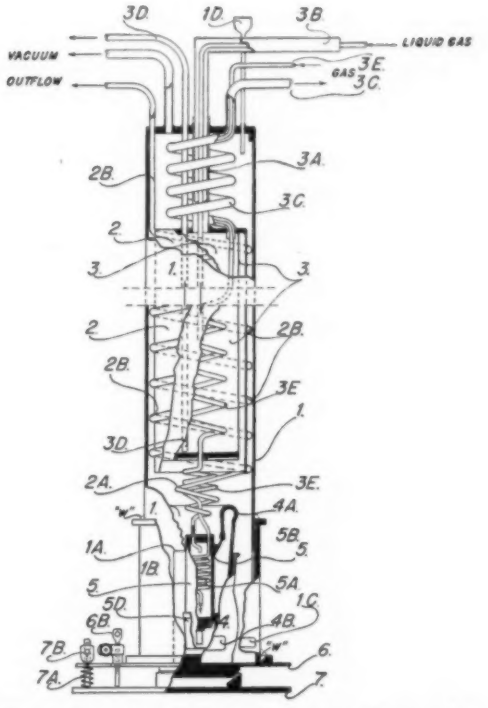

FIG. 1. Semischematic view of cryostat. The numbers designate isothermal parts of the system: 1. Outer shell; 2. shield of gas container; 3. container for liquid gas; 4. glass-support of crystal holder; 5. crystal holder; 6. base attached to cryostat; 7. base attached to spectrometer.

The windows (1*a*) of the outer wall can be closed by the lowering of the outer sleeve (1*b*), which itself carries two small windows (1*c*), which are covered with aluminum foil in a vacuum-tight fashion. As the outer assembly remains at room temperature, (1*b*) can be sealed vacuum-tight to the base and to (1) with Picein at the places indicated by "*W*." All leads to the inside of the cryostat enter the top plate of (1) and as they are soldered, (1) forms a vacuum-tight system which can be exhausted to vacuum of the order necessary for thermal adiabacy. The container (3) is supplied with liquid gas through the metal-Dewar-syphon (3*b*) inserted into (3*a*). The evaporated gas is led to the outside through the vent (3*c*). The liquid gas can be blown out of (3) through the drain tube (3*d*), which leads to the bottom of (3) and is operated by closing (3*b*) and (3*c*). (This device is used while changing from liquid air over to liquid hydrogen: in this

[19] R. C. Hergenrother, Physics **2**, 211 (1932).
[20] A. Goetz, Rev. Sci. Inst. **7**, 307 (1936).

case (3*b*) is closed and hydrogen pressure of 0.5 atmos. is applied to (3*c*), and the liquid hydrogen is admitted only after the last drop of liquid air has left (3*d*).)

The type of measurements described in this paper made it necessary to have the possibility of cooling the crystal to any intermediate temperature between 25° and 300° abs. It was for this reason that the constant flow of a gas independent of the gas in the cryostat was used, He or H_2. The obvious advantage of this arrangement is that one can adjust the temperature by the rate of the flow of the gas; also that one can maintain a certain temperature by adjusting the flow so as to compensate for the influx of heat from the outside. A further advantage of this method is that no part of the cryostat has to be dimensioned for high pressures. Thus the danger of clogging fine capillaries and the nuisance of large heat capacities is avoided.

The gas to be used for the cold transfer enters at (3*e*), and joins (3*c*) for a preliminary heat exchange before entering the container (3), where it is cooled down to the boiling point of the liquid gas. (3*e*) leaves the bottom of (3) and brings the cooled gas through a coil (in order to provide mechanical flexibility) into the crystal holder (5). After a heat exchange with the latter, it leaves (5) through (2*a*) (coiled for the same reason) and enters a long coil (2*b*), which is mounted isothermally upon the shield (2). Thus a protection against radiation losses of (3) against (1) is afforded without waste of liquid gas. Finally the gas is led through the top of (1).

The considerable danger of thermal distortion of the crystal holder and its mountings inside such a complex apparatus as this cryostat was avoided—as tests have shown—by mounting the crystal holder (5) into a cylinder of Nonex glass (4). The crystal holder consists of a fairly heavy-walled, closed, copper cylinder, into which the gas is led from (3*e*) where it passes a spiral (5*a*). After the gas has left the latter, it returns through the tube (5*b*), connected with (2*a*). The heavy bottom of (5) carries a recess (5*c*), upon which a resistance coil is wound for the measurement of the temperature. At the center of the bottom a tapped hole is bored, which receives a small copper cylinder, the outside of which carries a corresponding male thread, into the inside of which the crystal is soldered. The latter is shielded against radiation from outside by a cylindrical shield (5*d*) which is equipped with windows. The shield (5*d*) is held in close contact with (5) and consists of copper. The windows are uncovered, the bottom is of massive copper.

The Nonex cylinder (4) is sealed with wax to the base of the cryostat. Opposite to the crystal it carries the windows (4*b*). Its upper end consists of a ground female cone. Into it fits the male cone (4*a*), which is bent inward in order to provide for sufficient elasticity of the ring seal with respect to the cylindrical copper rim, which latter forms an integral part of the copper tank of the crystal holder. The ground surfaces are covered with colloidal graphite for a smooth fit. The inner part of (4) communicates with the vacuum in the outer container through the windows (4*b*). The separation of the Nonex cylinder into two parts by means of the cone is necessary for the facilitation of the assembly of the apparatus; also for changing the crystals.

The base plate (6) of the cryostat is adjustable in all directions: *a*. The crystal can be tilted over a solid angle of 6° by moving the cryostat on the spherical surface between (6) and (7). As the center of the sphere lies in the center of the crystal, no lateral displacement of the crystal takes place with this adjustment. The position thus obtained can be fixed by the compression of each of three coil springs with the nuts (7*b*) (only one of which is shown in the figure). After the final adjustment is reached, the fixation of the position can be insured with three adjustment screws (6*a*) (only one of which is shown in the figure).

The plate (7) rests upon a large-based cross-stage built similar to the construction used in a microscopic table. This arrangement permits the motions necessary for centering the crystal to the axis of the spectrograph.

The leads for the thermometer coils (5*c*) are brought through a German silver tube (1*d*) which ends in a cup at several inches distance from the top of (1). The wires are led through the cup and afterwards the cup is filled with Picein, insuring a vacuum-tight lead of the wires into the cryostat. The cup has to be kept at room temperature in order to avoid cracking of the wax.

The chief controlling factor of the temperature of the crystal—the flow rate of the gas—is measured with a flow meter[20] connected with (2*b*), whereas the inlet of the gas (3*e*) is connected with a sensitive pressure gauge. The thermometric measurements were taken with the potentiometric arrangement described previously.[20]

Although the method of changing and maintaining a temperature of the crystal used in this cryostat could be extended to temperatures above room temperature (by filling container (3) with heated oil, etc., and preheating thus the transferring gas), the temperature range in this direction is limited by the unavoidable use of soft solder in the instrument. Thus a different device for holding and heating the crystal was used for the range between room temperature and the melting point of Bi (271°C). It consists chiefly of a thermally isolated holder of the crystal, a heating and a thermometer coil around the base of the crystal. A hood of light material with Cellophane windows permitted one to surround the crystal with an atmosphere of carbon dioxide in order to avoid oxidation of the surface. A similar arrangement has been described previously by Goetz and Hergenrother.[16]

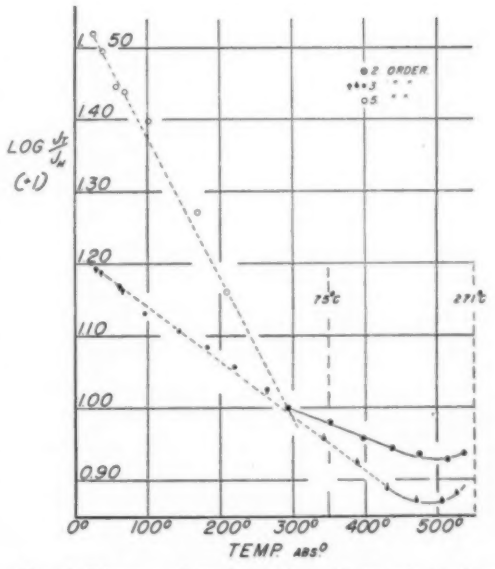

FIG. 2. Diagram of the logarithms of the relative integrated intensities of the 2nd, 3rd, 5th orders against temperature. The room temperature (=294° abs.) is taken for reference.

TABLE I. *Relative integrated intensity values for various orders.*

ORDER	T(abs.)	J_T/J_N	$\lg J_T/J_N$	$\lg (J_T/J_N)+1$	$\sin^{-2}\vartheta$	$\lg J_T/J_N \cdot \sin^{-2}\vartheta$
2	537.0	0.861	−0.064	0.936	30.3	−1.94
2	514.5	0.839	−0.076	0.924	30.3	−2.31
2	475.5	0.860	−0.064	0.936	30.3	−1.94
2	438.0	0.878	−0.056	0.944	30.3	−1.70
2	397.0	0.922	−0.042	0.958	30.3	−1.27
2	353.5	0.956	−0.020	0.980	30.3	−0.608
2	294.5	1.000	0.000	1.000	30.3	0.00
3	527.0	0.770	−0.120	0.880	13.9	−1.67
3	507.0	0.741	−0.130	0.870	13.9	−1.81
3	470.5	0.741	−0.130	0.870	13.9	−1.81
3	431.5	0.774	−0.111	0.889	13.9	−1.54
3	389.5	0.837	−0.077	0.923	13.9	−1.07
3	344.5	0.906	−0.042	0.958	13.9	−0.58
3	294.0	1.000	0.00	1.000	13.9	0.00
3	221.0	1.140	+0.057	1.057	13.9	+0.78
3	182.5	1.215	+0.084	1.084	13.9	+1.17
3	143.0	1.279	+0.107	1.107	13.9	+1.48
3	95.8	1.351	+0.131	1.131	13.9	+1.82
3	266.0	1.060	+0.026	1.026	13.9	+0.36
3	66.0	1.292	+0.164	1.164	13.9	+2.28
3	62	1.474	+0.170	1.170	13.9	+2.37
3	36	1.539	+0.188	1.188	13.9	+2.62
3	29	1.563	+0.194	1.194	13.9	+2.70
5	294.5	1.000	0.000	1.000	4.95	0.000
5	210.0	1.44	+0.160	1.160	4.95	+0.792
5	165.0	1.82	+0.270	1.270	4.95	+1.36
5	103.0	2.50	+0.398	1.398	4.95	+1.97
5	71.0	2.68	+0.428	1.428	4.95	+2.12
5	58.5	2.84	+0.452	1.452	4.95	+2.23
5	43.0	3.16	+0.500	1.500	4.95	+2.47
5	27.5	3.30	+0.519	1.519	4.95	+2.57

4. CRYSTALS

The crystals used were made from highly purified Bi (Braun Corporation) used in previous work and were tested for impurities by magnetic methods.[11] They were grown in "P_1" orientation ([111] $\perp$ to rod) after methods described previously.[21, 22] In order to increase the degree of purity the material was subjected to the process of repeated recrystallization, first developed by Schubnikow and de Haas.[23] Then the crystals were cleft on the cleavage goniometer and by optical methods the best cleavage was selected. The size of the cleavage planes approximated in width: 6–8 mm, in breadth: 4–5 mm.

5. RESULTS

The relative integrated intensity values (J_T/J_N) for the 2nd, 3rd, and 5th order obtained from Bi (111) with Mo-$K\alpha$ are given in Table I

[21] A. Goetz, Phys. Rev. **35**, 193 (1930).
[22] M. F. Hasler, Rev. Sci. Inst. **4**, 356 (1933).
[23] L. Schubnikow and W. J. de Haas, Kgl. Acad. Amsterdam **33**, Nr. 4 (1930).

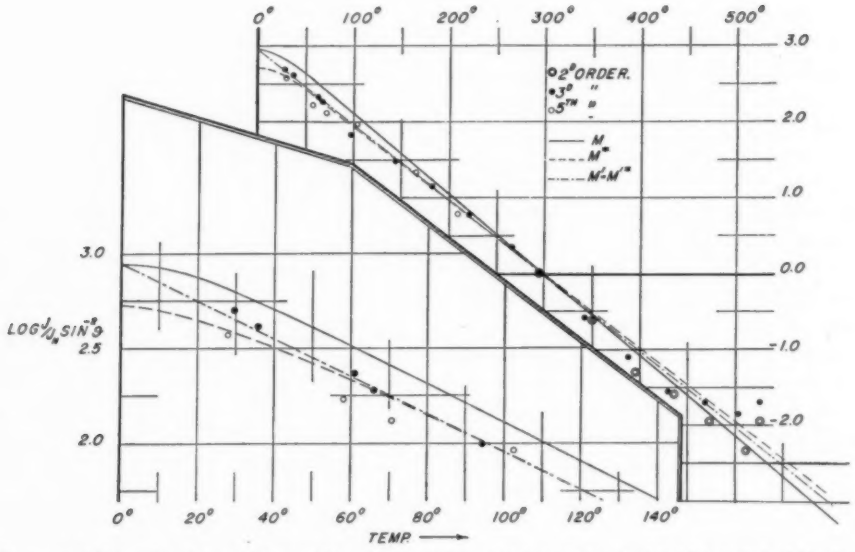

FIG. 3. Diagram of the reduced logarithms of the relative integrated intensities (lg (J_T/J_0) $\sin^{-2}\vartheta$ of the 2nd, 3rd, 5th order against temperature. The straight line extrapolation is marked —·—·—·—, the Debye function without zero-point energy is drawn full (for $\Theta=92.5°$), the same with zero-point energy is drawn dashed (for $\Theta^*=95.9°$). The auxiliary diagram on the left represents the range of $\Theta<T$ on an enlarged scale.

together with their algebraic modifications used in the diagrams. In Fig. 2 J_T/J_N is plotted in the usual logarithmic form against T. The different orders are indicated with different demarkations, the room temperature (T_N) is taken as reference temperature for J_N. (Some of the J_T/J_N values were taken at different dates—almost two years apart—and are marked as such in order to demonstrate the magnitude of error.)

In general the points for the 2nd, 3rd and 5th orders fall well on straight lines for the whole range of temperature except for the concave deviation beginning about 70° before the point of fusion. Disregarding this range of the highest temperatures for the moment it is thus well established that the exponential relation (Eq. 1) for $M=M'T$ holds over a temperature range of at least 400° even down to $T=0.27\Theta$ within the limits of experimental error.

In Fig. 3, lg $(J_T/J_N)/\sin^2\vartheta$ is plotted against T. The demarkation of the observations at different orders is the same as in Fig. 2. The fair coincidence of the observations of different orders proves the validity of the $\sin^2\vartheta$ relation, the small magnitude of a systematic experimental error and a good verification of the above relation.

This simple exponential relation being only a rough approximation used for higher temperatures it has been attempted to compare the data with the exact relation predicting

$$J_T=J_0\cdot e^{-2M\cdot\sin^2\vartheta}\cdots, \tag{1}$$

where J_0 is the reflection at the absolute zero and

$$M=c\cdot\sin^2\vartheta\cdot\Theta^{-2}(\phi(\Theta/T)\cdot T), \tag{2a}$$

$$M^*=c\cdot\sin^2\vartheta\cdot\Theta^{*-1}[T/\Theta^*\cdot\varphi(\Theta^*/T)+0.25] \tag{2b}$$

with and without assuming zero-point energy, where

Θ = characteristic temperature (proportional to the maximum elastic frequency),
ϑ = Bragg angle,
$c=6h^2\cdot m^{-1}\cdot k^{-1}\cdot\lambda^{-2}$,
λ = the x-ray wave-length used $(=7.1\cdot10^{-9}$ cm for Mo-$K\alpha)$,
m = mass of a Bi atom $=3.45\cdot10^{-22}$ g,
$h=6.55\cdot10^{-27}$ erg. sec.,
$k=1.37\cdot10^{-16}$ erg. deg.$^{-1}$.

Accordingly, $c=1.05\cdot10^2$,

$$\varphi(\Theta/T)=T/\Theta\int_0^{\Theta/T}\xi d\xi/e^{\xi}-1 \text{ (Debye-Function).}$$

TABLE II. *Value of M for different temperatures.*

T	Θ/T	$\frac{\varphi(\Theta'/T)\cdot c}{\Theta'/T}$	Θ^*/T	$\frac{C}{\Theta^*}\left[\frac{\varphi(\Theta^*/T)}{\Theta^*/T}+\frac{1}{4}\right]$
0	∞	0	∞	0.238
10	9.25	0.0177	9.59	0.252
20	4.63	0.0692	4.79	0.304
30	3.08	0.144	3.19	0.377
40	2.31	0.237	2.40	0.459
50	1.85	0.324	1.92	0.544
60	1.54	0.436	1.60	0.638
70	1.32	0.538	1.37	0.731
80	1.16	0.636	1.20	0.834
90	1.02	0.735	1.06	0.918
100	0.92	0.831	0.96	1.014
200	0.46	1.875	0.48	1.990
294	0.32	2.902	0.33	4.842
400	0.23	4.038	0.24	3.900
500	0.19	5.075	0.19	2.938

As for practical purposes J_N for $T_N=294°$ is used for reference, Eq. (1) is changed into

$$J_T/J_N=J_0/J_N\cdot e^{-2M\cdot\sin^2\vartheta}. \qquad (1a)$$

It has been shown above that our observations are represented in sufficient first approximation by assuming the Debye function ($\varphi(\Theta/T)$) to be invariant with T. Thus Eqs. (2a) and (2b) change into

$$M'=c\cdot T_N\cdot\Theta'^{-2}\cdots;\quad M'^*=c/\Theta'^*\cdot(T_N/\Theta'^*+0.25)$$

or in combination with Eq. (1)

$$M'=M'^*=\lg\,(J_0/J_T)\cdot\alpha/2\,\sin^2\vartheta\cdots,$$

where α is the modulus of the natural logarithms.

The value of $\lg\,(J_0/J_N)\,\sin^{-2}\vartheta=2.95$ is obtained by linear extrapolation according to Fig. 3 (—·—·—). This results in $M'=3.38$ and in the value for the inclination of the straight line

$$M'/T=c\cdot\Theta'^{-2}=1.15\cdot10^{-2}\cdots.$$

Thus: $$\Theta'=(c\cdot T_N/M')'=95.6°\cdots. \qquad (3b)$$

In the same way the value of Θ'^* with consideration of the zero point energy is derived according to Eq. (2b):

$$\Theta'^*=\frac{c}{8M'}\left[1+\left(\frac{64M'\cdot T_N}{c}+1\right)^{\frac{1}{2}}\right]=99.5°\cdots. \qquad (3b)$$

The exact solution is now derived by considering $\varphi(\Theta'/T)$, for the numerical evaluation of which the obtained approximate values of $\Theta\sim\Theta'$ and $\Theta^*\sim\Theta'^*$ can be used. Thus the second approximations of Θ and Θ^* are derived from Eqs. (3a) and (3b) as follows:

$$\Theta=\left(\frac{c\cdot T_N\cdot\varphi(\Theta'/T)}{M}\right)^{\frac{1}{2}}=92.5°\cdots, \qquad (4a)$$

and analogously:

$$\Theta^*=\frac{c}{8M}\left[1+\left(\frac{64M}{c}\cdot T_N\cdot\varphi(\Theta'^*)/T)+1\right)^{\frac{1}{2}}\right]$$
$$=95.9°\cdots. \qquad (4b)$$

It is interesting to compare these values for Θ with values obtained hitherto by other methods (specific heat measurements or elastic constants).

In his first paper already, Debye[24] gives an estimated value for Bi as $\Theta=111°$ derived from elastic measurements. Later Anderson[25] found from specific heat measurements $\Theta=147°$; his measurements, however, were not extended far into the $T<\Theta$-region. The best values so far are given by Keesom and van den Ende[26] with $\Theta=92.3°$ for $T=10°$, and $\Theta=104.1°$ at $T=20°$. Thus the difference with our Θ^* value and that of Keesom is less than 10 percent which agreement is satisfactory especially in view of the fact that a single Debye function is strictly not sufficient to describe an irregular system—in fact a simple consideration shows that in case of Bi the resulting function:

$$\phi=(\varphi_{\parallel}+2\varphi_{\perp})/3.$$

According to the existence of different maxima of the elastic spectrum in different directions of the crystal there exist different Θ values. This fact is reflected in the results of Keesom[26] who finds at sufficient low temperatures a dependence of Θ on T.

In order to demonstrate the agreement of our observations with the theory, both functions (Eq. (1)) were calculated for Θ and Θ^*, i.e., without and with considering zero point energy, and plotted in Fig. 3 (the former full drawn, the latter dashed). Table II gives some of the numerical values. The lower left side of the diagram presents the range of the last 120° on an enlarged scale.

Although it is obvious that more measurements should be available and the scattering of the points should be less, it is easily seen that a better agreement exists with the lower than with

[24] P. Debye, Ann. d. Physik **39**, 817 (1912).
[25] C. T. Anderson, J. Am. Chem. Soc. **52**, 2720 (1930).
[26] W. H. Keesom and S. N. van den Ende, Kgl. Acad. Amsterdam **33**, 243 (1930).

the upper curve, i.e., *with* the assumption of the zero point energy. For $T > T_N$ the observations fall systematically below the M^* curve and are better, but not sufficiently fitted by the M curve. There are several tentative explanations possible if one does not wish to ascribe the deviation to a systematic error. The assumption of a change of the value of Θ^* with higher temperatures is unlikely as Θ^* had to be smaller (Eqs. (2a) and (b)) and our value is already smaller than that of other authors. For the same reason the above mentioned superposition of several functions should not alter the curve in the desired direction.

It seems more likely that an increase of secondary extinction sets in at higher temperatures which should be very influential, in view of the strong tendency of Bi towards mosaic malformation, this effect would support the assumption of the process of decrystallization (see Section 1).

Concerning the aforementioned pseudoallotropic transformation point at 75°C, the diagrams indicate neither a discontinuity in $J_T/J_N(T)$ nor a change of M, although we are to report[27] a change of the thermal expansion coefficient of the lattice as observed at the same crystals in a following paper. The absence of a change of the integrated intensities at this point seems to speak against the implication that the alleged allotropy of Bi was just due to the triple eutectic point of the system Bi-Pb-Sn. The high purity of the crystals used in our experiments excludes the presence of Pb or Sn in larger concentrations than 10^{-4} and it could hardly be assumed that these small traces of impurities could form eutectic segregations. But even if this were the case and certain sections of the lattice consisting of such eutectic segregations of minute size would melt at 75°C, one should assume a discontinuous change of the extinction of the crystal and with it a change of the integrated intensity.

From Figs. 2 and 3 is seen that the intensities begin to deviate in a positive direction from the straight line relation 50°–80° before the melting point. Contrary to the relatively small negative deviation mentioned above this appears to be a large discrepancy with the temperature function anticipated by the theory which cannot easily be

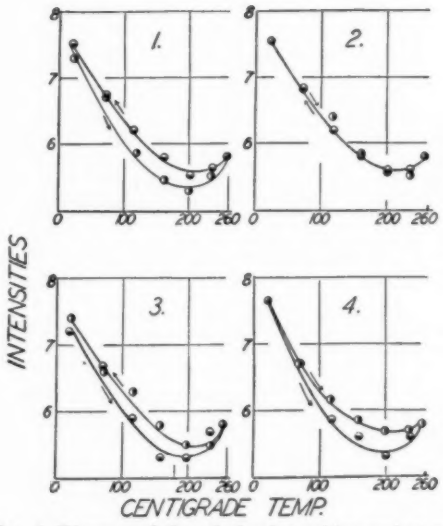

FIG. 4. Diagram of the relative intensities against temperature in the neighborhood of the melting point for different thermal histories of the crystal. (3rd-order only.) In cases 1 and 3 the crystal was "quenched" before measurements were taken. In case 2 the crystal had been annealed. In case 4 the crystal was heated after annealing (upper curve), then "quenched" and reheated (lower curve). The arrows indicate the temperature direction of the measurement. Points of equal demarcation belong to the same direction of measurements.

ascribed to an experimental error.[28] A special study of the behavior of the crystal was made by approaching the melting point as closely as possible, that is, up to a temperature at which the crystal began to sag. For these experiments, only the third order was used. As diagram 2, Fig. 4 shows, the integrated intensities do not decline as fast as is expected beyond approximately 180°C. In fact the curve goes through a minimum around 210°C after which the intensities *increase* with increasing temperature in such a way that, for instance, the intensity at 260°C is the same as the intensity around 160°C. As no anomaly of the specific heat or the elastic properties is known to exist in this region a change in the secondary extinction, i.e., in the mosaic discontinuities of the crystal is more likely the cause. In this case, one should expect a dependence of this anomaly upon the thermal history of the crystal and accordingly one should observe an hysteresis between the intensities and the temperature if the crystal is cooled faster

[27] R. B. Jacobs and A. Goetz, Phys. Rev., following paper.

[28] Against such an error speaks the much tested reproducibility as well as the reversibility with (T) of the phenomenon which excludes, e.g., an oxide layer on the crystal face as a cause.

than is necessary for it to assume a mosaic configuration stable at the particular temperature.

Accordingly intensity measurements were performed on crystals of different thermal history while increasing or decreasing the temperature. The results are presented in the diagrams 1, 3 and 4 in Fig. 4 and it is seen that the expected hysteresis occurs. Whereas the crystal which does not show hysteresis (diagram 2) has been kept at high temperature for a considerable time and cooled very slowly, diagrams 1 and 3 represent crystals which, before the measurement was taken, had been heated to 220°C and were quenched in liquid air before they were heated for the intensity measurement. Both diagrams show that the annealing of the crystal in the neighborhood of the melting point results in a decrease of the extinction, in other words, the crystal is a better reflector after the heat treatment than before. In order to make sure that the hysteresis was not caused by a temperature lag in the apparatus, which would cause lower intensity measurements when the temperature was increased or higher intensity values when the intensity was decreased, a carefully annealed and slowly cooled crystal was reheated while the intensities were measured (upper curve, diagram 4, Fig. 4). Then the crystal was quenched and reheated while another set of intensity measurements was taken. The result proved to be the same as in the other measurements, indicating that *the extinction is largest in a crystal, the mosaic configuration of which is not in temperature equilibrium.* The fact that the "repair" of the crystal sets in only in the neighborhood of the melting point is in agreement with the experience that the recrystallization temperature of bismuth lies very close to the point of fusion. It is easily seen that the increase of J_T/J_N with the temperature is caused to some extent by this "repair." Nevertheless, there remains sufficient curvature even for the perfectly annealed crystal to indicate another phenomenon for which a satisfactory explanation cannot be suggested.

In conclusion the authors wish to express their indebtedness to Dr. A. B. Focke and Dr. M. F. Hasler for growing the crystals and refining the metal used, to Dr. E. Donat and Dr. C. Gregory for assistance in the production of liquid hydrogen and in the temperature measurements and Mr. Charles Edler for a great deal of technical assistance.

FEBRUARY 1, 1937 PHYSICAL REVIEW VOLUME 51

The Thermal Expansion of the Bi Lattice Between 25° and 530° Abs.*

ROBERT B. JACOBS† AND ALEXANDER GOETZ
Cryogenic Laboratory, California Institute of Technology, Pasadena, California

(Received October 24, 1936)

The thermal expansion of the lattice of Bi crystals between 25° and 530° abs. is measured with a Bragg spectrometer equipped with a movable slit between crystal and ionization chamber. The 2d, 3d and 5th orders of Mo $K\alpha$ reflections on (111) were used. α_{II} thus obtained varies from 8.3×10^{-6} to 17.4×10^{-6} at 25° abs. and 120° abs., respectively, beyond the latter temperature it stays unchanged until the melting point. Only the range between −15°C and +75°C forms an exception where the expansion coefficient drops to 13.8×10^{-6}. This seems to indicate the existence of a separate "phase," not characterized by a change of the lattice configuration and confirms certain previous findings of discontinuities at +75°. A definite divergence between the lattice and the integral expansion beginning 30° before the melting point was found. The Grüneisen rule (α/c_p=const) is found to hold in first approximation for the whole temperature range. The relation of the α_{II} values obtained to those of other authors is discussed.

1. INTRODUCTION

THE thermal expansion of a crystalline substance may be measured by two distinct methods. The first is the usual optical method which sums the thermal expansion of every volume element over the whole length of the crystal. In the second type of measurement, x-ray diffraction is employed to measure the change of the crystal lattice spacing due to change of temperature, and the values of the expansion so obtained present the expansion only

* Partly contained in: R. B. Jacobs, thesis 1934, Cal. Inst.

† Now at Harvard University.

of those volume elements of the crystal which contribute to the diffraction. As an actual crystal ("Realkristall") does not necessarily consist entirely of elements of sufficiently well aligned atomic configuration, it is conceivable that the results of both types of measurement can differ.

For a number of reasons this problem seems to be particularly interesting in the case of Bi crystals. Here the integral expansion has been measured by a number of authors, whose results are given in Table I, as far as the coefficient of the thermal expansion parallel to [111] is concerned. These measurements are in fair agreement (with the exception of Bridgman's value) and give a nearly constant value for $\alpha_{\parallel}$ between room temperature and 30°–50° of the melting point of the metal; certain detailed differences, however, will be discussed later. Goetz and Hergenrother[1] were the first to measure the lattice expansion systematically and compare them with the dilatometric (integral) values of $\alpha_{\parallel}$ obtained previously. Their results indicated that there exists a considerable difference between the microscopic (lattice) and the integral expansions. Jay,[2] in a later paper, performed similar measurements on a number of crystalline substances (Ag, SiO_2, Bi) and concluded that his lattice expansion coefficients agreed quite well with the known values for the integral expansion.

Differences between Jay's work and that of Goetz and Hergenrother are immediately evident: The latter authors find a continuous variation of $\alpha_{\parallel}$ from room temperature to a temperature slightly below the melting point of Bi (271°C), i.e., from 14.4×10^{-6} to 20.3×10^{-6}, whereas the former finds a value of $\alpha_{\parallel}$ which is essentially invariant with the temperature between 20° and 150°C, i.e., $16.9\pm0.5\times10^{-6}$. Beyond 150° Jay's x-ray lines overlap with control lines, making further measurements of $\alpha_{\parallel}$ impossible. He was, however, able to determine the values of $\alpha_{\perp}$ (expansion coefficient normal to [111]) for the whole region between the melting point and room temperature, which are of considerable value, as an approximate proportionality between $\alpha_{\parallel}$ and $\alpha_{\perp}$ for higher temperatures can safely be assumed. These values are:

20°– 70°	$=11.0\times10^{-6}$
80°–160°	$=11.9\pm0.2\times10^{-6}$
160°–240°	$=12.1\times10^{-6}$.

Two points are of special interest in Jay's observations: The existence of a discontinuity in the region of 75°C and the occurrence of an actual contraction of the lattice for the last 25° before the melting point, which would necessitate a negative expansion coefficient. Whereas these results are in fair agreement with dilatometric values up to about 248°C, they disagree with the dilatometric observations for higher temperatures, since no observer has found a contraction. Recent investigations by Buchta and Goetz[3] concerning this particular temperature range showed only a decrease in $\alpha_{\parallel}$, but always a positive value for the expansion coefficient. The size and the nature of this decrease was found to depend to a large extent upon the presence of small traces of impurities in the metal. In the light of these discrepancies it appears that Jay's results cannot be offered as complete proof of the equality of the integral and the lattice expansion coefficients.

In addition to the question of whether the integral expansion of a single crystal is identical with the lattice expansion, another problem needed investigation concerning the validity of the Grüneisen rule[4] (predicting a constancy of the ratio between the expansion coefficient and the specific heat (c_p) of a metal) which obviously does not hold for the integral expansion coefficient (as a decrease of the specific heat in the

TABLE I. *Integral expansion of bismuth crystals parallel to 111 axis as measured by various authors.*

OBSERVER	$\alpha_{\parallel}\cdot10^6$	TEMPERATURE INTERVAL
H. Fizeau[1]	16.4	20°– 80°C
P. W. Bridgman[2]	13.96	20°C
J. K. Roberts[3]	16.2	20°–220°C
T. L. Ho and A. Goetz[4]	16.6	20°–150°C

[1] H. Fizeau, Comptes rendus **68**, 1125 (1869).
[2] P. W. Bridgman, Proc. Nat. Acad. **10**, 411 (1924).
[3] T. K. Roberts, Proc. Roy. Soc. **A106**, 385 (1924).
[4] T. L. Ho and A. Goetz, Phys. Rev. **43**, 213 (1933).

[1] A. Goetz and R. Hergenrother, Phys. Rev. **40**, 643 (1932).
[2] A. H. Jay, Proc. Roy. Soc. **143**, 465 (1934).
[3] J. W. Buchta and A. Goetz, Phys. Rev. **46**, 1042 (1934).
[4] Strictly speaking, the volume coefficient is implied, but owing to the apparent constancy of $\alpha_{\parallel}/\alpha_{\perp}$ for Bi, either of the latter may be substituted.

neighborhood of the melting point would have to be postulated). Goetz and Hergenrother, however, found the validity of this rule by introducing the lattice expansion coefficient instead of the integral α_{II}. Nevertheless, this agreement would be considered substantiated only over the comparatively small temperature range over which c_p values were available. Meanwhile, the range from helium temperatures to the point of fusion has been covered with the exception of 40°.[5-7]

2. Method and Apparatus

In the work being reported in this paper, the values of the lattice expansion coefficient (α_{II}) are determined over an extended temperature range, that is, from near the boiling point of hydrogen to within a few degrees of the melting point of the crystal (30°–537° abs.).

In order to ensure the identity of the crystal material used in the dilatometric measurements, the Bragg method was employed for the determination of the change of the lattice spacing whereas the Debye-Scherrer method used by Jay necessitates the use of powdered crystals, the integral α values of which cannot be determined for the sake of comparison with the lattice values of α.

The spectrometer is the same as the one described in the preceding paper,[6] likewise the cryostatic and the thermostatic crystalholders. The only alteration introduced for a more sensitive and accurate determination of the position of the maximum reflection consists of providing the ionization chamber with a movable slit. A schematic view of the assembly is given in Fig. 1, where C is the cryostat, J the ionization chamber, S the aforementioned slit guided by an accurate micrometer spindle M, facilitating a measurable displacement of the former with respect to the chamber and thus also to the beam of the reflected x-rays. The exact position is given by the reading of the micrometer head. The (adjustable) width of the slit is kept small compared to the width of the beam. The record of a line profile $[J=f(\vartheta)]$ is thus taken in the

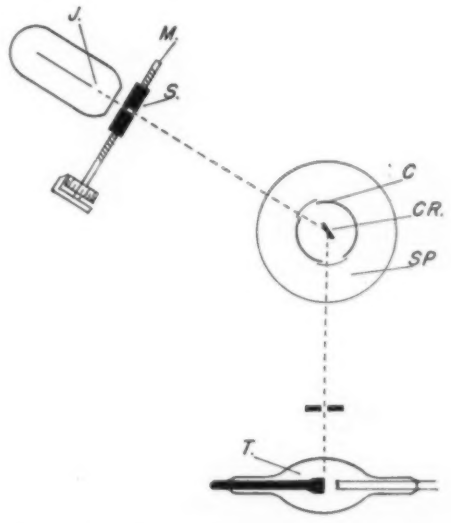

FIG. 1. Scheme of spectrometer assembly: *SP*, Spectrometer; *CR*, cryostat; *C*, crystal; *T*, x-ray tube; *J*, ionization chamber; *M*, micrometer spindle; *S*, movable slit.

following manner: When the crystal (Cr) has reached thermal equilibrium at the desired temperature, it is set together with the tube (T) somewhere near the center of the rocking angle corresponding to the order of reflection under observation. The slit system of the incident beam is then rigidly fixed in position. Now slit S is moved across the path of the reflected beam and the current in J is recorded for different slit positions. From this record the exact position of the maximum is found by interpolation. The temperature of the crystal is then changed, the procedure repeated and a new maximum found. The shift of the latter is then a measure of the change in ϑ, that is, in the lattice spacing.

The increase in accuracy of these experiments compared with previous work at this laboratory is partly due to the use of the movable slit in front of the ionization chamber instead of moving the crystal through the full rocking angle, the former technique making it possible to use several orders of reflection for comparison. Although Goetz and Hergenrother took observations of all of the first five orders, the resolving power of their method was not sufficient to permit the application of any but the fifth order. The present apparatus, however, resolves well

[5] L. G. Carpenter and T. F. Harle, Proc. Roy. Soc. **A136**, 243 (1932).
[6] A. Goetz and R. B. Jacobs, Phys. Rev., preceding paper.
[7] W. H. Keesom and S. N. van der Ende, Kgl. Acad. Amsterdam **33**, 243 (1930).

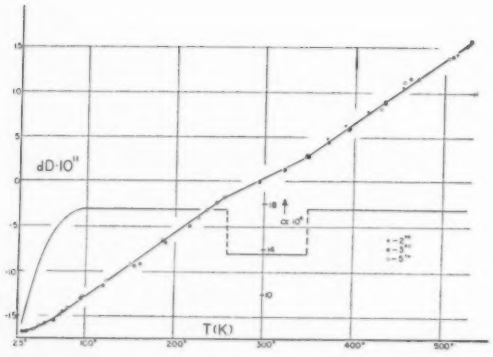

FIG. 2. The temperature function of the lattice spacing along [111] of Bi and of the expansion coefficient $\alpha_{\parallel}$. The abscissa is common to both, the ordinate of the latter is indicated in the center.

enough even the second order. The advantage obtained thus is obvious, as a simple geometrical consideration shows that any displacement of the crystal due to thermal distortion in its mountings, etc., will to a first approximation result in an *equal* angular displacement for *each* order of reflection. However, a change in the lattice spacing will give *different* angles for *different* orders in accordance with the Bragg equation. It is thus easily possible to distinguish between a $\Delta\theta$ caused by a displacement of the crystal as a whole or one caused by the thermal dilatation within the lattice.[8]

The wave-length used was that of Mo-$K\alpha$ radiation. Only the [111]-direction in the crystal was used as only (111) produces a plane satisfactory for this type of work.

3. MATERIAL

Most of the crystals used in this work are identical in origin with the crystals used in previous work.[6] The metal used for measurements above room temperature comes from stock identical to the crystals used by Ho (reference 4, Table I). The crystals used below room temperature were produced in a vacuum and are identical with those used by Buchta and Goetz.[3] No essential difference between the two different stocks is known.

[8] Aside from the aforementioned possibility of using large individual crystals instead of powder, the above method should be capable of higher accuracy than the Debye-Scherrer method employed by Jay. Owing to the larger intensity required in a photographic method, the practical limit of the distance between crystal and film is around 4–5 cm. These factors are limited to a much less degree in the Bragg method and 5–10 times larger distances can easily be used. (The distance in these investigations varies between 21.5 and 31.5 cm.) Furthermore, the obvious advantage of the D.-S. method in using extremely high orders with a large displacement corresponding to an increment of the lattice spacing is, in our opinion, outweighed by the indeterminacy of the position of the photometric maximum of the reflection on the photographic record—in addition to the gain of the above factor due to the increased distance.

4. RESULTS

In Table I the experimental data are given. The change in the lattice spacing ($dD\times10^{11}$) for each temperature is calculated with reference to the room temperature (294° abs.). Measurements of the 2nd, 3rd, and 5th order of reflection have been used, as the first is too much influenced by the surface condition of the cleavage plane, and the 4th is not sufficiently intense. In Fig. 2 the values of dD (Table II) are plotted against the temperature, observations of different orders being marked by different designations. The small scattering of the observations of different orders demonstrates the smallness of a systematic error.

The curve reveals two distinct changes of inclination, occurring at about −15° and +75°C,

TABLE II. *Expansion data.*

Order of Refl.	Abs. Temp.	$dD\times10^{11}$	Order of Refl.	Abs. Temp.	$dD\times10^{11}$
2	294.2	0.0	3	395.5	6.08
"	323.0	1.44	"	435.1	8.97
"	350.0	2.88	"	472.0	11.80
"	371.2	4.94	"	511.3	14.08
"	391.3	6.35	"	531.2	15.28
"	416.4	7.78	5	32.7	−16.8
"	434.5	9.11	"	42.6	−16.55
"	454.6	10.70	"	48.5	−16.15
"	472.3	11.63	"	56.0	−15.60
"	514.9	14.32	"	64.5	−15.20
"	533.4	15.51	"	71.8	−14.95
3	30.2	−16.85	"	81.2	−14.15
"	35.0	−16.75	"	97.0	−12.85
"	56.1	−15.80	"	123.9	−11.0
"	63.9	−15.70	"	151.2	− 9.20
"	75.2	−14.60	"	186.3	− 6.41
"	96.3	−13.20	"	216.8	− 4.21
"	123.0	−11.65	"	226.0	− 4.03
"	154.6	− 9.41	"	236.3	− 3.16
"	162.1	− 9.25	"	294.2	0
"	189.7	− 6.85	"	348.2	2.88
"	217.2	− 5.0	"	394.5	5.92
"	247.0	− 2.4	"	430.8	8.20
"	294.2	0	"	461.3	11.3
"	323.5	1.46	"	505.9	13.7
"	346.3	2.90	"	536.7	15.9
"	349.5	2.97			
	373.0	4.48			

aside of which it approaches except for the lowest temperatures a fairly straight line. The decline of the expansion in the $T<\theta$ region is obvious and to be expected—it shall be discussed below in connection with the validity of the Grüneisen rule.

It is noteworthy that in agreement with Jay's values for $\alpha_\perp$ and in discrepancy with Goetz and Hergenrother the pseudoallotropic transformation is found to be marked in the lattice expansion, whereas it could not be found in the intensities-temperature function.[8] Also, new to our knowledge is the existence of a change in direction at -15°C which appears to be the reversal of the change at $+75$°C. Hence the curve suggests the existence of a separate phase within this temperature interval, which phase is, however, not a case of normal allotropy, as the lack of a discontinuity in the temperature function of the lattice spacing proves.[9] Since this problem has been discussed already in the preceding paper it may suffice to call attention to the fact that within the range of this phase the expansion rate is abnormally low.

This point is made more obvious by the temperature-function of the expansion coefficient α_{11} derived from the previous curve by differentiation. The function is plotted also in Fig. 2 on a separate ordinate, the numerical data are given in Table III.

The temperature function of α_{11} has therefore three distinctly different sections: The range where $T<\theta-(0°$–$100°)-$, where α_{11} shows large variation with temperature, the range where $T>\theta-100°$–$538°-$ where α_{11} does not vary appreciably with T. Within this region lies the interval of a separate "phase" within which $-258°$–$348°$—α_{11} is apparently constant but considerably smaller than in the range bordering this "phase."

TABLE III. *Values of coefficient of expansion.*

TEMP. (ABS.)	$\alpha_{11}\times10^6$
30°	7.2
35°	8.3
45°	11.2
55°	14.0
70°	15.6
80°	17.0
90°–258°	17.4
258°–348°	13.8
348°–538°	17.4

[9] The apparent reversibility of this "transformation" establishes a certain analogy to the $\alpha\rightarrow\gamma$ and $\gamma\rightarrow\delta$ transformation of Fe which is an almost perfect reversal. Of course these transformations are *not* analogous with respect to the true allotropy of Fe.

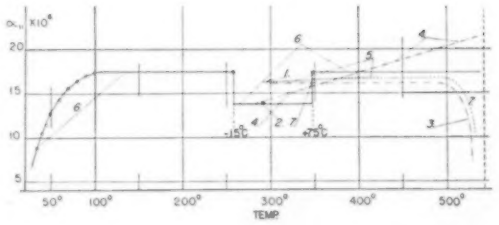

FIG. 3. Compilation of α_{11} values of different authors: "*1*" Fizeau; "*2*" Bridgman; "*3*" Roberts; "*4*" Goetz and Hergenrother; "*5*" Jay; "*6*" authors; "*7*" Ho and Goetz.

5. DISCUSSION

As there exists considerable disagreement among the different observers a compilation of the data so far available is presented in Fig. 3. It is seen that even at room temperature the agreement is not good but that the results fall into two groups:

The dilatometric values of Fizeau ("*1*"), Roberts ("*3*"), Ho ("*7*"), and the x-ray value of Jay ("*5*") are consistent in giving a value of α for room temperature which is between 16.2 and 16.9×10^{-6}. The other group comprises Bridgman's value ("*2*") for the integral expansion and for the expansion of the lattice the observations of Goetz and Hergenrother ("*4*") and of the authors ("*6*") ranging from 13.6 to 14.4×10^{-6}. It appears difficult to explain this discrepancy. Furthermore: at 75°C Ho's dilatometric values and our x-ray values give indications of a discontinuity in α_{11}, whereas other authors fail in finding it, as does Jay. This is all the more surprising when it is remembered that in measuring $\alpha_\perp$ Jay found a definite indication of a sudden change in lattice spacing (i.e., $\alpha=\infty$) at 75°C. Beyond this temperature and up to about 240°C there is considerably better agreement among the various observations, with the exception of the results of Goetz and Hergenrother which indicate a continually increasing value of α_{11} from 16.2 to 19.4×10^{-6}, respectively. In view of the present results which were taken by the same method, the quantitative results of the former paper for higher temperatures have to be dis-

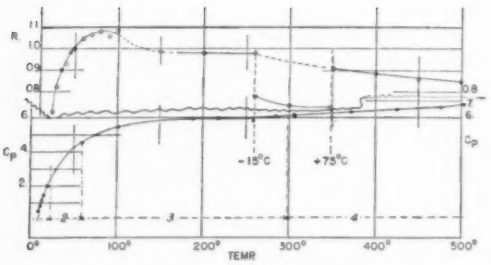

FIG. 4. Lower section: The c_p function of Bi; "*1*" Keesom and van der Ende; "*2*" interpolated; "*3*" Anderson; "*4*" Carpenter and Harle. Upper section: The relative variation of $R=\alpha_{II}/c_p$ for $R_0=3.0$. The dashed line between $-15°$ and $+75°$C indicates R in case of the absence of a "transformation."

carded, probably due to the lack of comparison with other orders and of a sufficient number of readings at different temperatures.

Only four sets of values continue beyond 240°, as Jay's measurement terminated at 150°. The 2 dilatometric values—that of Ho and of Roberts—agree on assigning a decline to α_{II} between 240° and the melting point. However, neither our present values on lattice expansion nor those of Goetz and Hergenrother gave any indication of such a decline. As Buchta and Goetz[3] have shown this anomaly of the dilatometric expansion to be influenced by very small concentrations of foreign atoms in the lattice it appears certain that this anomaly is not a property of the lattice but is caused by those regions of the crystal which do not contribute to the diffraction. (See reference 1.) This is supported by the fact that the anomaly of the temperature function of the integrated intensities begins in the same temperature range as the anomaly of the expansion coefficient.

This, however, leaves Jay's finding of an anomaly of the lattice expansion unsupported.

Finally the relation of our values of the expansion coefficient with the specific heat shall be discussed briefly: The Grüneisen rule postulating $\alpha/c_p=$const. (at least for cubic systems) was found by Goetz and Hergenrother to hold remarkably well for their values of the lattice expansion. Since our present values differ considerably from those of the former work and extend over a much larger temperature range—a compilation of the recent c_p values was made which are plotted in the lower section of Fig. 4. The work of three different authors was used, since no measurement extending over the whole of the temperature range is available. Keesom and van der Ende[7] ("*1*") measured from He temperatures to 25° abs., Anderson[10] ("*3*") from 60°–300° and Carpenter and Harle[5] from room temperature to beyond the melting point ("*4*"). Hence the range between 60° and 25° has to be interpolated ("*2*"). Considering the resulting function it is noteworthy that beyond $-15°$C c_p begins to rise with T instead of being constant, although the two "transformation" points are not marked by a discontinuity of c_p. Unfortunately the observations in the range "*4*" are taken over too large intervals of temperature to be decisive about any similar change of dc_p/dT at $+75°$C.

In order to find the relative variation of α_{II}/c_p from constancy, the values of $R=\alpha_{II}/R_0c_p$ are plotted against T. As an approximate *average* value, $R_0=\alpha_{II}/c_p$ was taken as 3.0. A possible systematic variation is indicated by a curve. As a whole this variation amounts to 20–30 percent of R_0, nevertheless the constancy should be considered fair in view of an almost 400 percent variation in c_p and of the uncertainty of the interpolation of c_p in "*2*" and finally of the inaccuracy of the determination of any α value for large $d\alpha/dT$. Thus the validity of the Grüneisen rule as a fair approximation even for the $T<\theta$ region seems to be established. It is obvious that this validity is nonexisting between $-15°$ and 75° due to the absence of a measurable heat of formation. It may be mentioned that the Grüneisen rule would require so large a change in c_p at $-15°$ and $+75°$ that it could not have escaped observation.

[10] C. T. Anderson, J. Am. Chem. Soc. **52**, 2720 (1930).

The Index of Refraction of Cerussite for X-Rays

J. E. FIELD AND GEORGE A. LINDSAY
University of Michigan, Ann Arbor, Michigan
(Received November 4, 1936)

The refractive index of cerussite ($PbCO_3$) has been measured for some fourteen wave-lengths lying in the spectral regions from 2500 to 3600 X.U. and from 4800 to 5400 X.U. In this neighborhood are found also the five M absorption limits of lead. On account of the high density (6.6 g per cc) of cerussite, the unit decrement $\delta(=1-\mu)$ is much larger than that of such crystals as calcite, quartz, etc. From the theory of dispersion δ/λ^2 should decrease considerably in the vicinity of the absorption limits. A general decrease in the value of δ/λ^2 was found, especially toward the higher wave-lengths, but it is not evident that there is a very large change in the immediate vicinity of an absorption edge. The method used differs somewhat from those previously employed.

INTRODUCTION

PERHAPS the chief difficulty in determining the index of refraction for x-rays is due to the very small deviation of the beam in passing from one medium to another, even when the glancing angle is small. Several different methods have been used in the past to measure the index for various substances. Among the methods used is one proposed by Bergen Davis and used by von Nardroff,[1] Larsson[2] and others. The essential principle of this method consists in increasing the deviation of a refracted ray of a certain wave-length by reflecting it from a crystal in such a manner that the ray enters or leaves the crystal at a very small angle with the crystal face, instead of at the regular angle given by the Bragg law of reflection. With the exception of von Nardroff's work on iron pyrites (density about 5 g per cc) most of the measurements made by this method, as well as by the method of direct transmission of a ray through a prism of the material, have been for lighter materials such as calcite, quartz, glass, etc. The advantage with lighter materials is, of course, that the absorption is much less—a very important consideration for the longer wave-lengths. For the method of total reflection the absorption is not so serious, but for the elements of higher atomic number the critical angle at which total reflection occurs becomes very indefinite.[3]

The present work takes advantage of the principle suggested by Bergen Davis, but with this difference; instead of artificially preparing a face on a crystal at a certain angle with the atomic planes, a natural face (in this paper referred to as the bevel face) was used, while the spectrum was formed from planes parallel to the other natural face, here called the Bragg face.

Crystals of cerussite ($PbCO_3$) often possess such natural faces making suitable angles with each other, while at the same time the substance is very dense (6.6 g per cc), so that a relatively large value of the unit decrement $(1-\mu)$ is obtained. The faces used were such that the wave-lengths having suitable angles of reflection lie in the portion of the spectrum containing the M absorption edges of lead. Anomalous refraction near the absorption limits has been investigated extensively by Larsson,[2] whose work dealt with the K edges. It was hoped that some similar effect could be observed near the M edges of lead.

The same substance, $PbCO_3$, has been investigated by Hoyt and Lindsay[4] by a somewhat different procedure. In the latter work a single beam was reflected from two faces of the crystal at once, while the present method determines the position of the ray refracted from the bevel face of the crystal by measuring its distance from a reference line reflected from the Bragg face of the same crystal. When both the reference line and the line whose refraction is being investigated are reflected from the Bragg face their separation is the normal one, each line, of course, being displaced slightly by refraction as all lines are in ordinary reflection. Now, if the crystal is turned so that the reference line is still reflected from the Bragg face, while the other is reflected from the bevel face, the separation of the two lines is changed, since the deviation of the ray issuing

[1] R. von Nardroff, Phys. Rev. **24**, 143 (1934).
[2] A. Larsson, Dissertation, Upsala (1929).
[3] E. Nahring, Physik. Zeits. **31**, 799 (1930).
[4] H. C. Hoyt and Geo. A. Lindsay, Phys. Rev. **49**, 498 (1936).

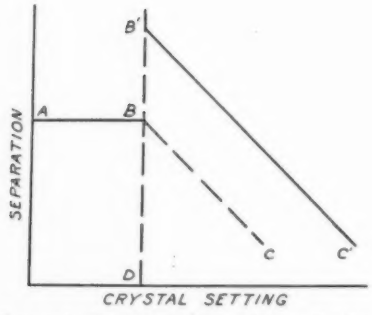

FIG. 1. Separation between reference line and refracted line as crystal is turned.

from the bevel face has been greatly increased. If now we plot the separation between the two lines as measured on the photographic plate, as a function of the angular setting of the crystal, we find a constant separation as long as the two lines are reflected from the Bragg face, but as soon as one line passes to the bevel face there is a sudden change in separation as shown by BB' in Fig. 1. As the crystal is turned further the position of the line from the bevel face changes uniformly because it is no longer reflected from atomic planes passing through the axis of rotation of the spectrograph. Since the angle between the two faces is accurately known, however, the slope of the portion of the line $B'C'$, expressed as the number of millimeters per minute of arc by which the line coming from the bevel face is displaced, simply due to rotation of the crystal, and not at all due to refraction, is given by

$$\frac{\Delta s}{\text{min.}} = \frac{0.104 \sin\alpha \cos\theta}{\sin(\alpha+\theta)} \text{mm/min.} \qquad (1)$$

The angles α and θ are shown in Fig. 2. The numerical factor 0.104 is two times the arc, expressed in mm, which is subtended at a distance equal to the radius of the spectrograph by an angle of one minute.

The line of intersection of the two crystal faces should be placed accurately in the axis of the spectrometer, and no line should be reflected from so near the intersection that it becomes unsymmetrical, for in such a case the measurement of its middle point would be in error.

It becomes necessary to locate with some accuracy the setting of the crystal such that the center of the line falls on the intersection of the two faces. This setting was calculated by taking a continuous spectrum from the Bragg face, with the line to be refracted a short distance from the sharp limit where the continuous spectrum is terminated by the junction between the two faces. From the distance between the line and the termination of the continuous spectrum it is easy to calculate how much more the crystal should be turned to bring the line exactly at the junction of the two faces. This calculation at once gives the point D (Fig. 1).

Apparatus

The photographs were taken with a Siegbahn vacuum spectrometer of radius 179.2 mm. The slit was 0.035 mm wide. An important feature of the method is that the only special apparatus needed was a crystal holder capable of being tipped about two axes at right angles to each other and also capable of being displaced parallel to these axes. By means of this table the crystal was set so that the line of intersection of the faces remained fixed in position as the crystal was rotated. Thus the line of intersection of the faces was made coincident with the axis of the spectrometer. Suitable spectrum lines were obtained by placing various substances on the anode of the x-ray tube.

Geometry of the Crystal Used

Cerussite is orthorhombic in form. Its density is 6.6 g per cc.[5] The axial ratios as determined by the authors and by Hoyt[4] are

$$a : b : c = 0.6102 : 1 : 0.7229.$$

These ratios were obtained by measurement of the grating spaces of several faces of the crystal

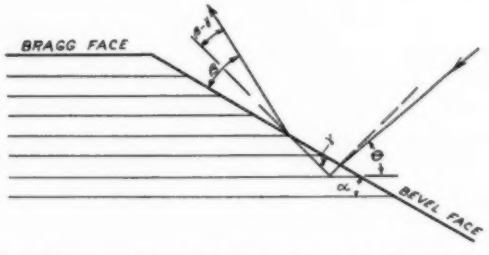

FIG. 2. Reflection and refraction of a ray at a bevel face of the crystal.

[5] *International Critical Tables.*

used, and they agree very well with values given in crystallographic tables. In all, sixteen different determinations of δ were made. For these the (001) face of cerussite was used as the Bragg face six times, the (110) face six times, the (100) face twice, and the (130) face twice. The angle between the Bragg face and the bevel face must be known rather accurately because δ is proportional to the tangent of the angle β, which is the difference between the Bragg angle θ and this angle α between the two faces (see Fig. 2). Since β was only of the order of 2° or 3°, it is evident that α should be known to about 1′. The angle α was measured optically with a spectrometer and found to be as follows. Between faces (110) and (100), 31° 23′ 30″; (110) and (130), 29° 58′ 30″; (001) and (102), 30° 37′ 0″. The face (102) was not used as a Bragg face. The values of the grating space d as measured by a precision method for the remaining four faces denoted above were determined to be as follows.

Face	(110)	(100)	(130)	(001),
d in X.U.	4416	2586	2480	3065.

Formulas for the Calculation of the Index

In Fig. 2 a monochromatic ray is shown entering the bevel face at nearly normal incidence

Table I. *Data for Ca $K\alpha_1$ line. Reference line: Ni $K\alpha_1$ (2nd order). Bragg face (001), (d=3065 X.U.); bevel face, (102); angle α between the faces=30°−37′−00″; angle θ for Ca $K\alpha_1$=33°−09′−09″; angle $\beta=(\theta-\alpha)$=2°−03′−09″; slope of $B'C'$=0.0494 mm/min.; r=179.2 mm.*

Plate number	Crystal setting	Separation (mm) Ca $K\alpha_1$ − Ni $K\alpha_1$	
262	274°–28′	3.030	
256′	30′	3.020	
256	30′	3.025	
263	32′	3.035	
264	40′	3.025	
		3.027 mean	
		Ca $K\alpha_1$ − Edge of cont. spec.	
256′	30′	2.453	
256	30′	2.428	
	53.4′	setting for Ca $K\alpha_1$ incident on crystal edge.	
		Ca $K\alpha_1$ − Ni $K\alpha_1$	BB' (mm)
260	58′	3.085	0.285
257	275–00′	2.970	.269
258	02′	2.890	.288
259	04′	2.780	.277
261	06′	2.675	.271
			0.278 mean

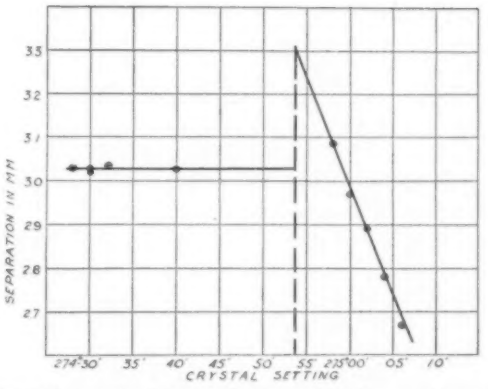

Fig. 3. Separation between Ca $K\alpha_1$ and Ni $K\alpha_1$ as reference line.

and emerging at a very small grazing angle γ inside the crystal, β outside, so that $\beta-\gamma$ is the deviation of this ray on emerging from the crystal. Hence we have

$$\mu=1-\delta=\cos\beta/\cos\gamma, \tag{2}$$

$$\delta=\frac{\cos\gamma-\cos\beta}{\cos\gamma}=\frac{2\sin\tfrac{1}{2}(\beta+\gamma)\sin\tfrac{1}{2}(\beta-\gamma)}{\cos\gamma}. \tag{3}$$

Since $\beta-\gamma$ is small, $\tfrac{1}{2}(\beta+\gamma)=\gamma$ nearly, and $\sin\tfrac{1}{2}(\beta-\gamma)$ may be put equal to $\tfrac{1}{2}(\beta-\gamma)$.

$$\therefore\quad \delta=(\beta-\gamma)\tan\beta. \tag{4}$$

Referring to Fig. 1, BB'/r, where r is the radius of the spectrograph, should be the angle by which the ray is deviated by refraction on emerging from the bevel face. It is necessary, however, to add to this angle a small amount, because of the refraction of the ray from the Bragg face, for BB' is only the *change* in the displacement when the ray passes from the Bragg face to the bevel face. We may write, then

$$\beta-\gamma=BB'/r+\Delta\theta, \tag{5}$$

where $\Delta\theta$ is the deviation of the same ray on refraction at the Bragg face. From Eq. (4)

$$\Delta\theta=\delta/\tan\theta, \tag{6}$$

hence

$$\delta=\frac{BB'}{r}\cdot\frac{\tan\beta}{1-\cot\theta\tan\beta}. \tag{7}$$

By means of this last formula the values of δ were calculated. Fig. 3, plotted as explained in connection with Fig. 1, is a sample of the results

from which BB' may be read off at once. It should be remembered that the slope of the lines is known from Eq. (1); it is not necessary to estimate their slope from the positions of the points. BB' was also calculated from each individual observed point of the sloping lines by means of Eq. (1). Of course the average of these calculations agrees closely with the graphical distance BB'. Table I contains a sample of such calculations, together with data on the measurement of plates for the Ca $K\alpha_1$ line. Fig. 3 is based on these measurements. The values of BB' in Table II are the mean of graphical values from plots like that of Fig. 3 and the average of the values calculated from the individual points as just explained.

The dispersion theory of x-rays, as developed by several writers[6, 7, 8] results in the following expression.

$$\frac{\delta}{\lambda^2}=\frac{e^2AZ\rho}{2\pi mc^2M}\left[1+\sum_k\frac{N_k}{N}\left(\frac{\lambda}{\lambda_k}\right)^2\ln\left\{1-\left(\frac{\lambda_k}{\lambda}\right)^2\right\}\right], \quad (8)$$

where A is Avogadro's number, Z the total number of electrons per molecule of the refracting medium, ρ the density, and M the molecular weight. N is the total number of electrons per cubic centimeter, while N_k is the number of electrons of kind k per cubic centimeter. On the short wave-length side of an absorption edge, where $\lambda<\lambda_k$, $\ln\{1-(\lambda_k/\lambda)^2\}$ in Eq. (8) should be replaced by $\ln\{(\lambda_k/\lambda)^2-1\}$. The values of δ/λ^2 are calculated from formula (8) and are compared with those from the observations. The comparison is made in Table II and in Fig. 4.

Experimental Procedure

In using the Bragg method, in which the distance of the axis of the spectrograph from the

[6] R. de L. Kronig, J. Opt. Soc. Am. **12**, 547 (1926).
[7] H. Kallman and H. Mark, Ann. d. Physik **82**, 585 (1927).
[8] J. A. Prins, Zeits. f. Physik **47**, 479 (1928).

Table II. *Summary of results.*

Line	λ(X.U.)	Ref. line	BB' (mm)	Bragg face	Bevel face	$\delta/\lambda^2\times10^6$ Meas.	Calc.
Va $K\alpha_1$ Va $K\alpha_2$	2498 2502	Ni $K\alpha_1$ (2) Zn $K\beta_1$ (2)	0.123	(110)	(100)	6.4	6.9
Ti $K\alpha_1$ Ti $K\alpha_2$	2743 2747	Cu $K\beta_1$ (2)	0.135	(130)	(110)	7.0	6.8
"	"	S $K\alpha_1$ (1)	0.063	(110)	(100)	6.8	
Cs $L\alpha_1$	2886	Cu $K\beta_1$ (2)	0.215	(100)	(110)	6.8	6.7
"	"	" "	0.083	(130)	(110)	6.4	
Sc $K\alpha_1$ Sc $K\alpha_2$	3025 3028	Cu $K\alpha_1$ (2)	0.122	(100)	(110)	6.4	6.5
Sb $L\beta_1$	3218	Sn $L\beta_2$ (1)	0.543	(001)	(102)	5.5	6.2
Te $L\alpha_1$ "	3282 "	Cu $K\alpha_{1,2}$ (2) Ca $K\beta_1$ (1)	0.320	(001)	(102)	5.3	6.2
Ca $K\alpha_1$	3352	Ni $K\alpha_{1,2}$ (2)	0.280	(001)	(102)	5.3	6.1
Sn $L\beta_1$	3378	Ni $K\alpha_{1,2}$ (2) Ca $K\alpha_{1,2}$ (1)	0.229	(001)	(102)	6.0	6.0
Sb $L\alpha_1$	3432	Ni $K\alpha_{1,2}$ (2)	0.166	(001)	(102)	5.2	5.9
Sn $L\alpha_1$	3592	Co $K\alpha_{1,2}$ (2)	0.126	(001)	(102)	5.7	5.9
Ru $L\alpha_1$	4835	Cu $K\alpha_{1,2}$ (3)	0.572	(110)	(100)	4.5	3.8
Mo $L\beta_1$	5166	Ni $K\alpha_{1,2}$ (3)	0.274	(110)	(100)	4.9	4.6
S $K\alpha_1$	5361	Ti $K\alpha_{1,2}$ (2)	0.215	(110)	(100)	5.0	4.9
Mo $L\alpha_1$	5395	Cu $K\beta_1$ (4)	0.223	(110)	(100)	5.4	4.9

slit and from the photographic plate are equal, the position of a spectrum line remains fixed when the crystal, mounted with its face containing the axis of rotation, is turned to a new position. In this work the crystal was mounted so that both the Bragg and the bevel faces contained the axis of rotation. The line to be refracted and a convenient reference line were photographed together, both being reflected from the Bragg face. Several such photographs were taken, the crystal being moved about 1′ each time. Then several more photographs were taken with the reference line still reflected from the Bragg face, but the other line reflected from the bevel face. Different settings of the crystal were made here also. The method of locating the point D (Fig. 1) which gives the setting of the crystal for which the line whose refraction is to be studied is reflected at the line joining the two crystal faces, has already been described. This point was probably located to an accuracy of about 15 seconds.

The direction of the rays on striking the crystal was always in the sense shown in Fig. 2, and never in the opposite sense; for in the latter sense all rays of a certain wave-length would leave the crystal in almost exactly the same direction from both faces, and hence there would be practically no separation due to refraction.

When the rays leave the bevel face at a grazing angle less than one degree the absorption is very great and the refracted line is not sharp; hence most of the measurements were taken of lines of such a wave-length that the rays left the bevel face at an angle of from one to five degrees.

Results

In Table II are collected the complete results. The first column contains the symbol of the line whose index is to be found, the second its wave-length, the third the reference line. The numbers in parentheses in the third column indicate the order of the reference line. The fourth column contains BB' of Fig. 1 and Eq. (7). In column five are the Miller indices of the Bragg face, in column six those of the bevel face. The last two columns contain the values of δ/λ^2 calculated from formulas (7) and (8), respectively.

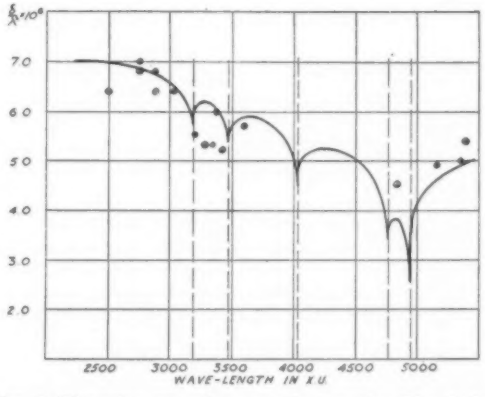

FIG. 4. Dispersion curve for x-rays in cerussite. The circles represent experimental values.

Discussion of Results

In Fig. 4 we have the curve for the value of δ/λ^2 for lead carbonate in the spectral region of the five M absorption edges of lead. The angles between the crystal faces were not suitable for measurements in the middle portion of the region, but the results indicate a falling value for δ/λ^2 as we approach M_{I} and M_{II}, then a rise again after M_{V} is passed. Only one good line could be found very near an edge. This was Sb $L\beta_1(\lambda = 3218)$ which is probably about 6 X.U. above M_{I} in wave-length. There was no evidence of any smaller value of δ/λ^2 for this particular line. However, in a substance with so many electrons per molecule as $PbCO_3$ one must approach very closely to the edge before there is any marked change in δ/λ^2. The point for Ru $L\alpha_1$ also fails to indicate the especially low value for δ/λ^2 to be expected in the narrow region between M_{IV} and M_{V}. The values of δ/λ^2 are probably accurate to some 10 percent. While the quantity undoubtedly shows a general diminution in value in the region of the M edges, it does not seem to decrease so much as required by Eq. (8), which results from the theory of anomalous dispersion.

The Radiations Emitted from Artificially Produced Radioactive Substances

III. Details of the Beta-Ray Spectrum of P^{32}

HUGH C. PAXTON
Radiation Laboratory, Department of Physics, University of California, Berkeley, California

(Received October 19, 1936)

The high energy portion of the distribution of β-rays from P^{32} was investigated by means of a hydrogen-filled cloud chamber in a magnetic field. A Konopinski-Uhlenbeck distribution was followed practically to the cutoff of 8200 $H\rho$ predicted by an extrapolation of the K-U plot. But it is possible to account for all tracks in excess of a straight line dropping to 6950 $H\rho$ by a spreading due to the estimated probable error of ± 3.8 percent. Accordingly, this work is best interpreted as indicating a sharp deviation from the K-U relation near the high energy limit, dropping to an upper limit of about 6950 $H\rho$. This discrepancy might be eliminated by modifying the K-U formula to apply to a doubly forbidden type of disintegration. However, for the allowed transitions from N^{13} and F^{17}, there is evidence from disintegration data that experimental upper limits are to be taken instead of the K-U extrapolations. The low energy part of the P^{32} β-spectrum was obtained from a very thin source suspended at the center of the expansion chamber. This distribution approached the origin almost as predicted by the K-U relation. There appeared to be no irregularities such as those observed by H. O. W. Richardson in the case of RaE.

WITHIN the past year several groups of workers[1-3] have used cloud chamber methods to investigate β-ray spectra from a number of artificially produced radioactive substances. All have found promising agreement between experimental curves and those predicted by the Konopinski-Uhlenbeck[4] modification of the Fermi theory. However, data in the neighborhood of the high energy limit have been so meagre that they present almost no evidence concerning the extremely flat tail of the K-U distribution.

The present work is an attempt to obtain detailed information about the upper limit of the β-ray spectrum of radio-phosphorus (P^{32}). This activity was chosen because of its comparatively long half-life ($14\frac{1}{2}$ days) and its freedom from γ-radiation. Further, this spectrum is the one investigated most completely by Kurie, Richardson and Paxton.

EXPERIMENTAL SET-UP

A target of red amorphous phosphorus pressed onto a pitted copper surface was activated by means of deuterons from the magnetic resonance accelerator of Lawrence and Livingston.[5] The target was liquid air-cooled during the course of bombardment in vacuum to prevent sublimation of the phosphorus. The active target was put away for three weeks before finally being investigated, in order to eliminate any known β-ray contaminant which may have been present in the phosphorus or its copper backing. The copper was allowed to remain an integral part of the source because reflected electrons would have little effect on the high energy portion of the β-spectrum.

The β-ray distribution was determined by measuring magnetically produced curvatures of electron tracks in a hydrogen-filled expansion chamber. The apparatus used was that described by Kurie, Richardson and Paxton with the addition of an external collimating channel between the source and chamber. Because this work is primarily concerned with the small fraction of tracks lying near the high energy spectrum limit, it was believed desirable to have some dispersing arrangement to prevent too much interference by the great body of low energy tracks. The method used was to collimate the beam of β-rays from the target, this being accomplished in an evacuated arm separated from the chamber itself by a thin (0.001″) mica window in the chamber wall. Thus, all β-particles enter the chamber not only at nearly the same place, but in essentially the same direction. Under these circumstances the analyzing magnetic field

[1] Kurie, Richardson and Paxton, Phys. Rev. **49**, 368 (1936).
[2] Fowler, Delsasso and Lauritsen, Phys. Rev. **49**, 561 (1936).
[3] Gaerttner, Turin and Crane, Phys. Rev. **49**, 793 (1936).
[4] Konopinski and Uhlenbeck, Phys. Rev. **48**, 7 (1935).
[5] Lawrence and Livingston, Phys. Rev. **45**, 608 (1934).

tends to fan out the spectrum, curling the lower energy tracks to one side, taking them out of the way of those of higher energy which continue in a more nearly forward direction.

A check calibration of the Helmholtz coils providing the analyzing magnetic field differed from that given by Kurie, Richardson and Paxton. A careful recalibration by several methods gave a best value of 31.5 gauss per amp. on field ammeter. This value applies to the magnetic field at the chamber center. The field decreased radially from this point, dropping to 97 percent at an inch from the chamber edge. The working area was consequently kept within this region. The ammeter in series with the coils was found to read 1.8 percent lower than when used by Kurie, Richardson and Paxton. As the change may have taken place after the present work, the results here reported may be too low by this amount.

Experimental Results on the Upper Limit

2660 exposures were obtained with an analyzing field of about 500 gauss. This gave a radius of curvature of 16 cm to the highest energy track found. Consequently, it was possible to measure radii of curvature to the nearest half centimeter by fitting arcs of circles scratched on celluloid to reprojections of normal size. In the case of higher energy tracks template measurements were checked by means of a traveling microscope focused on the negative itself. Because a comparatively heavy background made tracks on them more difficult to follow under the microscope, the first 860 photographs were disregarded in the final results. This was done in spite of the close agreement between the distribution of template measured tracks from the discarded pictures and that remaining.

Each track was critically examined in the course of measurement, the following points being kept in view. (1) It was necessary that the portions between apparent nuclear deflections be sufficiently distinct to permit fitting to the nearest half centimeter radius on the template. (2) Any track was discarded if there was an apparent change in curvature over its course. (3) Because of field nonuniformities near the chamber edge, portions of tracks appearing within an inch of the edge were disregarded. To avoid poor judgment due to fatigue, no more than fifty tracks were measured at a sitting. It is believed that in maintaining the above criteria for measurable tracks, very little distortion was introduced into the natural β-particle distribution, until one reaches a region far enough below the upper limit that the tracks belonging there were mostly lost in the large number with lower energy.

Fig. 1 shows representative exposures, tracks that were actually measured being indicated by the arrows. All tracks of 7000 $H\rho$ or above are included in this figure. The distribution of tracks against $H\rho$ values is shown in Fig. 2. Ordinates corresponding to $H\rho$ values of less than about 5750 are certainly deficient because the interference of low energy tracks cuts out an appreciable number that should be included. The complete spectrum from P^{32} as obtained by Kurie, Richardson and Paxton is shown in Fig. 3. The upper limit distribution adjusted to fit the main curve as well as possible at the $H\rho$ values 5875, 6125 and 6375 is represented by the circles.

Error Considerations

As mentioned above, the curvature of each track above 7000 $H\rho$ was checked by measuring coordinates of the droplets constituting it. The number of points so obtained ran from 46 to 83 per track. These were plotted, allowing curvature measurements to be made independent of other tracks in the neighborhood, varying droplet sizes, background influences, etc. In a few cases small angle nuclear scattering (1° to 2.5°) showed up where it had been obscured in ordinary reprojection. Typical plots of tracks so measured are shown in Fig. 4. By comparing microscope and corresponding reprojection determinations of radii of curvature it was indicated that the ordinary measuring process contributes about ± 2.3 percent to the probable error of radius of curvature near the spectral upper limit.

The influence of small angle nuclear scattering of β-rays was estimated through an expression for the probable total angular deflection in terms of the differential elastic scattering cross section for an electron in hydrogen. This was obtained by geometrical addition of the contributions from

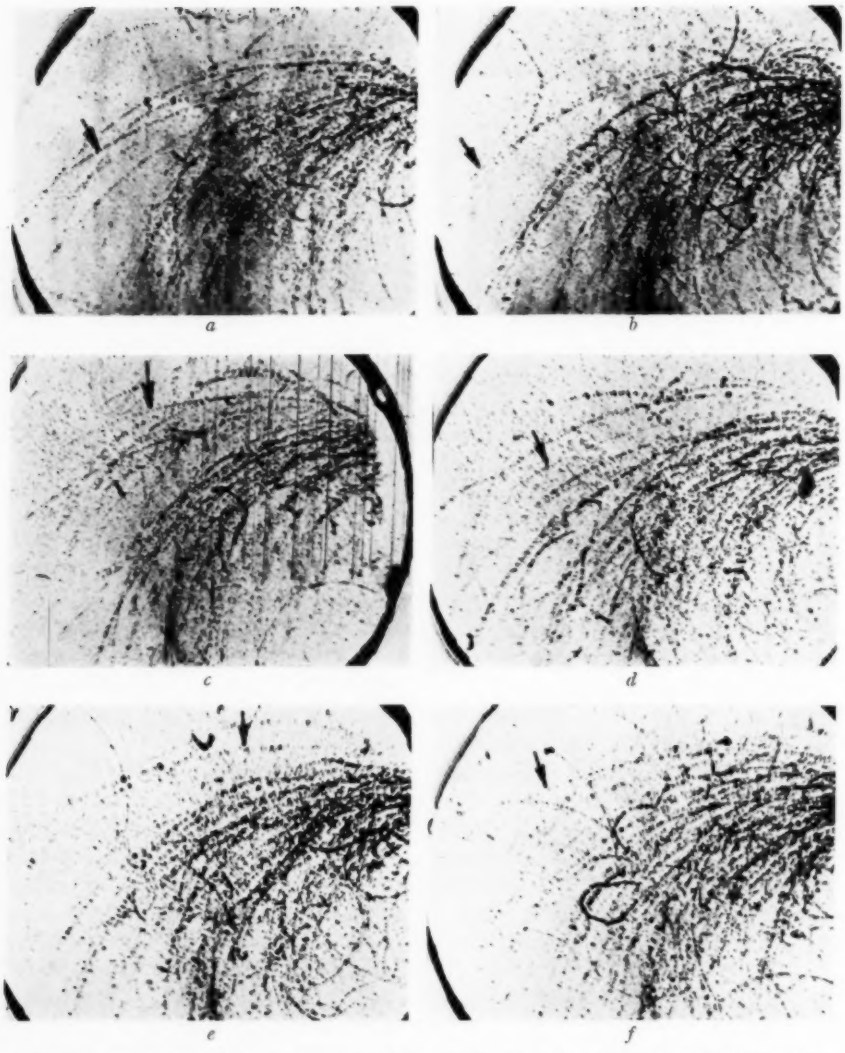

FIG. 1. Photographs including all measured P^{32} β-ray tracks of $H\rho$ above 7000. Track numbers and $H\rho$ values are: (*a*) No. 1912, 7380 $H\rho$; (*b*) No. 2162, 7260 $H\rho$; (*c*) No. 2247, 7210 $H\rho$; (*d*) No. 2762, 7150 $H\rho$; (*e*) No. 2695, 8200 $H\rho$; (*f*) No. 2697, 7480 $H\rho$.

all increments of scattered angle between 0° and the maximum individual deflection which one would just fail to detect by microscopic examination of a track (about 1°). The evaluation was made by a graphical integration involving values of differential cross section tabulated against scattering angle which Mott and Massey[6] have obtained from Born's first approximation, valid for the elastic scattering of high velocity electrons. The contribution to probable error in radius of curvature by the scattering influence of hydrogen and isopropyl alcohol vapor was finally estimated to be about ± 0.1 percent at the upper limit.

A third error factor comes about through unknown variations in the analyzing magnetic

[6] Mott and Massey, *The Theory of Atomic Collisions* (Oxford, 1933), p. 120.

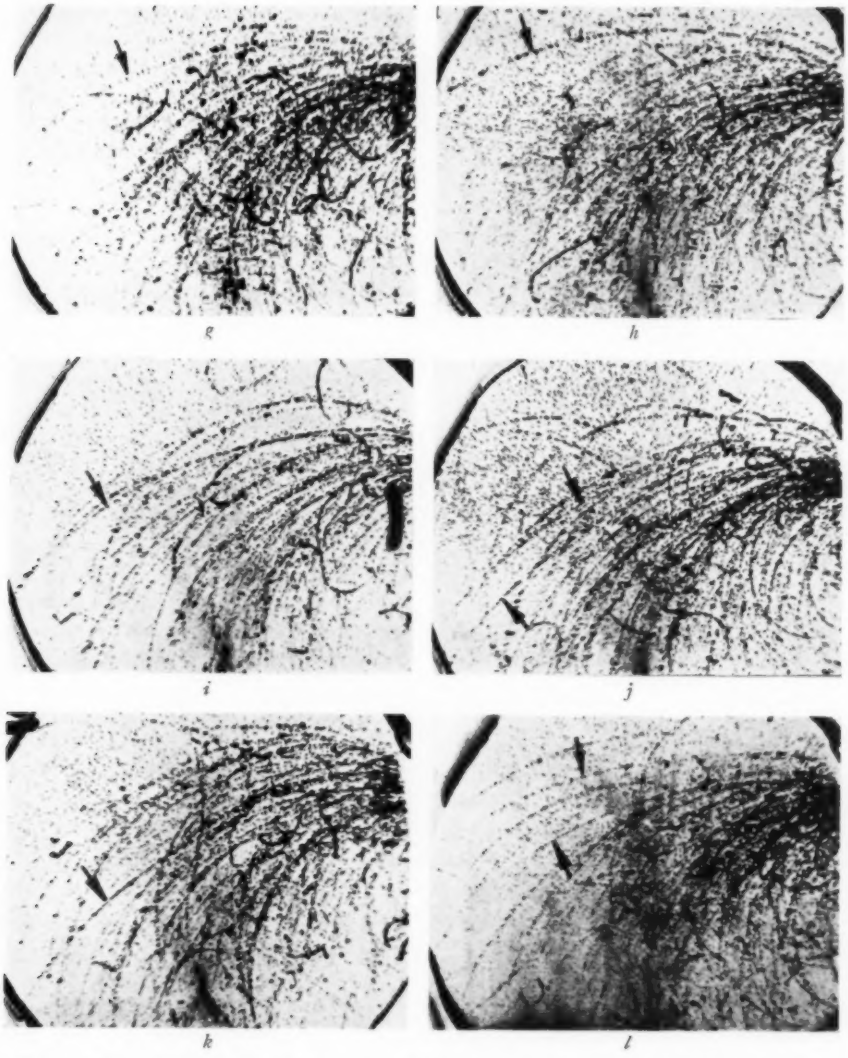

FIG. 1. Photographs including all measured P^{32} β-ray tracks of $H\rho$ above 7000. Track numbers and $H\rho$ values are: (*g*) No. 2853, 7240 $H\rho$; (*h*) No. 3028, 7240 $H\rho$; (*i*) No. 3178, 7140 $H\rho$; (*j*) No. 3146A, 7780 $H\rho$; No. 3146B, 7780 $H\rho$; (*k*) No. 3470, 7580 $H\rho$; (*l*) No. 3789A, 7300 $H\rho$; (No. 3789B, 6410 $H\rho$).

field. Power for the field was provided by a 50 kw motor generator set, each of the two generators delivering about 110 volts d.c. During operation, this generator set was used exclusively for the cloud chamber, the chief power drains being the magnetic field current supplied by one generator, and the flashing carbon arc for chamber illumination being fed by the other. As no fluctuations in Helmholtz coil current greater than one percent had been observed in much previous work, it was considered suitable to read the current about every 25 expansions, this being sufficient to follow changes in field due to heating of resistances. However, doubt was thrown on the constancy of field when it was noticed that two of the three tracks of highest energy

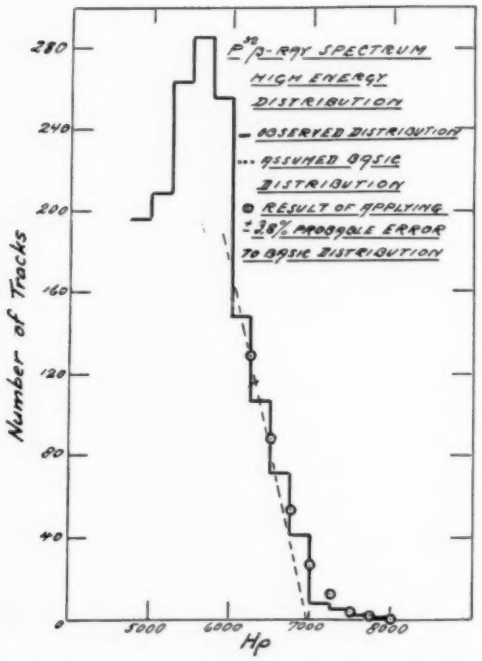

FIG. 2. Distribution of high energy tracks from P^{32}. The peak is introduced by geometrical discrimination against tracks of low energy.

appeared on the same photograph and that the third was but two exposures from another track of moderately high energy. Other high energy tracks were apparently distributed at random among expansions. As the result of this, 830 expansions were taken solely to investigate field fluctuations. It was found that all deviations from the normal heating drift could be connected with a change in sound of the carbon arc, the current sometimes decreasing as much as 5 or 6 percent in the expansion (sometimes two expansions) during which the arc would sputter just before extinguishing itself. This variation had not been noticed in regular operation because the adjustment of a sputtering arc had always held precedence over the reading of current.

It is difficult to estimate the probable error contribution to $H\rho$ by these field fluctuations; so it was rather arbitrarily taken as ± 3 percent. The asymmetric error tending to increase the apparent $H\rho$ may legitimately be replaced by a symmetrical error because the difference introduces a very slight change at the upper limit.

Further error is introduced because the magnetic field, due to its falling off near the chamber edge averages about 1 percent below its value at the center. This might give something near $\pm\frac{1}{2}$ percent to the probable error in $H\rho$ from the chance that some tracks lie along the edge of this region, while most cut across it not far from the center.

A summary of the main contributions to probable error in $H\rho$ (those which may be approximated by a gaussian distribution) at the upper limit of the spectrum is:

1.	Measurement uncertainties	±2.3 percent
2.	Elastic scattering	±0.1 percent
3.	Field fluctuations	±3.0 percent
4.	Field nonuniformities	±0.5 percent.

The total probable error from these influences is then about ±3.8 percent.

An additional uncertainty comes from the fact that all tracks are treated as though lying in the median plane of the chamber, whereas they are actually distributed through a region one centimeter deep (45 cm from the camera lens). The error so introduced, which is ±1 percent maximum, is not included in the above group because of its distinctly nongaussian nature. If it were put in as a $\pm\frac{1}{2}$ percent probable error component, its effect on the total probable error would be completely negligible.

Analysis of Upper Limit Data

The histogram representing the experimental distribution of tracks against $H\rho$ (Fig. 2) was transferred to the K-U plot shown in Fig. 5. The

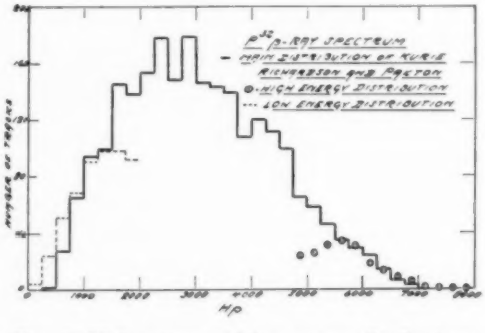

FIG. 3. High energy and low energy distributions of tracks from P^{32} fitted to the main distribution of Kurie, Richardson and Paxton.

main distribution of Kurie, Richardson and Paxton is shown by the circles in Fig. 6, the filled circles giving the upper limit curve adjusted to agree with the main distribution at 5875, 6125 and 6375 $H\rho$. These K-U plots were made as described by Kurie, Richardson and Paxton, and so involve approximations which are strictly applicable only to allowed transitions. When corrected to apply to a spin change of two as is involved in the disintegration $P^{32}\rightarrow S^{32}+e^-$, the functions plotted should drop below the straight line of Fig. 6 as the upper limit is approached, according to unpublished calculations by Lamb.

Before accepting the apparent confirmation of the uncorrected Konopinski-Uhlenbeck relation, it is well to follow the lead of Fowler, Delsasso and Lauritsen in estimating the influence of the probable error on the upper limit tail. By trial the line $y=-0.175x$ representing the actual spectrum cutoff (x being measured from the upper limit so defined) was found to give the distribution corresponding to the circles superposed on the upper limit histogram in Fig. 2, when each element is spread out by a probable error of 3.8 percent. Accordingly, it is hardly permissible to insist that these data support a tail of higher order contact than the straight line shown in Fig. 2. When represented as a K-U plot, this line gives the crosses on Fig. 5.

Assuming the linear cutoff of Fig. 2, the upper limit is 6950 $H\rho$ (corrected to the mean analyzing field which is 1 percent below that at the chamber center; also the stopping power of the mica window is taken into account). This is to be compared with a K-U limit of 8200 $H\rho$. This interpretation gives results essentially in agreement with recent findings of Lyman.[7] In working with his magnetic spectrograph of very high resolving power, he has found the K-U plot for P^{32} to drop sharply away from a straight line just before striking an upper limit at 7150 $H\rho$. This limit, however, includes a slight tail beyond a nearly linear drop on the distribution in $H\rho$ curve.

This difference is of the order indicated by Lamb's correction terms for a doubly forbidden disintegration. However, if this explanation holds, the K-U limits should apply to allowed

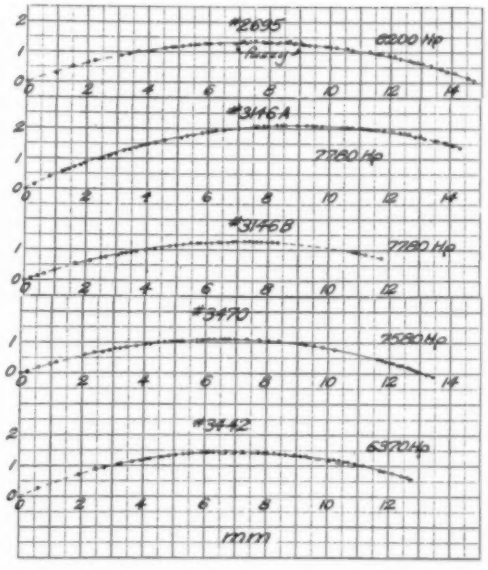

FIG. 4. Typical plots of droplets constituting higher energy tracks. Coordinates were determined by comparator measurements on the photographic film. These tracks are listed in Fig. 1; they may be identified by the noted track numbers and $H\rho$ values. Uncertain parts of the plots are indicated by dotted portions of the approximately fitted circles. Some elastic deflections are indicated by overlapping arcs of equal radii.

transitions such as the disintegration of N^{13} and F^{17}. These are involved in the following sets of reactions which Dr. E. McMillan has kindly detailed.

$$C^{12}+H^2\rightarrow C^{13}+H^1+\begin{cases}2.66\pm0.06\text{ Mev}^8\\ \text{or } 2.71\pm0.04\text{ Mev}\end{cases}$$

the second value which includes a correction by Bethe (unpublished) will be used in the following.

Further, $C^{12}+H^2\rightarrow N^{13}+n-0.37\pm0.05$ Mev[9]

and $$N^{13}\rightarrow C^{13}+e^++(e^-)+E_1.$$

E_1 is interpreted as the upper limit of the positron distribution, as no γ-radiation appears in this decay. These relations give $E_1=H^1-n+(2.71\pm0.04)+(0.37\pm0.05)-(1.03)$. A weighted mean of the results on the photodisintegration of the deuteron by Chadwick and

[7] Lyman, Phys. Rev. **51**, 1 (1937).

[8] Cockcroft and Lewis, Proc. Roy. Soc. **A154**, 261 (1936).
[9] Bonner and Brubaker, Phys. Rev. **50**, 308 (1936).

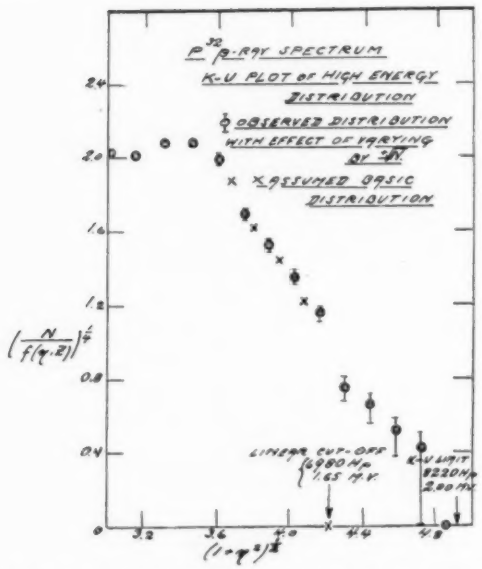

FIG. 5. Konopinski-Uhlenbeck plot of the high energy P^{32} distribution of Fig. 2. The crosses correspond to points on the dotted line of Fig. 2, assumed to be the normal distribution undistorted by probable error.

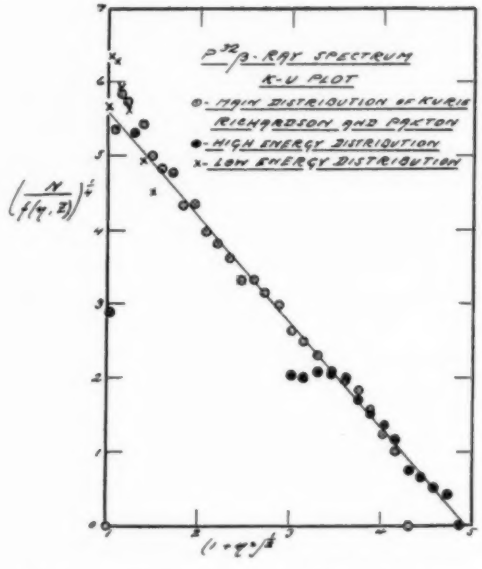

FIG. 6. Konopinski-Uhlenbeck plots of the high energy, low energy and main distributions of P^{32} fitted together in Fig. 3.

Goldhaber[10] and by Feather[11] as recalculated by Bethe and Bacher[12] gives

$$H^2 \rightarrow H^1 + n - 2.20 \pm 0.06 \text{ Mev.}$$

Also $$2H^1 - H^2 = 1.42 \pm 0.03 \text{ Mev,}$$

from the almost identical mass-spectrographic measurements of Bainbridge and Jordan[13] and Aston.[14] These combine to give $n - H^1 = 0.78 \pm 0.07$ Mev which leads to $E_1 = 1.27 \pm 0.10$ Mev as the upper limit of the N^{13} positron spectrum.

For F^{17}

$$O^{16} + H^2 \rightarrow O^{17} + H^1 + 1.91 \pm 0.03 \text{ Mev}^{5}$$
$$O^{16} + H^2 \rightarrow F^{17} + n - 1.8 \pm 0.2 \text{ Mev,}^{15}$$

the excess energy being obtained from the reaction threshold rather than from the neutron energy as in the case of carbon. These, with $F^{17} \rightarrow O^{17} + e^+ + (e^-) + E_2$, give as the upper limit of the positron spectrum from F^{17}:

$$E_2 = 1.90 \pm 0.22 \text{ Mev.}$$

[10] Chadwick and Goldhaber, Proc. Roy. Soc. **A151**, 479 (1935).
[11] Feather, Nature **136**, 467 (1935).
[12] Bethe and Bacher, Rev. Mod. Phys. **8**, 123 (1936).
[13] Bainbridge and Jordan, Phys. Rev. **49**, 883 (1936).
[14] Aston, Nature **137**, 357 (1936).
[15] Newson, Phys. Rev. **48**, 790 (1935).

Expressed in terms of $H\rho$, these limits are 5700 ± 310 $H\rho$ for N^{13} and 7900 ± 750 $H\rho$ for F^{17}. The K-U limits[16] of 6000 $H\rho$ and 9100 $H\rho$ differ from these values by $5\frac{1}{2}$ percent and 15 percent, respectively. These might be compared with the 18 percent difference between the K-U limit and the straight line cutoff for P^{32}. Upper limits[16] of 5600 $H\rho$ for N^{13} and 8150 $H\rho$ for F^{17} which were obtained by inspection from the positron distributions of Kurie, Richardson and Paxton are on the other hand consistent with the disintegration values. Consequently, it appears that these experimental data are not completely consistent with the Fermi-Konopinski-Uhlenbeck theory.

THE LOWER LIMIT OF THE BETA-SPECTRUM OF P^{32}

H. O. W. Richardson[17] in a cloud chamber investigation of the low energy part of the RaE β-spectrum found that there appeared frequency peaks near 500 $H\rho$ and 750 $H\rho$. It was believed worth while to look at the lower limit of the P^{32} β-ray distribution in more detail than had been done previously, to see whether any such rise at

[16] Corrected for magnetic field recalibration.
[17] Richardson, Proc. Roy. Soc. **147**, 442 (1934).

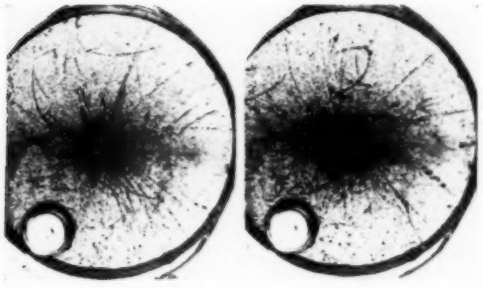

FIG. 7. Exposures representative of those from which the low energy distribution of P^{32} was obtained.

the low energy end of the spectrum might be present in this case.

To do this, a thin collodion film containing some active phosphorus which had stood for $2\frac{1}{2}$ weeks was suspended at the center of the cloud chamber described above. 225 expansions were photographed with the analyzing field reduced to 168 gauss. Conditions were otherwise the same as for the upper limit work. Representative exposures are shown in Fig. 7.

Because β-ray scattering becomes increasingly serious as the energy decreases, all tracks of sufficient length were measured as well as possible in spite of bad curvature changes, in order to prevent distribution distortion from selection criteria. Measurements were made by reprojection and template fitting. A length of track equal to about two-thirds of its diameter was roughly considered as just measurable, until limited further by the chamber radius. This, of course, introduced a variable effective solid angle, increasing with decreasing energy.

The distribution of tracks obtained directly is given by the full line in Fig. 8. The dotted line involves an approximate correction for the variation in solid angle just mentioned. This distribution when adjusted to agree with the main distribution at 875, 1125 and 1375 $H\rho$ is given by the dotted line in Fig. 3. From its contribution to

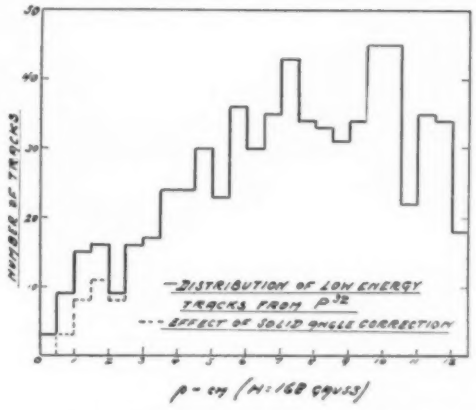

FIG. 8. Distribution of low energy tracks from P^{32}. The dropping off for larger radii is introduced by geometrical discrimination against tracks in that range.

the K-U plot as shown by the crosses on Fig. 6, the distribution appears to go into the origin not quite as rapidly as predicted by the K-U relation. But the difference is within experimental error.

To look into the possibility of there being many tracks of $H\rho$ less than 100, on the first 50 photographs the number of short uncertain tracks originating within one centimeter of the source was compared with the number apparently arising in the gas in the annular region between $1\frac{1}{2}$ and $2\frac{1}{2}$ cm from the source. These numbers were found to be nearly identical, 54 in the first case and 52 in the other, although more secondaries might be expected to come from the region containing the solid material. So there is no indication of a sudden rise in distribution in the neighborhood of the origin such as that found by Richardson in the β-spectrum of Ra E.

I wish to thank Professor E. O. Lawrence, Dr. F. N. D. Kurie and Mr. W. E. Lamb for many discussions concerning this work. This investigation has been aided by grants from the Research Corporation, the Chemical Foundation and the Josiah Macy, Jr. Foundation.

The Radioactive Isotope of Potassium

W. R. SMYTHE AND A. HEMMENDINGER
Norman Bridge Laboratory of Physics, California Institute of Technology, Pasadena, California
(Received November 25, 1936)

By means of a high intensity mass spectrometer we have separated the three isotopes of potassium. Measurements of the radioactivity of the isotopic samples indicate that K^{40} is radioactive. Comparison of the beta-particle emission from the isotopic samples and from KCl shows that K^{40} is responsible for both of the known beta-ray bands.

INTRODUCTION

MUCH work has been done in many laboratories on the radioactivity of potassium since its discovery in 1905 by J. J. Thomson.[1] Since the emission of beta-particles by such a light element is rather surprising, D. Dobrosserdow[2] and others have suggested that it must be due to the widespread existence of "eka-caesium," atomic number 87, as an impurity in ordinary potassium. Many attempts to remove this activity by chemical methods have failed, so this idea seems to have been generally abandoned. The discovery by Aston and Thomson[3] in 1921 that potassium has two isotopes, K^{39} and K^{41}, made it of interest to ascertain which of these is radioactive. G. v. Hevesy and M. Logstrup[4] prepared, by fractional distillation, a specimen slightly heavier and slightly more radioactive than ordinary potassium. They concluded that the active isotope has a mass greater than 39. Elaborate experiments, carried out to find the end product, Ca^{39} or Ca^{41}, of this disintegration, were unsuccessful. This suggested the possibility that a rare isotope K^{40} is responsible for the radioactivity, with the well-known Ca^{40} as the end product. Further measurements with a Geiger-Müller counter by G. v. Hevesy, W. Seith, and M. Pahl[5] on the heavy samples of potassium showed an increase in the radioactivity of 4.43 ± 0.53 percent. A determination of the atomic weight by Hönigschmid and Goubeau[6] indicated an increase in the concentration of K^{41} of 4.2 ± 0.84 percent. They asserted that these results prove the radioactivity of potassium to be due to K^{41} and that they definitely exclude a hypothetical K^{40}. More precise measurements of the atomic weight of potassium[7] and of v. Hevesy's heavy potassium,[8] together with recent measurements of the abundance ratio[9, 10] of K^{39} and K^{41}, raised doubts as to the correctness of v. Hevesy's conclusion:* they showed that the fractional increase in concentration of K^{41} was 10.6 percent. Finally, it was discovered by Nier,[9] and confirmed by Brewer,[10] that K^{40} constitutes about 1 part in 8300 of ordinary potassium. Meanwhile, theoretical reasons, the most cogent of which has already been mentioned, had been advanced for the assignment of the radioactivity to K^{40}. Klemperer[11] and Newman and Walke[12] considered that of the hypothetical group, K^{39}, K^{40}, K^{41}, K^{42}, the only one which could give the observed activity was K^{40}, and that this is consistent with v. Hevesy's observations if the latest values of atomic weights and abundance ratios are used. After the discovery of K^{40} Sitte[13] pointed out that, since Ca^{40} and A^{40} are both well-known stable atoms, if K^{40} atoms can disintegrate with the emission of electrons they should also disintegrate with the emission of positrons. Because careful investigations have failed to detect positrons he concludes that the

[1] J. J. Thomson, Phil. Mag. (6) **10**, 584 (1905).
[2] D. Dobrosserdow, Phys. Ber. **7**, 1414 (1926).
[3] F. W. Aston, Phil. Mag. **42**, 436 (1921).
[4] G. v. Hevesy and M. Logstrup, Zeits. f. anorg. allgem. Chemie **171**, 1 (1928).
[5] G. v. Hevesy, W. Seith and M. Pahl, Zeits. f. physik. Chemie, Bodenstein Festband, 309 (1931).
[6] O. Hönigschmid and Goubeau, Zeits. f. anorg. allgem. Chemie **163**, 93 (1927); **177**, 102 (1928).
[7] G. P. Baxter and W. M. MacNevin, J. Am. Chem. Soc. **55**, 3185 (1933).
[8] G. P. Baxter and C. M. Alter, J. Am. Chem. Soc. **55**, 3270 (1933).
[9] A. O. Nier, Phys. Rev. **48**, 283 (1935).
[10] A. K. Brewer, Phys. Rev. **48**, 640 (1935).
* G. v. Hevesy in a recent article predicts a radioactive isotope, K^{40}. Naturwiss. **23**, 583 (1935).
[11] O. Klemperer, Proc. Roy. Soc. **A148**, 638 (1935).
[12] F. H. Newman and H. J. Walke, Phil. Mag. **19**, 767 (1935).
[13] K. Sitte, Zeits. f. Physik **96**, 593 (1935).

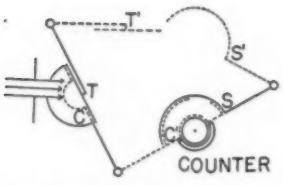

FIG. 1. Solid lines show collector, C, in collecting position and screen, S, in counting position for R_0. C' and S show collector and screen in counting position for R.

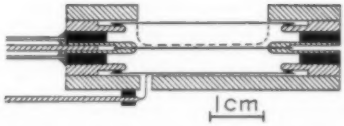

FIG. 2. Longitudinal section of Geiger counter showing amber insulation in black and brass parts cross hatched. The dotted line outlines the exposed area of aluminum foil wall of the counting region. A cross section of the counter appears in Fig. 1.

experimental evidence is against the radioactivity of K^{40}, and suggests that some other unknown isotope, probably K^{43}, is responsible. Clearly, only the determination of the radioactivity of each isotope, separately, can answer this question conclusively. The only known method of preparing a pure isotopic sample from a group of three or more is that of mass spectroscopy.

APPARATUS

Of these instruments only the high intensity mass spectrometer described by Smythe, Rumbaugh, and West[14] gives sufficient intensity. Minor changes have been made in the instrument. The heating elements now consist of tungsten helices enclosed in MgO tubes,[15] constructed by West. The Kunsman K^+ ion source is now prepared by fusing the nitrates of potassium and iron together and igniting. The resultant oxide mixture is reduced in hydrogen, pounded into the grooves in the source block until it forms a layer of solid metal, placed in the spectrometer and is again reduced in hydrogen. After the spectrometer is evacuated the source is outgassed for a day before using. An automatic voltage regulator, which controls the field current of the generator supplying the accelerating potential for the ions, keeps the voltage, usually about 5000, constant within 0.2 percent. The only attention required by the spectrometer after it is set for collecting a given mass is the adjustment every eight hours of the source heater current and the magnetic field current, and the renewal of the liquid air on the mercury trap.

The collecting end of the apparatus has been entirely changed. K^+ ions have a very destructive effect on any target upon which they impinge, so that not only the potassium but also the material of the target is sputtered on all neighboring objects. To collect the potassium we set a tungsten target at an angle such that few of the sputtered atoms would retrace the path along which they came as ions, and surrounded it by a box through a hole in which the positive rays entered, as shown in Fig. 1.

A Geiger-Müller counter seemed to be the most satisfactory instrument for measuring the emitted beta-particles. Four requirements are imposed upon this counter. First, to minimize its background its volume must be small. Second, to avoid absorption of beta-particles the walls must be thin. Third, the counter must subtend a large solid angle at the collector. Fourth, to avoid possible contamination the collector should be handled as little as possible, preferably not at all. After a few unsuccessful experiments with external counters we followed Mr. Harper's suggestion that we make a counter which is not vacuum-tight, and place it inside the collecting chamber, admitting air to the whole apparatus to adjust the pressure in the counter.

The design of the thin-walled counter is shown in Fig. 2. The cylinder, 3.5 cm long, was made by wrapping 0.0254 mm aluminum foil around a mandrel 0.93 cm in diameter and fastening the overlapping portions with Duco cement. The central wire is steel, 0.254 mm in diameter. The cylinder is mounted in a brass tube which is cut away on one side to expose the aluminum. The mounting is designed to shield electrostatically the sharp ends of the aluminum and to guard it against leakage from the wire across the amber insulators. The background of all counters not so constructed

[14] W. R. Smythe, L. H. Rumbaugh and S. S. West, Phys. Rev. **45**, 724 (1934).
[15] W. H. Swanger and F. R. Caldwell, Nat. Bur. Stand. J. Research **6**, 1131 (1931).

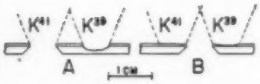

FIG. 3. *A* shows the destructive action of 13.5 mg of 5000 volt K^{39} ions striking a brass slit faced with 0.15 mm of molybdenum. The maximum penetration from the surface is 1 mm. *B* shows the action of 20.4 mg of the same ions striking a brass slit faced with 0.5 mm of tungsten. The maximum penetration from the surface is 0.37 mm.

was large and unsteady, but that of the counter used is extremely steady. A lead box with walls 5 cm thick and open at one end was constructed to slide over the whole collecting chamber. The massive iron pole-pieces of the spectrometer formed the sixth side of the box. The background of the counter was 1 count per minute when surrounded by the lead and 3 counts per minute when not. This is just the ratio of cosmic-ray ionization to total ionization in this laboratory and indicates that the counter background is an absolute minimum.

The circuit devised by Neher and Harper[16] for coupling the counter to the amplifier proved to be of great value, for it requires no especially good insulation of the counter.

The transfer of the collected sample from the collecting position to the counting position is accomplished by the arrangement shown in Fig. 1. The collector *C*, covering the face of the target *T*, is a half-cylindrical box, partially closed at the ends, with a hole through which the positive rays can enter. Except for the small amount escaping through this hole and the ends, and adhering to the target outside of the bombarded area, all the potassium impinging on *T* is collected on the inside of the box. During the collection the counter is protected by a cylindrical screen, *S*. The screen, target, and collector may be turned, in this order, to the position shown by the dotted lines. The screen may then be turned back to cover the hole in the collector. Thus all measurements are independent of the contamination of the walls of the collecting chamber. The procedure for investigating a single isotope is as follows: after the apparatus has been evacuated long enough to remove the moisture, air is admitted to 5.6 cm pressure and counts are made alternately on *S* and *C* for

[16] H. V. Neher and W. W. Harper, Phys. Rev. **49**, 940 (1936).

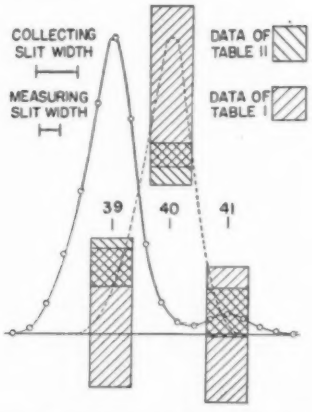

FIG. 4. The solid curve, giving the collecting current plotted against mass, is measured with a 2 mm slit and shows the resolution maintained during the collection of all samples except the K^{39} sample of Table II. The width of the cross-hatched areas shows the positions of the collecting slit. The ordinates of the center of the cross-hatched areas are the measured activities, and the lengths are twice the probable errors, all reduced to samples of the same size. All scales of ordinates are arbitrary.

one-half hour intervals until at least 400 counts have been made on each; the apparatus is then evacuated and the sample collected on *C*; air is admitted and pumped out several times until the potassium, which always collects on the walls of the apparatus near the source, is so oxidized that it no longer removes oxygen from the air rapidly (the counter would never operate stably without oxygen); alternate counts are then made on the collector and screen as before. During a set of counts the counter is operated at a fixed voltage and pressure. The collected sample is always mixed with tungsten sputtered from the target. There seems to be no easy way of eliminating this sputtering without adopting an entirely different collecting technique.

When collecting, a slit which is set in the focal plane of the spectrometer 3 mm in front of the hole in the collector is opened to 4 mm. The destructive effect of the intense positive ion beam on the slit material is shown in Fig. 3. The slit edges were originally of 1.6 mm beveled brass. The ion beam widened a 4 mm slit to 5.5 mm. The brass was then inlaid with 0.15 mm molybdenum, and 4 mg of K^{39} ions drilled a hole through the molybdenum and 1 mm into the brass. Tungsten proved to be more resistant under ion bombardment: a hole 4×6 mm in

area and with a maximum depth of 0.37 mm was made in tungsten by 20.4 mg of K^{39} ions. Thus it was necessary to replace the tungsten slit edges after each run. The sputtering of the target was less severe, for the beam is there spread over an area of 17×10 mm. For these 5000 volt ions the mass of the sputtered tungsten was approximately five times that of the impinging potassium.

All collections were made at good resolving power, except the last item in Table II. The curve of positive ion current plotted against atomic weight, taken with a focal plane slit 2 mm wide, is shown in Fig. 4. The usual collecting current, with a 4 mm slit, is about 0.12 ma. Although greater collecting currents are easily obtained by increasing the source temperature, this usually broadens the peak and greatly shortens the life of the source. The maximum amount of potassium that can be collected in one run is not known: at the end of the run, one week long, in which the 20.4 mg sample was collected the collecting current was still near its maximum, the resolving power was good, and there was no sign of exhaustion of the source.

Measurements

Two complete sets of measurements were made on potassium. The first set was completed without opening the apparatus, with each sample of potassium deposited on top of the previous one, so that the count was cumulative. The results are shown in Table I. The *counting ratio* R in each case is the ratio of collector-counts to screen-counts. The error is computed in the standard way:[17] the probable error in N counts is $0.675\sqrt{N}$; the probable error in R $(=N_2/N_1)$ is $0.675R(1/N_1+1/N_2)^{\frac{1}{2}}$.

In the second set of measurements larger deposits of each isotope were made. This involved opening and cleaning the apparatus and renewing the source between runs. The results are shown in Table II. Unfortunately the resolving power went bad several times during the collection of the K^{39} sample, perhaps because a different batch of emitter and new heater insulation were used, so that it is contaminated with an unknown amount of K^{40}.

If all the collector current were due to K^+ ions and if all these ions, after neutralization, were deposited on the collector, the factor c in Tables I and II would be one. Somewhat indirect measurements indicate that from 5 percent to 15 percent of the collector current is due to the escape of secondary electrons. A visual inspection of the deposit on the collector and target indicates that from 60 percent to 80 percent of the potassium striking the target adheres to the collector. Thus the factor c appears to lie between 0.5 and 0.75.

The data of Table III were obtained from two counts made on a nickel sheet when it was coated with a thin layer of KCl and the second after this had been washed off with distilled water.

Calculations and Results

The *activity* of each sample is defined as $R-R_0$, where R_0 and R are the counting ratios taken before and after deposition on the collector. The significance of $R-R_0$ can be seen from the following:

Let N = the background of the counter,
N_1 = the count due to the screen,
N_2 = the count due to the collector,
and N_3 = the count due to the deposit.

Then $R_0=(N+N_2)/(N+N_1)$, $R=(N+N_2+N_3)/(N+N_1)$, and these ratios are independent of the voltage of the counter. The difference,

TABLE I. *β-particle counts from the collector as deposits of K^{41}, K^{40} and K^{39} were added successively.*

Collector Deposit	Counting Ratio	Probable Error
No deposit	1.04	0.05
(1) 4.35 c/14 mg K^{41}	1.04	0.05
(2) 4.06 c/8300 mg K^{40}+(1)	1.28	0.06
(3) 4.7 c/1 mg K^{39}+(1)+(2)	1.30	0.06

TABLE II. *β-ray counts from separate deposits of K^{41}, K^{40} and K^{39}.*

Collector Deposit	Counting Ratio	Probable Error
No deposit	1.07	0.05
13.4 c/14 mg K^{41}	1.14	0.06
No deposit	1.10	0.05
20.4 c/8300 mg K^{40}	1.93	0.08
No deposit	1.03	0.05
13.6 c/1 mg K^{39}	1.26	0.06

[17] H. Bateman, Phil. Mag. **20**, 704 (1910).

TABLE III. *β-ray counts from natural potassium.*

COLLECTOR DEPOSIT	COUNTING RATIO	PROBABLE ERROR
67.2 mg KCl on Ni foil	3.22	0.12
Clean Ni foil	1.03	0.05

$R-R_0=N_3/(N+N_1)$, is thus proportional to the number of beta-particles emitted by the deposit.

The data of Tables I and II are presented graphically in Fig. 4.

There are 32.9 mg of K^{39} in 67.2 mg of KCl. The activity of this sample, after correcting for absorption of both bands of the beta-particles in KCl on the assumption that the mass absorption coefficients are the same as for aluminum,[18] is 2.58. The correction for absorption in tungsten in Tables I and II is quite negligible. Measurements by Bocciarelli[19] show that 60 percent of the emitted beta-rays lie in the low energy band and the remainder in the high energy band. Taking the weighted mean of the measured activity of K^{40} from Tables I and II, reducing to a standard sample of 20 mg, and comparing with the activity to be expected from the measurements of Table III, also reduced to 20 mg, we have, for the three possible assumptions as to which bands belong to K^{40}, the results shown in Table IV. This clearly indicates that K^{40} is responsible for the entire known activity of potassium.

TABLE IV. *Comparison of the measured activity of K^{40} with that to be expected upon various hypotheses.*

HYPOTHESIS	MEASURED ACTIVITY $c=0.75$	MEASURED ACTIVITY $c=0.5$	EXPECTED ACTIVITY
K^{40} emits high energy band	1.08	1.62	0.63
K^{40} emits low energy band	1.08	1.62	0.94
K^{40} emits both bands	1.08	1.62	1.57

ACKNOWLEDGMENTS

We wish to acknowledge our debt to those who have worked on this problem in its earlier stages, particularly Dr. West, and to Mr. Harper, who lent us his amplifier and assisted in some of the counter work. We are grateful also for the assistance in the laboratory of Mr. R. H. Mansfield.

[18] N. R. Campbell and A. Wood, Proc. Camb. Phil. Soc. **14**, 15 (1907).
[19] D. Bocciarelli, R. C. Accad. Lincei (6) **17**, 830 (1933).

FEBRUARY 1, 1937 PHYSICAL REVIEW VOLUME 51

The Disintegration of Beryllium by Protons*

J. S. ALLEN
Ryerson Physical Laboratory, University of Chicago, Chicago, Illinois
(Received October 24, 1936)

The disintegration of Be by protons of energies from 45 to 125 kv has been studied. The yield curve for a thick target has been determined and the ratio of the number of alpha-particles and deuterons ejected from the target has been determined for various voltages. The ratio was very close to unity. The ranges of both groups of particles were found to be 7.1 mm. From the energy relations the mass of Be^8 was found to be 8.0074. The experimental value of the effective area for collision was found to be of the same magnitude as that predicted by Gamow's theory of the penetration of a potential barrier by protons having zero angular momentum.

ALTHOUGH much work has been done on the disintegration of Be by protons, it seemed worth while to investigate the two possible reactions in order to determine their relative probability of occurrence. According to Oliphant, Rutherford and Kempton,[1] the two reactions are:

$$_4Be^9+{}_1H^1={}_3Li^6+{}_2He^4, \quad (1)$$

$$_4Be^9+{}_1H^1={}_4Be^8+{}_1H^2. \quad (2)$$

They found that the H^2 and the He^4 particles

* A dissertation submitted to the faculty of the division of the physical sciences in candidacy for the degree of Doctor of Philosophy. Private edition, distributed by the University of Chicago Libraries, Chicago, Illinois.

[1] Oliphant, Rutherford and Kempton, Proc. Roy. Soc. **A150**, 241 (1935).

were present at all bombarding energies and were in the ratio of 4 to 3 singly charged to doubly charged particles. The observed range of both groups was 7.4 mm of air. Neuert[2] investigated the same reactions by means of a Wilson cloud chamber and found a group of particles with a range of 7.5 mm of air. He concluded that they were alpha-particles and that the second reaction was improbable.

Another object of this research was to determine the form of the yield curve for thick and thin targets and to find the effective area for collision from these data. The excitation curve was compared with that predicted from Gamow's theory of the penetration of the potential barrier around the Be nucleus by protons of zero angular momentum.

Apparatus and Method

A. Production of protons

The proton source was of the low voltage arc type similar to that used by Tuve, Hafstad and Dahl.[3] The ions were drawn from the arc by a probe at a potential 3 kv negative with respect to the metal body of the arc space. This divergent beam was focused by a cylindrical lens having a potential of 10 kv. Total ion currents of the order of 40 microamperes were obtained. The proton current was about one-third of the total ion current.

The accelerating tube had two sections with cylindrical electrodes 3.5 cm in diameter and 11.6 cm long with a separation of 2.5 cm. The system was evacuated by two stages of oil diffusion pumps. The tube was operated at a pressure of 5×10^{-5} mm of Hg.

The high potential source consisted of a 200 kv transformer with half-wave rectification. The output of this transformer as well as that of the proton source was filtered with condensers so that the energy spread of the proton beam was not more than a few percent. The high potential source was calibrated both by means of a spark-gap and by the energy of the protons as measured in the magnetic field.

B. Target assembly

A diagram of the target assembly is given in Fig. 1. The proton beam was bent through 90° in the arc of a circle of 9.2 cm radius and its position was limited by two 1.0 cm holes at the edges of the magnetic field. The strength of the magnetic field was measured with a Bi spiral previously calibrated at the National Bureau of Standards. The field was found to be quite uniform out to the edges of the pole pieces. The fact that this same target assembly and magnetic field had been used by H. D. Doolittle[4] for a study of the disintegration of Li by protons furnished an additional check on these measurements. The targets of metallic Be were supported at an angle of 45° with the proton beam.

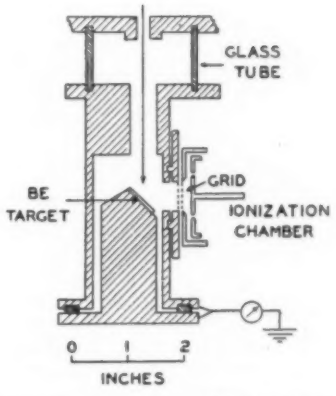

Fig. 1. The target assembly and ionization chamber.

The window for allowing the disintegration particles to pass into the ionization chamber was supported on a thin phosphor-bronze sheet having 71 holes, each 0.046 cm in diameter. The windows were made in the following manner. A drop of a mixture of 50 percent Merck flexible collodion and 50 percent amyl acetate was placed upon a surface of distilled water. After the film had dried for 15 minutes it was removed on a wire frame and dried at a temperature of 100°C. The films were waxed to the grid with paraffin. In this manner windows having an air equivalent of about 2 mm were prepared.

C. Amplifier and measurement of proton current

A four-stage linear amplifier using Dunning's[5] circuit was utilized. The ionization chamber was 1.5 cm in diameter and 2.5 mm deep. In order to

[2] Neuert, Physik. Zeits. **36**, 629 (1935).
[3] Tuve, Hafstad and Dahl, Phys. Rev. **48**, 241 (1935).
[4] H. D. Doolittle, Phys. Rev. **49**, 779 (1936).
[5] Dunning, Rev. Sci. Inst. **5**, 387 (1934).

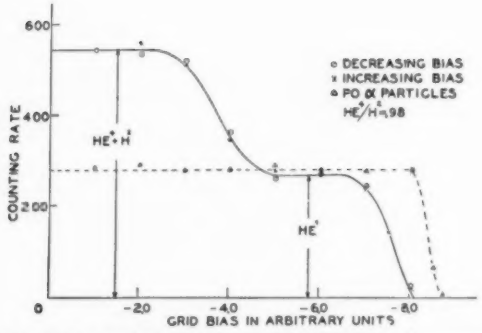

FIG. 2. The variation of the counting rate with thyratron grid bias for protons having an energy of 104 kv.

insure a uniform field between the collecting electrode and the grid the front of the chamber was covered with a metal grid. The particles were recorded by means of a thyratron scale-of-two counting circuit and a Cenco impulse counter. The magnitude of the pulses could be observed visually by means of a cathode-ray oscillograph.

The proton current was measured by a micro-ammeter which could be read to 0.05 micro-ampere. Readings were taken every half-minute and the results averaged to give the proton current. The currents ranged from 1 to 6 micro-amperes.

RESULTS AND CONCLUSIONS

A. Range measurements

In order to remove the uncertainty in the range measurements introduced by the use of a grid in front of the ionization chamber, it was calibrated with Po alpha-particles. The air equivalent of the window was determined for Po alpha-particles about one cm from the end of their range. Using a window of 3.5 mm air equivalent, the counting rate was determined as the ionization chamber was moved away from the window. For protons of 80 kv energy the range was 7.1 mm. There was no indication of a group of particles with another range.

B. Energy relations

The energy released in reaction (1) is given by:[6]

$$9.0138+1.0081=6.0163+4.0034+E.$$

From this relation E is 0.0022 mass unit and the velocity of the ejected alpha-particle is 7.7×10^8 cm/sec. From the data of Blackett and Lees[7] this corresponds to a range of 6.9 mm in air. The observed value of 7.1 mm is seen to be in good agreement with that predicted from nuclear masses.

According to the relation derived by Bethe,[8] the range of a particle of mass M, and charge Z, is proportional to M/Z^2. Thus, a deuteron should have twice the range of an alpha-particle of the same velocity. Assuming this relation to hold, the velocity of the deuterons ejected in reaction (2) is equal to 4.4×10^8 cm/sec. This corresponds to a release of energy equivalent to 0.0003 mass unit. The mass of Be^8 is then given by:

$$Be^8=9.0138+1.0081-2.0142-0.0003,$$
$$Be^8=8.0074.$$

This value is somewhat higher than the mass of 8.0071 determined by Oliphant, Rutherford and Kempton[1] from the same nuclear reaction.

C. Relative number of $_2He^4$ and $_1H^2$ particles

Since an alpha-particle produces many more ions along its path in air than does a deuteron of the same velocity, if both reactions (1) and (2) exist, two types of pulses should appear on the oscillograph. It was found that for all proton energies there were two types, one about twice the height of the other.

In order to determine the relative number of the two groups, a curve shown in Fig. 2 was plotted between the number of particles and the negative grid bias on the thyratrons. Since the amplification of the recording circuit was approximately linear, the amount of ionization produced by the passage of a particle through the ionization chamber was proportional to the height of the pulses. The counting rate decreased

TABLE I. *Ratio of He^4/H^2 at various voltages.*

V	He^4/H^2	NUMBER COUNTED
47,000	0.9	200
66,000	0.7	1000
81,000	0.8	3000
93,000	0.8	10000
105,000	1.2	5000
116,000	1.0	8000

[6] The values of the nuclear masses used in this paper are as given by Oliphant in the paper by Cockcroft and Lewis, Proc. Roy. Soc. London **A154**, 261 (1936).

[7] Blackett and Lees, Proc. Roy. Soc. **A134**, 663 (1932).

[8] Bethe, Ann. d. Physik **5**, 325 (1930).

rapidly whenever the grid bias was slightly greater than the height of a particular type of pulse. Thus, the solid curve represents two groups of particles, one producing about twice the ionization of the other. The former must be alpha-particles since they produce about the same ionization as Po alpha-particles near the end of their range as indicated by the dotted curve. From curves similar to Fig. 2 the proper grid bias for recording just alpha-particles or both groups was determined and observations were made on the relative number in the two groups. Table I gives the relative numbers at various proton energies and also the total number counted for any given voltage. The ratio He^4/H^2 appears to increase with the energy of the protons. The increase at 47 kv may be due to the rather large probable error in the determination of the counting rate since only about 200 particles were recorded. From 1000 to 10,000 particles were recorded for each of the other two ratios. The data seem to suggest that the ratio approaches unity at higher proton energies.

At first it was thought that the two types of pulses were due to two particles entering the ionization chamber within the resolving time of the amplifier. Due to the small time constants of the circuit, this was unlikely, but it was checked by reading at very slow and very fast counting rates. The ratio did not change appreciably with the counting rate. This proved that the two types of reaction actually did occur.

D. Excitation curve

To obtain the excitation curve the grid bias was adjusted so that both groups of particles were recorded. Due to the appearance of a brown carbon deposit, the targets were not used for more than 10 minutes. With the exception of the points at the two lowest voltages, 10,000 particles were counted for each point. Since there were two grids between the target and the ionization chamber, and since they were separated by only 2.1 cm, there was considerable uncertainty in the calculation of the solid angle subtended by the window. In Fig. 3 the excitation curve for a thick target is shown.

The shape of the curve is similar to that for the disintegration of Li by protons. Disintegrations were detected at 46 kv. From the curve

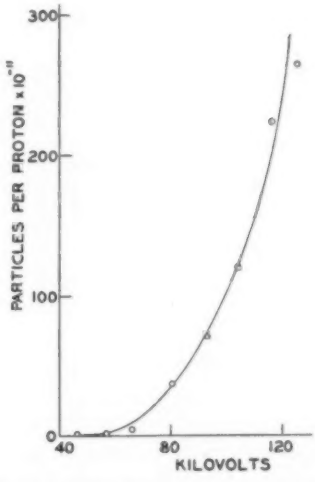

FIG. 3. The excitation curve for a thick target of beryllium. Thyratron grid bias set for the recording of both groups of particles.

Kv	47	57	66	81	93	104	116	125
Particles per proton	0.3×10^{-11}	1.6	4.6	37	71	120	224	264

the threshold voltage for disintegration to occur is at about 45 kv. No disintegration was detected below this voltage.

A thin film yield curve was determined by differentiation of the thick target yield curve in a manner similar to that used by Herb, Parkinson and Kerst.[9] However, the yield was determined for a film of sufficient thickness to reduce the energy of the protons by 5 kv. According to the work of Blackett and Lees[7] and Mano,[10] the range of protons in air is given approximately by $R=KV^{0.7}$ where R is the range in cm, K is a constant, and V is the energy of the protons in electron volts. This relation holds only for energies from 45 to 130 kv. Since there are no data concerning the range of protons of various energies in Be, this relation was assumed to hold instead of the usual $R=KV^{1.5}$.

According to Gamow's theory the probability of disintegration by protons for a thin target is proportional to:

$$(1/E_p)\exp -(e^2/\hbar)(2m_p/E_p)^{\frac{1}{2}}Z(2U_0-\sin 2U_0),$$

where $\cos^2 U_0=r_0E_p/Ze^2$.

E_p and m_p are the energy and mass of the

[9] Herb, Parkinson and Kerst, Phys. Rev. **48**, 118 (1935).
[10] Mano, J. de phys et rad. **5**, 628 (1934).

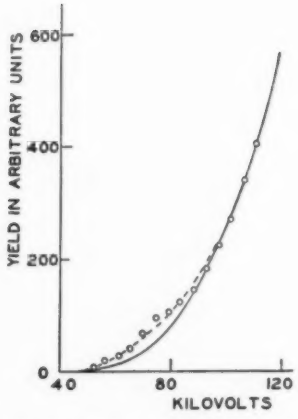

FIG. 4. Excitation curve for a thin target of beryllium. Dash line, experimental curve; solid line, Gamow's theory.

protons, e is the charge of the electron, Z is the atomic number of the bombarded nucleus, and r_0 is the nuclear radius. The nuclear radius was assumed to be 5×10^{-13} cm. When the numerical values of the constants have been substituted into the equation above the yield is given to a close approximation by:

$$Y=\frac{C}{V}\exp 3.84\times10^{3}\cdot V^{-\frac{1}{2}},$$

where V is the energy of the protons in electron-volts. In Fig. 4 the thin target data are compared with the curve given by the equation above. The experimental values of the proton energies have been multiplied by 0.9 to correct for the recoil motion. The value of the constant C, was adjusted so that the experimental and theoretical curves coincided at 110 kv. For low energies the experimental yield rises more rapidly than does the theoretical curve. This discrepancy is made still worse if the range of the protons is assumed to be given by $R=KV^{1.5}$.

The collision cross section σ for either reaction may be determined from the relation $Y=RN\sigma$ where Y is the thick target yield at a given voltage, R the range of the protons in the target and N is the number of Be nuclei per cc of the target. From the data of Blackett and Lees[7] the range of a proton of 100 kv in air is 0.15 cm. The atomic stopping power[11] of Be relative to air is about 0.75. From this information we find that protons of 100 kv have a range of 0.81×10^{-4} cm in Be. At this energy Y is 1.0×10^{-9} and N is 1.24×10^{23}. The value of σ is then 5×10^{-29} cm^2. The value of σ calculated in a similar manner from the thin target data is 25×10^{-29} cm^2.

The effective cross section for a thin target may be calculated from Gamow's equation. It is then given by:

$$\sigma=\frac{\pi\hbar^2}{2m_pE_p}\exp -3.84\times10^{3}\cdot V_p^{-\frac{1}{2}}\text{ cm}^2,$$

where E_p is the energy of the protons in ergs and V_p is the energy in electron volts. The value obtained at 100 kv is 3.2×10^{-29} cm^2. Since σ increases rapidly with the energy of the protons, the thin target value should be somewhat higher than that for thick films. The experimental results agree with this prediction, but the thin target value is about eight times that predicted by Gamow's theory. This discrepancy may be due to the use of an incorrect range relation. The value of the thin target σ would be affected more by an error in this relation than the thick target value. The disagreement may also be due to an error in the calculation of the solid angle although it is doubtful whether this could cause an error greater than 20 percent. Finally, there is some doubt as to how accurately the cross section is expressed by Gamow's relation. However, we may conclude that the effective cross section is between 5 and 25×10^{-29} cm^2.

In conclusion, the author wishes to express his appreciation to Professors A. J. Dempster and S. K. Allison for their valuable advice and discussions throughout the course of this work.

[11] Rutherford, Chadwick and Ellis, *Radiations from Radioactive Substances*, pp. 97–100.

A Note on the Capture of Slow Neutrons in Hydrogenous Substances

WILLIS E. LAMB, JR.
Department of Physics, University of California, Berkeley, California

(Received November 9, 1936)

A study is made of the effect of the chemical binding of the proton in hydrogenous substances on the capture of slow neutrons. It is shown that in contrast with the scattering cross section, no change is made by this in the radiative capture cross section. An estimate shows that the process of radiationless capture made possible by the binding will not play an important role.

INTRODUCTION

MUCH information about the nature of nuclear forces has been derived from experiments on the behavior of slow neutrons in substances containing hydrogen, but the interpretation of this work has been somewhat complicated by the fact that the protons in the materials available are not free, but are chemically bound, often having a zero point vibrational energy many times the kinetic energy of the neutron. Fermi[1] has studied the effect of the chemical binding of a single proton on its scattering of slow neutrons. He found that in the limit of zero neutron velocity, the scattering cross section becomes four times larger than the corresponding value for a free proton, as given by Bethe and Peierls and Wigner.[2]

It will be the purpose of the present work to examine the effect of the binding of the proton on processes of radiative and radiationless capture of neutrons in hydrogenous substances.

I. RADIATIVE CAPTURE OF NEUTRONS BY BOUND PROTONS

The important process for the capture of neutrons by protons is believed to be one of magnetic dipole radiation from a singlet S level of the continuum to the triplet S ground state of the deuteron. The theory of this process was also developed by Fermi,[3] but the effect of the chemical binding of the proton was not considered. As his derivation explicitly involved the value of the scattering cross section, one might possibly expect a changed capture cross section because the proton is not free. Since the experimental data on this capture radiation ought to give valuable information about both the magnitude and the sign of the singlet energy, it seems worth while to show how it is that the binding brings about no difference in the rate of combination.

We shall first outline, and refute, an argument which might lead one to anticipate a change. According to the theory of Fermi, the capture cross section varies inversely with the relative velocity of neutron and proton. Thus

$$\sigma_c = A/v_{\text{rel.}} \tag{1}$$

or A/v_0 if the free proton is at rest, where v_0 is the velocity of the incident neutron. This is simply the analytical expression of the fact that the chance of capture increases inversely with the time that the neutron spends in the vicinity of the proton. Now a bound proton does not have a definite velocity: from its wave function one can calculate the probability amplitude $\varphi(\mathbf{p})$ in momentum space and the distribution of momenta

$$N(\mathbf{p})d\mathbf{p} = |\varphi(\mathbf{p})|^2 d\mathbf{p}. \tag{2}$$

Let $\pi(\mathbf{v})$ be the corresponding distribution in velocity space. One has

$$\int \pi(\mathbf{v})d\mathbf{v} = 1. \tag{3}$$

Now consider those protons which have a velocity $\mathbf{v}$ in a certain interval $d\mathbf{v}$. These protons and the neutron have a relative velocity

$$v_{\text{rel.}} = |\mathbf{v} - \mathbf{v}_0| \tag{4}$$

[1] E. Fermi, Consiglio Nazionale delle Ricerche, Vol. II, No. 1–2 (1936).
[2] See, for example, the report of H. A. Bethe and R. F. Bacher, Rev. Mod. Phys. **8**, 82 (1936).
[3] E. Fermi, Phys. Rev. **48**, 570 (1935), also reference 1 or 2, §17.

and hence should contribute an amount

$$A(\pi(\mathbf{v})d\mathbf{v})/(|\mathbf{v}-\mathbf{v}_0|) \tag{5}$$

to the total cross section, which is then

$$\sigma_c = A\int \frac{\pi(\mathbf{v})d\mathbf{v}}{|\mathbf{v}-\mathbf{v}_0|}. \tag{6}$$

The integration gives A/v_0 if v_0 is great compared to the velocities which are likely in $\pi(\mathbf{v})$, but as the neutron's energy is lowered, one gets marked deviations from the A/v_0 law, and for $v_0=0$, a constant value

$$\sigma_c = A\int \frac{\pi(\mathbf{v})d\mathbf{v}}{|\mathbf{v}|} = \frac{A}{v_a}, \tag{7}$$

where v_a is an average proton velocity, corresponding roughly to the zero point energy. This result is not in agreement with several experiments[4] which speak strongly for a $1/v_0$ absorption by protons.

The error in the picture of the process which leads to the above calculation is that one has neglected the coupling between the various probability amplitudes of velocity which is introduced by the binding. Clearly, if one were dealing with a free proton described by the above wave packet, the calculation would have been made correctly. But long before a slow neutron could pass such a packet, complete spreading would have occurred, and the proton would then no longer be localized within a region of molecular size. A bound proton can at any time be represented by such a wave packet of plane waves, but only over a short interval, for actually the proton will remain localized. This is due to the chemical binding which causes it to move back and forth, i.e., there is interference between the various components of velocity. When a slow neutron passes such a proton, one might say that the chance of capture during a half-oscillation of the proton is proportional to $1/v_a$, but since the proton will have time for roughly v_a/v_0 such trips before the neutron wave function changes much, one will again expect a capture inversely proportional to v_0. But whether or not a numerical factor has to be introduced into the answer must be determined from the quantum mechanical calculation.

In order to make the calculation, we will first take the proton binding to be a fixed spherical trough $U(P)$ of depth U and radius b. Let $w_n(P)$ be the eigenfunctions in this trough, and let the proton be taken initially in the ground state $n=0$. The deuteron formed in the reaction may be in any of the states $w_m(R)$,[5] where R is its center of mass.

The initial state of the system has a wave function $\psi_0(N, P)$ which as Fermi[1] has shown is highly approximated to by

$$\psi_0(N, P) = w_1(P)\chi(r), \tag{8}$$

where $\mathbf{r}=\mathbf{N}-\mathbf{P}$, and $\chi(r)$ is the wave function for the relative motion in a singlet state met in the theory of scattering, and is normalized to be unity for $a\ll r\ll b$, where a is the radius of the potential $V(r)$. The final state has a wave function of the form

$$\psi_f = w_m(R)\chi_0(r), \tag{9}$$

where $\chi_0(r)$ corresponds to the triplet ground state of the deuteron. Transitions are induced by the coupling of the magnetic moments of the particles with the radiation field which is made possible by the spin-orbit interaction due to the admixture of a small amount of Heisenberg force in $V(r)$. The operator involved is

$$W = \boldsymbol{\mu}_P\cdot\mathbf{H}(P)+\boldsymbol{\mu}_N\cdot\mathbf{H}(N)$$
$$= \mu_0\{g_P\boldsymbol{\sigma}_P\cdot\mathbf{H}(P)+g_N\boldsymbol{\sigma}_N\cdot\mathbf{H}(N)\}, \tag{10}$$

where g_N, and g_P are the Landé factors for neutron and proton, $\mu_0=e\hbar/2Mc$ is the heavy Bohr magneton, $M=$ the proton mass, and the $\boldsymbol{\sigma}$ are Pauli spin matrices. For the magnetic field $\mathbf{H}$, we may take the expansion[6]

$$\mathbf{H}(x, t) = i(4\pi c^2)^{\frac{1}{2}}\sum_s[\mathbf{k}_s\times\mathbf{e}_s]\{q_s\exp i(\mathbf{k}_s\cdot\mathbf{x}-\nu_s t)$$
$$-q_s^*\exp -i(\mathbf{k}_s\cdot\mathbf{x}-\nu_s t)\}, \tag{11}$$

where $\nu_s=ck_s$ is the circular frequency, $\mathbf{e}_s$ is the polarization vector of the sth component of the radiation field, and q_s, q_s^* are matrices which

[4] For example, W. F. Libby and E. A. Long, Phys. Rev. **50**, 575 (1936).

[5] For a more general potential $U(P)$, one will have different eigenfunctions for the state m of the deuteron, but the result obtained is the same.

[6] Heitler, *Quantum Theory of Radiation*, p. 70.

act on the occupation numbers n_s. As we are interested in an emission process only, we get contributions from each s just from

$$(1_s|q_s|0_s)=(\hbar/2\nu_s)^{\frac{1}{2}} \tag{12}$$

and hence

$$(1_s|W|0_s)=i(2\pi\hbar c^2/\nu_s)^{\frac{1}{2}}[\mathbf{k}_s\times\mathbf{e}_s]$$
$$\cdot(\boldsymbol{\mu}_P\exp i\mathbf{k}_s\cdot\mathbf{P}+\boldsymbol{\mu}_N\exp+i\mathbf{k}_s\cdot\mathbf{N}), \tag{13}$$
$$\mathbf{P}=\mathbf{R}+\tfrac{1}{2}\mathbf{r},\quad \mathbf{N}=\mathbf{R}-\tfrac{1}{2}\mathbf{r}. \tag{14}$$

Since $k_s/\alpha\ll 1$, the matrix element between the initial and final states is

$$(f1_s|W|0_s0)=i\left(\frac{2\pi\hbar c^2}{\nu_s}\right)^{\frac{1}{2}}\int d\tau\psi_f^*$$
$$\times\{\mathbf{k}_s\times\mathbf{e}_s\cdot(\boldsymbol{\mu}_P+\boldsymbol{\mu}_N)\}\exp i\mathbf{k}_s\cdot\mathbf{R}\psi_0. \tag{15}$$

After a calculation similar to that given in the report of Bethe and Bacher (reference 2, page 128), one gets for the cross section for a capture which leaves the deuteron in state m

$$\sigma_m=\frac{\nu_s^2}{4v_0\hbar c^3}\frac{1}{\alpha\beta^2}\left(\frac{\alpha-\beta}{\alpha}\right)^2\mu_0^2(g_P-g_N)^2$$
$$\times\left|\int w_m^*\exp i\mathbf{k}_s\cdot\mathbf{R}w_0d\mathbf{R}\right|^2, \tag{16}$$

where β and α are the wave numbers for singlet and triplet states. This must be summed over all possible states m of the resultant deuteron. As the large values of m contribute very little, we may neglect the variation of ν_s with m, and find with the help of the completeness relation that

$$\sigma=\frac{2\pi\hbar\nu^3e^2}{M^2c^5v_0}\frac{|g_P-g_N|^2}{\alpha\beta^2}\left(\frac{\alpha-\beta}{\alpha}\right)^2. \tag{17}$$

This is in agreement with the result for a free proton.

The above proof needs some modifications if the proton is initially bound to a partner of comparable mass, but the capture cross section per proton turns out to be unaltered. Thus we see that the $1/v_0$ law indeed confirmed, and that there is no numerical factor to be introduced on account of the binding.

In fact, the $1/v_0$ law would seem unavoidable if one remembers that normalization of the incident neutron wave to unit flux insures it. The scattering cross section was introduced in Fermi's calculation for a free proton only to determine the size of the wave function $\chi(r)$. According to Eq. (8), the chemical binding does not alter the normalization of this, and hence no factor enters into the capture cross section.

II. Radiationless Capture of Neutrons by Protons

A deuteron could not be formed from a free neutron and proton without the emission of a gamma-ray because of the conservation laws of energy and momentum. If, however, the proton is bound, these can be satisfied when the center of mass of the deuteron takes on the energy I liberated, and the chemical binding takes up the excess momentum. To estimate the probability for this process, we add a term to the wave function of Eq. (8) which represents an outgoing wave of deuterons

$$\psi=\psi_0+w(R)\chi_0(r). \tag{18}$$

We have the wave equations

$$(T_R+T_r+V(r)+U(P)-E)\psi=0, \tag{19a}$$
$$(T_r+V(r)+I)\chi_0(r)=0. \tag{19b}$$

If stable, the singlet state will play the dominant role. I and α may refer to either state. Now from the integral equations which may be derived from Eq. (19a) one may show that ψ_0 fails to be an exact solution of the wave equation in the region $r\ll\lambda$ only because of the space variation of $w_0(P)$, which in turn is caused by $U(P)$. Hence the perturbation which induces transitions to deuteron states is just $U(P)$, and not for example, $V(r)$. This is important because for the validity of the whole theory of the effect of the binding it is essential that the waves of high frequency corresponding to the motion of the deuteron should have a small amplitude, and this condition would be less well satisfied if $V(r)$ were the perturbation in question.

For $w(R)$, one gets the wave equation

$$\{T_R+U(R)-I-E\}w(R)=$$
$$-\int d\mathbf{r}\,U(P)\psi_0\chi_0^*(r) \tag{20}$$

and from this, one sees easily that the cross section for deuteron formation without emission of radiation is of the order

$$\sigma \sim \frac{1}{\alpha^2}\frac{\hbar\alpha}{Mv_0}\left(\frac{MUb^2}{\hbar^2}\right)^2\frac{1}{(\alpha b)^7}, \qquad (21)$$

again obeying a $1/v_0$ law, but of negligible importance compared to the magnetic dipole capture process, unless there is a stable singlet level, extremely close to zero potential.

I wish to use this opportunity for expression of my gratitude to Professor J. R. Oppenheimer and Dr. Robert Serber for their generous interest and many valuable suggestions during the course of this work.

FEBRUARY 1, 1937 PHYSICAL REVIEW VOLUME 51

The Effect of Nuclear Motion in the Dirac Equation

IRVING S. LOWEN
New York University, Washington Square East, New York, N. Y.
(Received December 1, 1936)

Corrections to the Dirac equation, relativistic to the order v^2/c^2, due to the motion of the nucleus, for the case of an electron in the field of a heavy particle of mass M, are derived with the aid of the Breit two-body relativistic interaction, to the order m/M, m being the mass of the electron. A calculation of the value of the correction for a 1s electron gives a result in agreement with that obtained from the Schrödinger treatment to the order m/M.

1.

THE Dirac equation is limited in its application to such problems as the treatment of the energy levels of hydrogen, by the fact that it is valid only for the case of one body moving in an external field. As a consequence, the application to the energy levels of a single electron moving around a nucleus is justified only to the extent that the electron may be considered to move in a fixed field of force while a discussion of the effect of the nuclear motion on the energy levels by means of this equation is not available. A discussion of the "Mitbewegung" has been given by Bechert and Meixner[1] making use of the relativistic two-body interaction of Breit[2] in which both the nucleus and electron are treated in the Pauli approximation. The original treatment of Breit for the two-body interaction, however, suggests an approach in which the effect of the nuclear motion introduces small perturbing terms in the Dirac equation. In the discussion below these terms are evaluated to the order v^2/c^2 and $(m/M)^2$ m, M, being the mass of the electron and heavy particle, respectively. The correction due to the terms in $(m/M)^2$ turns out to be smaller than the hyperfine structure term by a factor m/M and may therefore be discarded as unobservable. We are therefore left with the equations (11), (12) in which the terms may be taken to represent the effect of the mitbewegung to the order m/M and v^2/c^2.

Our procedure in obtaining the desired corrections is to eliminate from the two-body equation of Breit, the "small" components of the wave function by expressing them in terms of the "large" components in the usual way in which the Dirac equation is reduced in the Pauli approximation. The large and small components mentioned refer of course only to the dependence on the nuclear coordinates.

2.

As our starting point, we consider the equation[2]

$$\left\{\frac{E}{c}+\frac{Ze^2}{cr}+\frac{e}{c}V+\boldsymbol{\alpha}_1\cdot\mathbf{p}_1+\boldsymbol{\alpha}_2\cdot\mathbf{p}_2+\beta_1 Mc+\beta_2 mc - \frac{Ze^2}{2c}\left(\frac{\boldsymbol{\alpha}_1\cdot\boldsymbol{\alpha}_2}{r}+\frac{\boldsymbol{\alpha}_1\cdot\mathbf{r}\,\boldsymbol{\alpha}_2\cdot\mathbf{r}}{r^3}\right)\right\}\Psi=0, \qquad (1)$$

[1] Bechert and Meixner, Ann. d. Physik **22**, 525 (1935).
[2] G. Breit, Phys. Rev. **34**, 553 (1929).

where the subscript 1 refers to heavy particle of mass M charge Ze, subscript 2 referring to electron; $\mathbf{r}$ vector distance between the two particles pointing from 1 to 2. The α's are the usual Dirac's α's while the wave function Ψ has sixteen components, and $V=V_1-ZV_2$, V_1 and V_2 being potentials at particles one and two, respectively, due to the external field. Disregarding the last term temporarily, (1) becomes, putting

$$p_0=\frac{E}{c}+\frac{Ze^2}{cr}+\frac{e}{c}V$$

$$\{p_0+\boldsymbol{\alpha}_1\cdot\mathbf{p}_1+\beta_1Mc \qquad (2)$$
$$+\boldsymbol{\alpha}_2\cdot\mathbf{p}_2+\beta_2mc\}\Psi=0,$$

setting $\Psi=\begin{pmatrix}\psi_a\\ \psi_b\end{pmatrix}$,

where ψ_a consists of the "small" components and ψ_b of the "large" components of the wave functions, referring to the heavy particle, (2) breaks up into

$$(p_0+Mc+\boldsymbol{\alpha}_2\cdot\mathbf{p}_2+\beta_2mc)\psi_a-\boldsymbol{\sigma}_1\cdot\mathbf{p}_1\psi_b=0. \quad (3)$$

$$(p_0-Mc+\boldsymbol{\alpha}_2\cdot\mathbf{p}_2+\beta_2mc)\psi_b-\boldsymbol{\sigma}_1\cdot\mathbf{p}_1\psi_a=0, \quad (4)$$

where the σ's are the negatives of Pauli's and both ψ_a and ψ_b are four component functions.

From (3), we obtain to the order $(m/M)^2$ and $(v/c)^2$

$$\psi_a=-\frac{1}{4M^2c^2}(\boldsymbol{\alpha}_2\cdot\mathbf{p}_2+\beta_2mc)\boldsymbol{\sigma}_1\cdot\mathbf{p}_1\psi_b$$
$$+(p_0+Mc)^{-1}\boldsymbol{\sigma}_1\cdot\mathbf{p}_1\psi_b.$$

Substituting this in (4), we obtain

$$\Big\{p_0-Mc+\boldsymbol{\alpha}_2\cdot\mathbf{p}_2+\beta_2mc$$
$$+\frac{1}{4M^2c^2}(\boldsymbol{\alpha}_2\cdot\mathbf{p}_2+\beta_2mc)\boldsymbol{\sigma}_1\cdot\mathbf{p}_1\boldsymbol{\sigma}_1\cdot\mathbf{p}_1$$
$$-\boldsymbol{\sigma}_1\cdot\mathbf{p}_1(p_0+Mc)^{-1}\boldsymbol{\sigma}_1\cdot\mathbf{p}_1\Big\}\psi_b=0. \quad (5)$$

The last term may be simplified as follows:

$$-\boldsymbol{\sigma}_1\cdot\mathbf{p}_1(p_0+Mc)^{-1}\boldsymbol{\sigma}_1\cdot\mathbf{p}_1=$$
$$-\frac{1}{2Mc}\left(p_1^2+\frac{Zeh}{c}\boldsymbol{\sigma}_1\cdot\mathbf{H}_1\right)$$
$$+\frac{p_0-Mc}{4M^2c^2}\left(p_1^2+\frac{Zeh}{c}\boldsymbol{\sigma}_1\cdot\mathbf{H}_1\right)$$
$$-\frac{Zeih}{4M^2c^3}(\mathbf{E}_1\cdot\mathbf{p}_1-i\boldsymbol{\sigma}_1\cdot\mathbf{E}_1\times\mathbf{p}_1),$$

$\mathbf{E}_1$ and $\mathbf{H}_1$ being the electric and magnetic intensities, use having been made of the following:

$$(p_0+Mc)^{-1}=\frac{1}{2Mc}\left(1+\frac{p_0-Mc}{2Mc}\right)^{-1}$$
$$=\frac{1}{2Mc}\left(1-\frac{p_0-Mc}{2Mc}\right) \qquad (6)$$

to terms of the order $(v/c)^2$, and of the result

$$(\boldsymbol{\sigma}\cdot\mathbf{A})(\boldsymbol{\sigma}\cdot\mathbf{B})=\mathbf{A}\cdot\mathbf{B}-i\boldsymbol{\sigma}_1\cdot\mathbf{A}\times\mathbf{B}, \qquad (7)$$

where $\mathbf{A}$, $\mathbf{B}$ are two vectors commuting with $\boldsymbol{\sigma}$.

Substituting in (5) and solving for p_0-Mc we obtain

$$\Big\{p_0-Mc+\boldsymbol{\alpha}_2\cdot\mathbf{p}_2+\beta_2mc$$
$$-\frac{1}{2Mc}\left(p_1^2+\frac{Zeh}{c}\boldsymbol{\sigma}_1\cdot\mathbf{H}_1\right)+\frac{p_1^4}{8M^2c^3}$$
$$-\frac{Zeih}{4M^2c^3}(\mathbf{E}_1\cdot\mathbf{p}_1-i\boldsymbol{\sigma}_1\cdot\mathbf{E}_1\times\mathbf{p}_1)\Big\}\psi_b=0. \quad (8)$$

We must now reduce the term

$$-\frac{Ze^2}{2c}\left[\frac{\boldsymbol{\alpha}_1\cdot\boldsymbol{\alpha}_2}{r}+\frac{\boldsymbol{\alpha}_1\cdot\mathbf{r}\,\boldsymbol{\alpha}_2\cdot\mathbf{r}}{r^3}\right]=-\frac{Ze^2}{2c}X$$

in a similar manner. Following a procedure of Breit's[3] instead of eliminating the small components from this term by the above procedure, it is convenient to calculate its average value and replace the small components in the integral for the average by their values in terms of the large. For this we require to calculate the integral of

[3] G. Breit, Phys. Rev. **39**, 616 (1932).

$$\overbrace{\psi_a^*\psi_b^*}\left[\frac{\boldsymbol{\alpha}_1\cdot\boldsymbol{\alpha}_2}{r}+\frac{(\boldsymbol{\alpha}_1\cdot\mathbf{r})(\boldsymbol{\alpha}_2\cdot\mathbf{r})}{r^3}\right]\begin{pmatrix}\psi_a\\ \psi_b\end{pmatrix}=$$

$$\overbrace{\psi_a^*\psi_b^*}\left[-\frac{\boldsymbol{\sigma}_1\cdot\boldsymbol{\alpha}_2}{r}-\frac{(\boldsymbol{\sigma}_1\cdot\mathbf{r})(\boldsymbol{\alpha}_2\cdot\mathbf{r})}{r^3}\right]\begin{pmatrix}\psi_b\\ \psi_a\end{pmatrix}=$$

$$-[\psi_a^*Q\psi_b+\psi_b^*Q\psi_a],$$

where $$Q=\frac{\boldsymbol{\sigma}_1\cdot\boldsymbol{\alpha}_2}{r}+\frac{(\boldsymbol{\sigma}_1\cdot\mathbf{r})(\boldsymbol{\alpha}_2\cdot\mathbf{r})}{r^3},$$

over the coordinate space of both particles.

Making use of (4a) this becomes

$$\psi_b\Big\{\frac{1}{4M^2c^2}[\boldsymbol{\sigma}_1\cdot\mathbf{p}_1(\boldsymbol{\alpha}_2\cdot\mathbf{p}_2+\beta_2mc)Q$$
$$+Q(\boldsymbol{\alpha}_2\cdot\mathbf{p}_2+\beta_2mc)\boldsymbol{\sigma}_1\cdot\mathbf{p}_1]-\boldsymbol{\sigma}_1\cdot\mathbf{p}_1(p_0+Mc)^{-1}Q$$
$$+Q(p_0+Mc)^{-1}\boldsymbol{\sigma}_1\cdot\mathbf{p}_1\Big\}\psi_b.$$

The first bracket may be simply transformed by exchanging $\boldsymbol{\alpha}_2\cdot\mathbf{p}_2+\beta_2mc$ with $\boldsymbol{\sigma}_1\cdot\mathbf{p}_1$ so that in the first term it finally operates on ψ_b^* and in the second on ψ_b. Furthermore, one can substitute in the first bracket to a sufficient degree of approximation

$$(\boldsymbol{\alpha}_2\cdot\mathbf{p}_2+\beta_2mc)\psi_b=-(p_0-Mc)\psi_b.$$

Thus we have for $\bar{X}$ at length, omitting the integral sign

$$\bar{X}=-\frac{1}{2Mc}\psi_b^*(\boldsymbol{\sigma}_1\cdot\mathbf{p}_1Q+Q\boldsymbol{\sigma}_1\cdot\mathbf{p}_1)\psi_b$$
$$+\frac{Zeih}{4M^2c^3}\psi_b^*(Q\boldsymbol{\sigma}_1\cdot\mathbf{E}_1-\boldsymbol{\sigma}_1\cdot\mathbf{E}_1Q)\psi_b, \quad (9)$$

where use has been made of (6).

Using (7) the first bracket is transformed as follows:

$$-\frac{1}{2Mc}\psi_b^*[\boldsymbol{\sigma}_1\cdot\mathbf{p}_1Q+Q\boldsymbol{\sigma}_1\cdot\mathbf{p}_1]\psi_b$$
$$=\frac{1}{Mc}\psi_b^*\Big[\frac{\boldsymbol{\alpha}_2\cdot\mathbf{p}_1}{r}+h\boldsymbol{\sigma}_1\cdot\frac{\mathbf{r}}{r^3}\times\boldsymbol{\alpha}_2$$
$$-\boldsymbol{\alpha}_2\cdot\mathbf{r}\frac{\mathbf{r}}{r^3}\cdot\mathbf{p}_1+\frac{ih}{2}\Big\langle\nabla\cdot\frac{\mathbf{r}}{r^3}\Big\rangle\boldsymbol{\alpha}_2\cdot\mathbf{r}\Big]\psi_b. \quad (10)$$

The term containing $\nabla\cdot\mathbf{r}/r^3$ is zero even for s states on account of the factor $\boldsymbol{\alpha}_2\cdot\mathbf{r}$ and may therefore be disregarded. This may be verified by a direct calculation for the special case of a Coulomb field which is the application with which we shall be concerned.

By a similar procedure, the second bracket of (9) can be reduced and when combined with (10) gives at length

$$X=-\frac{1}{Mc}\Big[\frac{\boldsymbol{\alpha}_2}{r}\cdot\mathbf{p}_1-h\boldsymbol{\sigma}_1\cdot\frac{\mathbf{r}}{r^3}\times\boldsymbol{\alpha}_2+\boldsymbol{\alpha}_2\cdot\mathbf{r}\frac{\mathbf{r}}{r^3}\cdot\mathbf{p}_1\Big]$$
$$+\frac{Zeh}{M^2c^3}\Big[\boldsymbol{\sigma}_1\cdot\mathbf{E}_1\times\frac{\boldsymbol{\alpha}_2}{r}+\frac{\boldsymbol{\sigma}_1\cdot\mathbf{E}_1\times\mathbf{r}}{r^3}\boldsymbol{\alpha}_2\cdot\mathbf{r}\Big]. \quad (10a)$$

Consequently the complete Hamiltonian may be written, in ascending order of magnitude in m/M

$$H=H_a+H_b+H_c,$$

where

$$\frac{H_a}{c}=-\Big(\frac{Ze^2}{cr}+\boldsymbol{\alpha}_2\cdot\mathbf{p}_2+\beta_2mc+\frac{e}{c}V\Big),$$

$$\frac{H_b}{c}=\frac{1}{2Mc}\Big(p_1^2+\frac{Zeh}{c}\boldsymbol{\sigma}_1\cdot\mathbf{H}_1\Big)$$
$$-\frac{Ze^2}{2Mc^2}\Big(\frac{\boldsymbol{\alpha}_2}{r}\cdot\mathbf{p}_1-h\boldsymbol{\sigma}_1\cdot\frac{\mathbf{r}}{r^3}\times\boldsymbol{\alpha}_2+\frac{\boldsymbol{\alpha}_2\cdot\mathbf{r}\mathbf{r}\cdot\mathbf{p}_1}{r^3}\Big),$$

$$\frac{H_c}{c}=\frac{Zeih}{4M^2c^3}(\mathbf{E}_1\cdot\mathbf{p}_1-i\boldsymbol{\sigma}_1\cdot\mathbf{E}_1\times\mathbf{p}_1)$$
$$+\frac{Z^2e^2h}{2M^2c^4}\Big(\boldsymbol{\sigma}_1\cdot\mathbf{E}_1\times\frac{\boldsymbol{\alpha}_2}{r}+\frac{\boldsymbol{\sigma}_1\cdot\mathbf{E}_1\times\mathbf{r}}{r^3}\boldsymbol{\alpha}_2\cdot\mathbf{r}\Big).$$

These results may be checked against those of Bechert and Meixner by eliminating the small components of the electron wave function in H_a and H_b in the usual way. We reduce then to the results 5, 6, 7 of their paper.

3.

We apply the preceding result to the calculation of the energy levels of a single electron in a Coulomb field. We may gain some idea of the relative importance of the various terms by

comparing them with the term of H_b

$$\frac{Ze^2}{2Mc^2}h\sigma_1\cdot\frac{\mathbf{r}}{r^3}\times\boldsymbol{\alpha}_2=-\frac{e}{c}\boldsymbol{\mu}\cdot\frac{\mathbf{r}}{r^3}\times\boldsymbol{\alpha}_2,$$

$\boldsymbol{\mu}$ being the magnetic moment of the heavy particle, to which is due the hyperfine structure. Simple considerations show that the terms in the second bracket of H_c are of the order $(m/M)\alpha^2Z^2$ while those in the first are $(m/M)\alpha Z$ in terms of the h.f.s. term. The contribution of H_c may therefore be dropped in applications to the derivation of the term values of a single electron in a central field. The terms in H_b on the other hand are either of the order of magnitude of the hyperfine structure term or differ from it by a factor of at most $1/\alpha Z$.

For application to s terms, these considerations require a slight refinement since H_c then becomes infinite. The more exact calculations result in the replacement of the factors M^2c^2 in the denominators of the terms in H_c by $(p_0+Mc)^2$. Since the chief contribution of these terms to the energy comes from a region $r=e^2/Mc^2\sim10^{-16}$ cm their meaning is doubtful unless we cut the wave functions off at about r equal to 10^{-13} cm. In this case also the terms in H_c may be dropped as being negligible. We take as the terms of our Hamiltonian for the one electron case in the Coulomb field of the nucleus assuming zero external magnetic field

$$\frac{H_a}{c}=-\boldsymbol{\alpha}\cdot\mathbf{p}-\beta mc-\frac{Ze^2}{rc}-\frac{e}{c}V,$$

$$\frac{H_b}{c}=\frac{p^2}{2Mc}-\frac{e}{c}\boldsymbol{\mu}\cdot\frac{\mathbf{r}}{r^3}\times\boldsymbol{\alpha}+\frac{Ze^2}{2Mc^2}\left(\frac{\boldsymbol{\alpha}}{r}\cdot\mathbf{p}+\boldsymbol{\alpha}\cdot\mathbf{r}\frac{\mathbf{r}}{r^3}\cdot\mathbf{p}\right),$$

where the substitution $\mathbf{p}=\mathbf{p}_1=-\mathbf{p}_2$ has been made. The subscripts have been omitted on the right since all the terms refer now to the electron.

We calculate the contribution of H_b to the energy for an s state first transforming to polar coordinates. In these coordinates we have[4] in the absence of an external field

$$\frac{H_a}{c}=-\epsilon p_r-i\epsilon\rho_3\frac{kh}{r}-\rho_3mc-\frac{Ze^2}{rc}, \tag{11}$$

$$\frac{H_b}{c}=\frac{1}{2Mc}\left(p_r^2-\frac{kh^2}{r^2}\rho_3+\frac{k^2h^2}{r^2}\right)+\frac{Ze^2}{2Mc^2}\left(\frac{2\epsilon}{r}p_r+i\epsilon\rho_3\frac{kh}{r^2}+\frac{i\epsilon h}{r^2}\right) \tag{12}$$

with the omission of the h.f.s. term, and the same definition of k as in Dirac. Thus for $s_{\frac12}$, $p_{\frac12}$, $p_{\frac32}$ states, k has values -1, 1, -2, respectively.

Use has been made here of the relations

$$r\epsilon=\boldsymbol{\alpha}\cdot\mathbf{r}, \tag{13a}$$

$$\mathbf{r}\cdot\mathbf{p}=rp_r+ih, \tag{13b}$$

$$\boldsymbol{\alpha}\cdot\mathbf{p}=\epsilon p_r+i\epsilon\rho_3(kh/r), \tag{13c}$$

where $\epsilon=\begin{pmatrix}0&-i\\ i&0\end{pmatrix}$, $\rho_3=\begin{pmatrix}1&0\\0&-1\end{pmatrix}$.

Finally by squaring (13c) we obtain

$$p^2=p_r^2-\frac{kh^2}{r^2}\rho_3+\frac{k^2h^2}{r^2}.$$

In terms of radial functions, the average value of H_b is given by

$$\Delta W=\frac{1}{2Mc^2}\int_0^\infty\left\{[E^2-(eA_0)^2+m^2c^4](\phi_1^2+\phi_2^2)+2Emc^2(\phi_1^2-\phi_2^2)+2Ze^2c\frac{kh}{r^2}\phi_1\phi_2\right\}dr, \tag{14a}$$

$$=\frac{h}{2Mc}\int_0^\infty\left\{(E-eA_0)\left(\phi_1\frac{d\phi_2}{dr}-\phi_2\frac{d\phi_1}{dr}\right)+2E\frac{k}{r}\phi_1\phi_2\right\}dr, \tag{14b}$$

where ϕ_1 and ϕ_2 satisfy the equations

$$\frac{d\phi_1}{dr}-\frac{k}{r}\phi_1+\frac{1}{hc}(E+eA_0-mc^2)\phi_2=0,$$

$$\frac{d\phi_2}{dr}+\frac{k}{r}\phi_2-\frac{1}{hc}(E+eA_0+mc^2)\phi_1=0,$$

where $eA_0=Ze^2/r$.

ϕ_1 and ϕ_2 are subject to the normalizing condition

$$\int_0^\infty(\phi_1^2+\phi_2^2)dr=1.$$

[4] Dirac, *Quantum Mechanics*, second edition, p. 266.

As a check on the calculations, it is convenient to use

$$\left(\frac{p^2}{2M}\right)=\frac{1}{2Mc^2}\int_0^\infty [(E+eA_0+mc^2)^2\phi_1^2 + (E+eA_0-mc^2)^2\phi_2^2]dr.$$

The first form (14) is convenient if one does not desire derivatives in the expression, the second is more compact and has the additional advantage that for $1s$ states

$$\phi_1\frac{d\phi_2}{dr}-\phi_2\frac{d\phi_1}{dr}=0.$$

For $1s$ states these expressions give

$$\Delta W=\frac{m}{M}\frac{mc^2}{2}\alpha^2Z^2.$$

This relativistic result is to be compared with what one might expect from naive considerations: $\Delta W=(m/M)mc^2(1-(1-\alpha^2Z^2)^{\frac{1}{2}})$. In the case of the former one has for $Z=90$, a correction $\Delta W=0.215(m/M)mc^2$ while the latter gives $.245\ (m/M)\ mc^2$. The strict relativistic treatment therefore gives an appreciable effect.

We close this section by giving the Mitbewegung corrections for the case of two electrons revolving around a nucleus. If we refer to the electrons by the subscripts 1 and 2, we have in place of H_b above, for two electrons, omitting the h.f.s. term

$$\frac{H_b'}{c}=\frac{(\mathbf{p}_1+\mathbf{p}_2)^2}{2Mc}+\frac{Ze^2}{2Mc^2}\left[\left(\frac{\boldsymbol{\alpha}_1}{r_1}\right)\cdot(\mathbf{p}_1+\mathbf{p}_2) + \left(\frac{\boldsymbol{\alpha}_1\cdot\mathbf{r}_1}{r_1^3}\right)\mathbf{r}_1\cdot(\mathbf{p}_1+\mathbf{p}_2)\right]+\frac{Ze^2}{2Mc^2}\left[\left(\frac{\boldsymbol{\alpha}_2}{r_2}\right) \cdot(\mathbf{p}_1+\mathbf{p}_2)+\left(\frac{\boldsymbol{\alpha}_2\cdot\mathbf{r}_2}{r_2^3}\right)\mathbf{r}_2\cdot(\mathbf{p}_1+\mathbf{p}_2)\right],$$

where $\mathbf{r}_1$ and $\mathbf{r}_2$ are vector distances pointing from the nucleus to the electrons 1 and 2, respectively. From this the generalization to any number of electrons may be simply made.

4.

Since in the derivation, Eq. (1) from which we start presupposes the existence of an equation of Dirac type for both particles and since present data on nuclear moments seems to indicate that the heavy particles are not described by such an equation, the question naturally arises as to the extent to which our results are limited by this condition. The answer to this question may be based on two circumstances. In the first place, the effect of the magnetic moment of the heavy particle is represented in our result by the term in $(10a)$

$$\frac{e}{c}\boldsymbol{\alpha}_2\cdot\frac{\boldsymbol{\mu}\times\mathbf{r}}{r^3},\quad\text{where}\quad\boldsymbol{\mu}=-\frac{Zeh}{2Mc}\boldsymbol{\sigma},$$

which is *formally* the same as that obtained from the single electron equation for a nuclear magnetic moment $\boldsymbol{\mu}$ so that by giving $\boldsymbol{\mu}$ appropriate values the h.f.s. is correctly given, insofar as it be considered to arise from a magnetic doublet at the heavy particle, by this calculation even though the heavy particle does not obey a Diracian equation. Presumably, then, the other terms which do not even involve the magnetic moment of the heavy particle are correct.

The other justification for believing our result to be correct to the stated degree of approximation is due to the fact that (1) may be derived in the case of two electrons by means of the quantum electrodynamics.[3] This derivation should hold also in case one of the particles is moving sufficiently slowly to be treated in the Pauli approximation in which case the applicability of the Dirac formalism to this particle would not then be a necessary prerequisite to the validity of the resulting interaction.

In conclusion it is a pleasure to acknowledge my indebtedness to Professor G. Breit for most generous advice and discussions. I should also like to express my thanks to the physics department of the University of Wisconsin for its kind hospitality during the past summer when part of this work was done.

The Nature of the Superconducting State

J. C. SLATER
Massachusetts Institute of Technology, Cambridge, Massachusetts
(Received December 4, 1936)

It is tentatively suggested that the superconducting state of metallic electrons may arise by application of perturbation theory to Bloch's theory. The excited states of a metal, on the usual theory, form a continuum whose lower boundary is the normal state. It is shown that under some circumstances there are nondiagonal matrix components of energy between states of this continuum, which would tend to depress a few of the lowest states below their normal positions. These special states of the metal would resemble a thermodynamic phase, stable only at the lowest temperatures, and having practically zero entropy, in agreement with present theories of the thermodynamics of superconductivity. They would also tend to have extremely low resistance, on account of the small concentration of energy levels per unit energy range. It is therefore suggested that these states may constitute the superconducting state. It is shown that superconductivity is not to be expected for the alkalies, or for Cu, Ag or Au; and that it is to be expected only at extremely small temperatures for transition metals, as W, Fe, Ni, Pt; thereby accounting for most of the metals which are known not to be superconducting at temperatures so far attained.

THE electron theory of metals has developed far enough so that it ought to be possible to explain superconductivity. And the study of the superconducting state itself has progressed, both experimentally and theoretically, so far that its explanation should not be too difficult.[1] The present paper does not present a complete theory of the superconducting state, but it does indicate a point in the electron theory, so far not explored, where we may very plausibly expect an interpretation of the phenomenon to be found. Briefly, the suggested explanation is the following. Almost all discussions of the metallic state have used the Bloch theory, or some refinement of it like that developed by Wigner and Seitz. The essence of such a theory is the use of a model where each electron moves in a periodic potential field, and where a wave function for the whole crystal can be made up by assigning to each electron of the metal a different wave function in such a periodic field. Brillouin[2] has attempted to show that a wave function of this type can exhibit superconductivity, but the criticisms of his attempt are generally believed to show that this is impossible. Instead, it is generally thought that a correct theory must depend on some sort of cooperative action between the electrons, of a type not describable by Bloch's theory. Theories of this sort have been suggested by Kronig[3] and Frenkel;[4] but neither one has made close enough connections with the accepted theory of metals to lead to any real hope of solving the problem. In contrast to those attempts, we shall proceed by well-known methods, asking how we should expect Bloch's method to be in error, and how to correct this error. In atomic structure, the analog to Bloch's method is the one-electron method, treating each electron as if it moved in a central field, and building up a wave function by assigning to each electron an orbit in the central field. It is at once observed, however, that there is degeneracy; using these unperturbed wave functions, a number of states, corresponding to different orientations of orbits and spins, prove to have the same energy. We proceed by computing the nondiagonal components of the energy matrix between such states, and carrying out a perturbation calculation, which yields perturbed energy levels falling into the well-known multiplet classification, with perturbed wave functions which are linear combinations of a number of the unperturbed functions. In the problem of metals, the present suggestion is that we must take the Bloch theory only as a first approximation; that, on account of degeneracy, we must find nondiagonal energy components between Bloch states, and make linear combinations according to perturbation theory.

[1] For a general review of superconductivity, with references, see H. G. Smith and J. O. Wilhelm, Rev. Mod. Phys. **7**, 237 (1935).
[2] L. Brillouin, J. de phys. et rad. **4**, 334 (1933); **4**, 677 (1933).
[3] R. de L. Kronig, Zeits. f. Physik **78**, 744 (1932); **80**, 203 (1933).
[4] J. Frenkel, Phys. Rev. **43**, 907 (1933).

Plausible reasons are given for the belief that, when this is done, while most of the energy levels of the electrons will not greatly change their nature, the very lowest states of the electronic system as a whole will be rather profoundly affected, and these will lead to the superconducting state. In the first section we consider this perturbation problem; in the second, we show that the resulting energy levels and wave functions may reasonably be connected with the existence of superconductivity.

1. Perturbations of Bloch Wave Functions

It is well known that the stationary states of an electron in a periodic potential field can be classified into certain energy bands. Each band contains a large number of levels, each of which can be occupied by one electron of each spin; in simple cases, a band contains as many levels as there are atoms in the crystal. The lowest stationary state of the crystal, on the Bloch picture, then arises when the electrons are placed in the lowest available levels. If the crystal is an insulator, the electrons will just fill some bands, leaving all the others entirely empty. For a metal, on the other hand, the number of electrons is such that one band at least is only partly full. If two or more bands overlap in energy at the top of the filled levels, each one will contain some electrons in its lower levels, but its upper levels will be unfilled. It is this case which we shall consider; for our considerations would indicate that the existence of more than one partly filled band is essential to superconductivity. For many purposes it is convenient to classify the levels according to the vector $\mathbf{k}$, the momentum or wave number vector, defined by the condition that the wave function is multiplied by a factor $\exp(i\mathbf{k}\cdot\mathbf{R})$ in going from one point of the lattice to a point removed by a distance $\mathbf{R}$, where $\mathbf{R}$ is the vector from the nucleus of one atom to that of another. We can then set up a $\mathbf{k}$ space, and can show that all the essentially different wave functions can be described by $\mathbf{k}$'s lying in a polyhedral cell surrounding the origin. Each energy band is represented by a set of $\mathbf{k}$ values filling this zone with uniform density. Energy contours can be drawn within the zone, and for the type of metal we are considering, there will be at least two zones for which only the levels within a certain energy contour will be filled.

Excited levels in the Bloch theory occur when one or more electrons are displaced from their original positions to other, necessarily higher, states. To a first approximation, the change in the energy of the system as a whole when an electron is displaced is given by the change in one-electron energy of this electron, and if only a few electrons are excited, we can add their separate excitation energies. It is now clear that above the lowest energy level of the system as a whole we have a continuum of excited levels. Any electron can be displaced to any unoccupied level; and if we choose to displace an electron which is just at the top of the occupied levels, and displace it to the bottom of the unoccupied ones, we shall do a negligible amount of work. There are so many electrons of this maximum energy, and so many unoccupied levels close above, that there are a great many states with energy hardly higher than the normal state. If the Bloch wave functions are correct, these excited levels of the system as a whole will really represent the excited levels of the metal. This will be the case if the matrix component of energy vanishes between any two levels of the continuum. But if these matrix components do not vanish, but instead have appreciable values, we must carry out a perturbation calculation; and since the states form a continuum, which is even worse than ordinary degeneracy, the perturbations may make important changes in the final energy levels and wave functions.

In the appendix, we consider the nondiagonal matrix component of energy between two Bloch states. We come to the following conclusions:

The matrix component is practically zero unless two, and only two, electrons have changed their levels from one state to the other.

The matrix component is zero unless the sum of the $\mathbf{k}$ vectors of all electrons is the same in the initial and final state. Since only two electrons are changing their $\mathbf{k}$'s, this means that the change in $\mathbf{k}$ of one should be equal and opposite to that for the other.

The matrix component is very small unless the two electrons which move in the transition were originally in two different energy bands;

and unless they are finally in two different energy bands. This shows that if we assume only one band to be partly occupied, as in an alkali metal, or Cu, Ag, Au, the Bloch states themselves will form good approximations, and no further perturbation calculation is necessary. Thus our theory would not lead to superconductivity for these metals, and it is significant that none of them have been observed to be superconducting.

In accordance with the matrix components just described, we can examine the perturbation problem. Let us start with a given low energy state of the metal as a whole, given by the Bloch theory. This will have matrix components to a great many other states, but we know from perturbation theory that the other states of almost the same energy will have the most effect. We shall therefore classify all the transitions from this state to others of about the same energy. In particular, we consider all transitions in which one electron changes its $\mathbf{k}$ value by $\Delta\mathbf{k}$, the other by $-\Delta\mathbf{k}$. We have two partly occupied energy bands, which we may call 1 and 2. Then we assume in the transition that an electron in band 1 goes into band 2, with change of $\Delta\mathbf{k}$, and an electron in band 2 goes into 1, with change of $-\Delta\mathbf{k}$. Furthermore, to have no appreciable increase of energy, each electron must have been originally at the top of the filled levels, and must have gone to the top of the filled levels in the other band. We may therefore obtain all the transitions of this type by the following construction. We start with our polyhedral zone, and plot in it the energy surface representing the top of the filled levels of band 1; we call this surface 1. Similarly we plot in the same zone the surface for band 2. We then displace surface 1 by the vector $\Delta\mathbf{k}$, and consider the line of intersection of the displaced surface 1 with surface 2. As a rule, these surfaces will actually intersect. Going back to the original surface 1, we can draw on it the line which was carried into the line of intersection by the displacement. Then we have lines on both surface 1 and surface 2, of the same shape, and the second displaced the amount $\Delta\mathbf{k}$ from the former. In other words, the electron which is removed in the transition from band 1 may come from any point of this line on surface 1, and by the displacement it will be carried to a point of the line on surface 2; and the electron which is removed in the transition from band 2 may come from any point of the line on surface 2, and by the equal and opposite displacement will be carried to a point on surface 1. If we allow a certain small tolerance in the energy values, it is clear that the surfaces will be replaced by thin shells, and their intersection by a thin filament of finite volume, so that there will be a finite number of such transitions for each value of $\Delta\mathbf{k}$, and a great many when we consider all possible values of $\Delta\mathbf{k}$. Thus it is clear that a given state will have nondiagonal matrix components to a great many other states, which however resemble it in having the same total number of electrons in each of the two bands, and in having the same vector sum of the $\mathbf{k}$'s. Of course, if we allow transitions to states with appreciably different energies, we have a great many more.

We shall make no attempt to solve the extremely complicated perturbation problem presented in this way. We can, however, make certain statements regarding the nature of the solution. First, we consider the perturbed energy levels. The second order perturbation theory cannot be applied quantitatively in the perturbation of a continuum of levels, but it leads qualitatively to the correct result: each unperturbed level is, so to speak, pushed away from every other level with which it has a matrix component, by an amount proportional to the square of the matrix component, and inversely proportional to the energy difference between the unperturbed levels. This means that in the middle of a continuum, a level will be pushed approximately equal amounts in both directions, and will as a result hardly be affected by the perturbations. But at the edge of a continuum, the push is entirely one-sided, and will result in the few levels near the edge being shoved away from the others, so that they will spread out into energy regions previously unoccupied. In our case, the unperturbed continuum has a lower boundary, coming at the lowest energy of the metal as computed by the Bloch theory. The effect of perturbations will be to spread out the few lowest states, so that they will lie lower than they otherwise would, and will correspondingly have a lower density of states per unit energy range. Effectively, there will be a relatively

small number of special states below the lowest Bloch states.

Next, we consider the wave functions. In such a perturbation of a continuum, the energy levels which are not much affected, lying in the middle of the continuum, will have wave functions which also are not much changed by the perturbation. But those which are repelled from the other states, at the bottom of the continuum, will have wave functions which are combinations of those unperturbed wave functions which do the repelling. Thus in our case one of these special states will have a wave function which is made up of all those Bloch states having the same vector sum of $\mathbf{k}$'s, the same number of electrons in each of the two bands, and approximately the same energy; and we have seen that there are a great many such states. These states will all be on a par in the calculation, and will have approximately the same coefficients in the linear combination; states satisfying all the conditions except that they have appreciably different energy will also appear, but with smaller coefficients.

A simple example of such a perturbation problem has been worked out by the writer and Shockley,[5] in a discussion of the absorption of light by an alkali halide crystal. The problem there discussed was essentially the following, if considered from the present point of view: there are electrons in two bands, but in particular one band contains only one electron, the other has all its levels but one occupied. All such states consistent with a given vector sum of the $\mathbf{k}$'s were set up, and the perturbation problem was solved, taking account of all these states. The problem was carried out only in one dimension, but this should hardly change the general results. It was carried out in terms of atomic functions rather than Bloch functions, but it is an easy matter to transform the unperturbed functions to the Bloch form. Thus it is seen that essentially this problem was specialized only in the small number of electrons in the second band, and while that simplifies the calculations greatly, it would hardly be expected to change the results profoundly. It was found, just as we have described in the preceding paragraph, that the energy levels and wave functions in the middle of the continuum were hardly affected by the perturbation, but that in this case just one level at the bottom split off, having an appreciably different energy, and a very different type of wave function, from the states of the continuum. Its wave function, as we have stated, was a combination of all the unperturbed functions, in which those of approximately the same energy are represented to approximately the same extent, but those of higher energy are not so strongly represented. While these results are not all at once apparent from the paper quoted, they can be derived from the discussion given there without difficulty.

The example mentioned above resembles the present problem not only mathematically, but fundamentally. To see this, let us adopt the same method used there, that of considering the energy levels of the system as a whole as a function of lattice spacing. To fix our attention on a definite case, let us consider the crystal of magnesium, which satisfies our condition of having two energy bands partly occupied, and which is known to be superconducting. At large distances, the band of $3s$ electrons is filled, the bands of $3p$ are entirely empty, so that the lowest state of the crystal is a single state, and the crystal would be an insulator. As with an alkali halide, the lowest excited state would come by removing one electron to the $3p$ band. If the bands are spread out at all, this will result in a continuum of excited states, depending on which $3s$ electron is removed, which $3p$ state it enters. But it was shown in the paper mentioned above that the very lowest excited states will not belong to the continuum. Instead, the lowest of all will come from the process which is described in an atomic model as excitation of the $3s$ electron of one atom to the $3p$ level of the same atom; next there will come discrete states arising from ionization of one atom, removing its $3s$ electron to the next nearest neighbor, and there creating a negative ion, with two $3s$ and one $3p$ electron; still further discrete levels will come from removal of the electron to further and further neighbors; and finally the continuum will arise from the process of removal of an electron from one atom to a distant atom, creating a widely separated pair of ions. These discrete levels lying below the continuum are

[5] J. C. Slater and W. Shockley, Phys. Rev. **50**, 705 (1936).

most marked at large distances, but while more and more of them merge with the bottom of the continuum as the lattice spacing diminishes, some of them are still separated from the continuum at the actual lattice space.

Now let us see how the situation is affected by the fact that in magnesium at small distances the $3s$ and $3p$ energy bands broaden so that the higher energies in the $3s$ band lie above the lower ones of the $3p$ band. Let us consider the state where the $3s$ band is full, the $3p$ empty, as a zero of energy at all lattice spacings. Then at the point where the overlapping of bands commences, the bottom edge of the continuum of excited levels will have descended to touch this zero of energy, and at smaller lattice spacings it will be lower than the zero. In other words, the state where $3s$ is full, $3p$ is empty, is no longer the lowest state in the Bloch theory; the energy will be diminished if the highest $3s$ electron goes into the lowest $3p$ state. But all this time, there is a discrete state even below the bottom of the continuum of excited levels. Therefore at the actual distance of separation, if we had the artificial state where all $3s$ levels were full, the transition of one electron which would make the greatest reduction in the energy of the system would not be a transition to an ordinary Bloch state at all, but rather would be this special type of transition, essentially to a state where the excited $3p$ electron is attached to the same atom from which, as a $3s$ electron, it was removed. Now this represents merely the gain in energy that can be produced by the transition of one electron; but clearly other electrons also will make transitions with reduction of energy, also to special states, until finally there will be an equilibrium.

We see, in other words, that by this method of tracing energy levels from large distances to small ones, just as by the direct perturbation method, we conclude that there will be special stationary states of the electrons of the system as a whole, lying slightly below the ordinary Bloch states, and representing special linear combinations of these low lying Bloch states, including a great many Bloch states with the same vector sum of the $\mathbf{k}$'s, the same number of electrons in each of the partly occupied energy bands, and about the same energy. It would be very difficult to make any accurate calculation of the exact nature of these states, but we shall show in the next section that the simple properties already mentioned are enough to make it very plausible that these states should represent the superconducting state of the metal.

2. The Superconducting State

At any temperature, the probability of finding the whole system in a state of energy E will be proportional to $\exp(-E/kT)$. Thus at the absolute zero only the lowest of our special states will have any chance of being realized. At very low temperatures, since the special states lie below the Bloch states, the chances will be very good that the system will be found in a special state. But as the temperature rises, so that the exponential $\exp(-E/kT)$ is not too small for the Bloch states, the latter can be occupied. Now the number of Bloch states per unit energy range will be enormously greater than the corresponding number for the special states. Thus when the probability that the Bloch states can be occupied at all becomes appreciable, on account of their great number the chance will become practically a certainty that the system will be found in the Bloch states. There will be, then, a gradual, but in the end an extremely rapid, change from the special to the Bloch type of state, as the temperature is increased. As we shall see, this is what is observed.

To an approximation, we may take the special states as representing one phase of the electrons, the Bloch states as another, forgetting that one sort really will merge smoothly into the other. The special phase will have a lower internal energy at the absolute zero of temperature than the Bloch phase; that is, the lowest special state has a lower energy than the lowest Bloch state. But, in thermodynamic language, the entropy of the special state at any temperature will be negligible compared with the entropy of the Bloch phase. The reason for this is that the entropy of a phase depends essentially on the number of stationary states which belong to that phase. Then we can get the equilibrium condition of the phases thermodynamically by equating the thermodynamic potentials Z of the two phases. At zero pressure, the thermodynamic

potential may be written $Z=E_0-\int_0^T SdT$, where E_0 is the internal energy at the absolute zero, S is the entropy as a function of the temperature T. Thus we see that the thermodynamic potential of the special phase will be approximately independent of temperature. On the other hand, for the Bloch state, the specific heat C_p is known to be proportional to the temperature, equal say to $C_p=AT$. Then the entropy is given by $S=\int C_p/TdT=AT$, so that the thermodynamic potential is $E_0-AT^2/2$. In other words, while the Bloch state has a higher thermodynamic potential than the special state at the absolute zero, its potential decreases with temperature. If ΔE represents the energy difference between the special and Bloch states at the absolute zero, it is clear that our approximation shows that the potentials of the two states should become equal when $\Delta E=AT^2/2$, $T=(2\Delta E/A)^{\frac{1}{2}}$, and that above this temperature the ordinary Bloch state should be the stable one. From known temperatures of transition and values of A we can get an approximate idea of the order of magnitude of ΔE necessary to explain superconductivity. Thus for silver A is of the order of magnitude of 0.00015 calorie per mole per degree. (We choose a nonsuperconducting metal to determine the value of A, since the superconducting ones cannot be followed to low enough temperatures in the Bloch state to separate the linear part of the specific heat from the T^3 part arising from the Debye function.) For most superconducting elements, the transition temperature is a few degrees absolute. Take for instance 7 degrees for T. Then ΔE becomes 0.0038 calorie per mole $=1.6\times10^{-7}$ electron volts per atom. In other words, our special states need be depressed below the Bloch continuum by only an excessively small energy of this order of magnitude to explain superconductivity.

The calculation we have just made seems to show without further hypothesis why the elements of the transition group (W, Fe, Ni, Pt in particular) have not been found to be superconducting. It is known that these elements have abnormally large values of the electronic specific heat, on account of their unfilled inner shells; that is, they have abnormally large values of the constant A, sometimes as large as 30 or 40 times the normal size. Then, if they have values of ΔE comparable with other metals, our formula shows that the transition temperature should be something like $\sqrt{40}$ times smaller, or six times smaller, than normal values. In other words, it seems plausible that these elements may really be superconducting, but that low enough temperatures have not yet been reached to show the effect. It is notable that our two categories of elements, first the alkalies and Cu, Ag and Au, and second the transition elements, include almost all the elements which have definitely been observed not to be superconducting at temperatures so far obtained.

The approximation of representing the superconducting and ordinary states of a metal as two phases, which we have just considered, is known to be a fair approximation, as is shown by the work of Rutgers, Gorter, Casimir, and others.[6] These writers have made a thorough study of the thermodynamics of superconductivity, and have shown, just as we have indicated, that the superconducting state must really have practically no entropy. They have further shown that if the superconducting state shields a conductor magnetically, as a perfect conductor should, the magnetic induction B will automatically be zero inside the conductor, and this introduces a magnetic term into the thermodynamic potential which automatically produces a change of equilibrium temperature with magnetic field, in quantitative as well as qualitative agreement with experiment. Thus we do not need to discuss the magnetic effect on the equilibrium between states. Furthermore, they have shown that the approximation of an ordinary phase change is too crude. In the absence of a magnetic field, there is no latent heat at the transition point, only a discontinuity of the specific heat, which means thermodynamically that the first derivative of Z with respect to T is not discontinuous, but only the second derivative. This suggests that the superconducting state really merges gradually into the ordinary state as the temperature rises. But that is just what our model would lead us to suspect; for there is no perfectly sudden change between our special states and the Bloch states, only a gradual change, which

[6] A. J. Rutgers, Physica **1**, 1055 (1934); C. J. Gorter and H. Casimir, Zeits. f. tech. Physik **15**, 539 (1934); J. A. Kok, Physica **1**, 1103 (1934); etc.

cannot be correctly described by dividing the states sharply into two classes. Thus we may conclude that as far as thermodynamic properties are concerned, our model of the superconducting state certainly shows the right general behavior, and does not contradict the known and well worked out theory in any particular.

In addition to the fact that the superconducting state forms a special phase of the electrons at low temperatures, which probably is the most fundamental property of this state, there remains its remarkable property of being able to carry a current for an indefinite time, without its dissipation in Joulean heat. This means that the probability of scattering of the electrons by the thermal motion of the lattice is zero, or excessively small, in the superconducting state. Now it is well known that the study of this scattering, and the deduction of the value of the resistance, is extraordinarily difficult for very low temperatures even in a normal metal; and we shall make no attempt to investigate the resistance of our special electronic states, and to show that the resistance is zero. There is, however, one fact which makes it very plausible that the resistance should vanish. The ordinary formula for resistance based on the Bloch theory contains as a factor the square of the density of one-electron energy levels at the top of the occupied levels. The reason for this is that the larger the number of unoccupied levels available for an electron to be scattered into, the larger is the probability of its being scattered. This idea has been used by Mott[7] to explain the large resistance of the transition metals, in terms of the large number of unoccupied states in the partly filled bands of d electrons. The argument is ordinarily stated in terms of one-electron levels; but it is clear that what is needed for large resistance is a large number of energy levels of the metal as a whole per unit energy range, in the neighborhood of its lowest level. It is significant that the same metals which, according to Mott, have an abnormally high resistance, are those which also have an abnormally high electronic specific heat, and therefore an abnormally high electronic entropy; for both these things come from the excess of energy levels.

Now the situation in our model of the superconducting state is just the opposite. In the neighborhood of the lowest energy level of the metal, the levels are spread out by the perturbation so that an extremely small number of levels comparatively is spread through a finite interval of energy. In other words, the number of available energy levels per unit range of energy, which an electron can be scattered into, is much smaller than normal. It is so much smaller that as we have seen the entropy appears to be practically equal to zero. By the same argument as before, then, the probability of electron scattering should be very much less for these states than for the normal states, and the resistance should be very much smaller. If this argument, which it is admitted is only qualitative, should be correct, the lack of resistance of the superconducting state would be tied up with its lack of entropy, and any theory which would explain one would explain the other. It would be very desirable to check this suggestion by an actual calculation of the distribution of the superconducting energy levels, and of the corresponding conductivity of the metal. But in the present state of the electron theory, this would be almost prohibitively difficult. Under the circumstances, it seems worth while bringing forward this tentative model of the superconducting state, even though it is only qualitative. If this state can be explained in terms of existing theories at all, it seems almost inevitable that it will be in some such way as is suggested here, in terms of further approximations starting with the Bloch theory as a beginning. And it seems significant that one can give at least likely reasons why such an attempt might be successful.

[7] N. F. Mott, Proc. Roy. Soc. **A153**, 699 (1936); *The Theory of the Properties of Metals and Alloys* (Oxford, 1936).

Appendix

The one-electron functions which we shall assume will be real solutions of the periodic potential problem, rather than Bloch's approximations to these solutions by means of atomic functions. Then the functions will be orthogonal to each other, and when we build up a function for the whole crystal, in the form of a determinant, the relations as far as matrix components of the energy are concerned will be as in the atomic problem. As in that problem, the non-diagonal matrix components of energy will come from the terms $2/r_{ij}$ in the potential energy, and will arise between

states differing in the wave functions of two electrons at most. If the initial wave functions of these two electrons are symbolized by A, B and the final ones by C, D, then it can be shown that the matrix component will be just as for a two-electron problem involving only these two electrons:

$$\tfrac{1}{2}\int \begin{vmatrix} A^*(1) & B^*(1) \\ A^*(2) & B^*(2) \end{vmatrix} (2/r_{12}) \begin{vmatrix} C(1) & D(1) \\ C(2) & D(2) \end{vmatrix} dv_1 dv_2.$$

If now A, B, C, D represent modulated functions, it is easy to show that unless the sum of the $\mathbf{k}$'s for A and B equals the sum for C and D, the integral over the crystal will vanish. If this condition is satisfied, however, the integration of dv_1 only over the cell surrounding one atom will lead to just $1/N$th of the whole integral, if N is the number of atoms. Furthermore, if dv_1 is integrated over one cell, the major contribution to the integral will come when dv_2 is integrated over the same cell. Now within a given cell, the wave functions of all the states of a single band are similar. Thus if A and B refer to states of the same band, the first determinant will be small, and if C and D states of the same band the second determinant will be small, verifying our statement that the matrix component is large only when A and B refer to different bands, and C and D refer to different bands.

FEBRUARY 1, 1937 PHYSICAL REVIEW VOLUME 51

Approximation to Discrete Quantum States by Iteration

L. H. THOMAS
Ohio State University, Columbus, Ohio
(Received November 23, 1936)

A method is described by which successive approximations to the wave functions and energies of stationary states can sometimes be obtained in a form allowing definite limits of error to be stated. Two examples in which the solution is otherwise known are worked out and the rate of approximation is found to be rapid.

THE ITERATION PROCESS

CONSIDER the homogeneous linear equation

$$N\psi = \lambda D\psi, \tag{1}$$

where N and D are two Hermitian operators operating on a range of functions ψ of certain variables x. Suppose a function φ_0 in the range can be expanded in the series

$$\varphi_0 = c_1\psi_1 + c_2\psi_2 + \cdots, \tag{2}$$

where ψ_r are proper functions of (1) corresponding to proper values λ_r (some of which may be distributed continuously). Then, if we operate on φ_0 repeatedly with $N^{-1}D$ giving the sequence of functions $\varphi_1, \varphi_2, \cdots$ such that

$$N\varphi_{n+1} = D\varphi_n, \tag{3}$$

we shall have $\varphi_n = \lambda_1^{-n}c_1\psi_1 + \lambda_2^{-n}c_2\psi_2 + \cdots$. (4)

Thus, if Eq. (1) has a discrete proper value of lowest absolute value, λ_s, and if the coefficient of the corresponding proper function ψ_s in φ_0, *viz.* c_s, does not vanish,

$$\varphi_n \sim \lambda_s^{-n}c_s\psi_s \quad (n\to\infty), \tag{5}$$

converging geometrically: and we have a process for approximating to ψ_s.

When a function φ approximating ψ_s has been found, if Eq. (1) has a discrete proper value next lowest in absolute value to λ_s, we can approximate in like manner to its corresponding proper function by replacing φ_n at each stage by

$$\varphi_n - \{(\psi^*\varphi_n)/(\psi^*\psi)\}\psi, \tag{6}$$

where ψ^* is the (Hermitian) conjugate to ψ and $(\psi^*\psi)$ means their summed product.

LIMITS OF ERROR

We can usually find from an approximate proper function ψ, by modifying it if necessary so that the zeros of $N\psi'$ and $D\psi'$ coincide, a function ψ' such that bounds μ and ν exist for which

$$\mu \leq (N\psi'/D\psi') \leq \nu \quad (\text{all } x). \tag{7}$$

There is then a corresponding proper value λ of (1) satisfying

$$\mu \leq \lambda \leq \nu. \tag{8}$$

If in particular D is positive definite, and if Eq. (1) has a discrete lowest proper value, λ_1,

so that the corresponding proper function ψ_1 is nodeless and minimizes $(\psi^* N\psi)/(\psi^* D\psi)$ in the range; then, for any nodeless function φ in the range, a lower bound μ exists such that

$$\mu \leq N\varphi/D\varphi \quad \text{(all } x\text{)}, \tag{9}$$

and then $$\mu \leq \lambda_1 \leq (\varphi^* N\varphi)/(\varphi^* D\varphi). \tag{10}$$

(If an upper bound ν also exists, the Ritz expression $(\varphi^* N\varphi)/(\varphi^* D\varphi)$ is less than ν and is a better approximation to λ_1.)

If in addition λ_1 is the proper value of least absolute value, then for the sequence given by (3) the successive ratios

$$(\varphi_0^* N\varphi_0)/(\varphi_0^* N\varphi_1)/(\varphi_0^* N\varphi_2)/\cdots \tag{11}$$

give successive approximations in excess to λ_1, (note that $(\varphi_0^* N\varphi_r) = (\varphi_s^* N\varphi_{r-s})$, so that alternate ratios are Ritz approximations using φ_0, φ_1, φ_2, $\cdots$); while the successive minimum values for varying x of the ratios

$$N\varphi_0/N\varphi_1/N\varphi_2/\cdots \tag{12}$$

(provided that the denominator is a nodeless function, which, after some point, it usually will be) give successive approximations in defect.

For problems involving absolute minima of quadratic expressions, better limits of error than that given by (10) can be obtained:[1] but the well-known comparison theorem results stated above seem to be the best available for relative minima, especially for proper values other than the lowest.

The Choice of the Operators N and D

Consider the simple case of the radial equation of S states of the hydrogen atom: in atomic units

$$-\tfrac{1}{2}\nabla^2\psi - \psi/r = E\psi, \tag{13}$$

of which the proper values are $E = -\tfrac{1}{2}, \cdots, -1/2n^2, \cdots$; $E>0$. Iteration with $N = -\tfrac{1}{2}\nabla^2 - 1/r$, $D=1$, even if it converged, would not lead to a state in which we are interested. We are not, however, limited to this form; change of scale brings the equation to

$$-\tfrac{1}{2}\nabla^2\psi - a\psi/r = b\psi \quad (a>0) \tag{14}$$

and iteration with D and N any linear combinations of ∇^2, $1/r$, and 1, would converge, if at all, to a solution of this equation (any a).

If
$$\begin{aligned} N &= -\tfrac{1}{2}\alpha\nabla^2 - \beta/r + \gamma, \\ D &= -\tfrac{1}{2}\delta\nabla^2 + \epsilon/r + \zeta, \end{aligned} \tag{15}$$

where, without loss of generality, $\alpha \geq 0$, $\delta \geq 0$: then $\epsilon \geq 0$ and $\zeta \geq 0$ are required to make D positive definite, and $\gamma > 0$ is required if $\lambda = 0$ is not to be in the continuous range of proper values, between γ/ζ and α/δ. If we take $\delta = 0$, $\zeta = 0$, there is no continuous range; and if further $\beta = 0$, the operation N^{-1} can be carried out reasonably easily.

We are thus led to take

$$\begin{aligned} N &= -\tfrac{1}{2}\nabla^2 - E \\ D &= 1/r \end{aligned} \tag{16}$$

or, in more general problems,

$$\begin{aligned} N &= T - E \\ D &= -V \end{aligned} \tag{17}$$

where T and V stand for kinetic and potential energies.

Finding the solutions of

$$T\psi - E\psi = -\lambda V\psi \tag{18}$$

corresponds to asking how large a potential energy of given form will lead to a state of energy E fixed in advance. In problems of the normal states of nuclei it is just this that we really desire to know. In problems of the normal states of atoms, a change of scale will bring the potential energy to its known value. In problems of the normal electronic states of molecules the change of scale also alters the size of the molecule; but that is in any case one of the parameters we wish to determine.

In (17) D is positive definite only if V is one-signed. This will not be true in electronic problems in general; and we shall have solutions corresponding to $-V$ also coming in; but the solution we want will usually be that for λ of lowest absolute magnitude: and once nodeless approximations to ψ are found they can be used to fix limits to E for given V from (10) with $N = T+V$ and $D=1$.

Various methods of obtaining and improving approximate wave functions have been suggested and applied by various authors:[2] the above

[1] Trefftz, Math. Ann. **100**, 503 (1928); Friedricks, Gott-Nach. Math.-Phys. Klasse, p. 13 (1929–30).

[2] E.g., Hylleraas, Zeits. f. Physik **48**, 469 (1928); Hartree, Proc. Camb. Phil. Soc. **26**, 542 (1930); Hasse, Proc. Camb. Phil. Soc. **24**, 89 (1928); Fock and Petraschen, Physik. Zeits. Sowjetunion **6**, 368 (1936).

method seems to be especially simple in theory and convenient in application to problems involving more than one variable x.

Two Examples Illustrating the Method

The exact solution in each of the following problems is known; and it happens that in each the iteration can be carried out analytically. In the first, radial distance; in the second radial momentum,[3] is used as independent variable.

The radial equation for a straight-sided potential hole in case of zero energy

The equation to be solved is

$$-\frac{d^2\psi}{dr^2}=\lambda V\psi, \quad \begin{matrix} V=1, & 0<r<1, & \text{with} & \psi(0)=0 \\ =0, & 1<r, & & \psi(\infty)\ \text{finite.}\end{matrix}$$

Thus

$$\varphi_{n+1}(r)=(1/r)\int_0^r\int_s^1 t\varphi_n(t)dtds, \quad r<1$$

$$=\int_0^1\int_s^1 \varphi_n(t)dtds, \qquad 1<r.$$

Taking $\varphi_0=r, \quad 0<r<1$

$$=1, \quad 1<r,$$

we get $\varphi_1=r/2-r^3/6, \quad \varphi_2=5r/24-r^3/12+r^5/120, \quad =1/3, \quad =2/15,$

$$\varphi_3=61r/720-5r^3/144+r^5/240-r^7/5040, \quad =17/315,$$

$$\cdots 0<r<1$$

$$\cdots \quad 1<r,$$

and the successive approximations in excess to λ (known to be $\pi^2/4=2.46740\cdots$) are 3, 2.5, $2.471\cdots$, $2.4678\cdots$; those in defect 0, 2, 2.4, $2.458\cdots$; (in each case the minimum is for $r=0$; note "$-\int\varphi_0\frac{d^2\varphi_0}{dr^2}dr$" $=\varphi_0(1)\left\{\frac{d\varphi_0}{dr_{1-0}}-\frac{d\varphi_0}{dr_{1+0}}\right\}=1$).

The radial equation for a simple exponential hole treated in momentum space

The equation

$$-d^2\chi/dr^2-c^2e^{-ar}\chi=-b^2\chi$$

is known to have the solution

$$\chi=J_{2b/a}((2c/a)e^{-(a/2)r}),^4$$

and $\chi(0)=0$ gives $J_{2b/a}(2c/a)=0$.

Transforming to momentum space by

$$\chi(r)=(2/\pi)^{\frac{1}{2}}\int_0^\infty \sin pr\,\psi(p)dp,$$

the equation becomes, if $\psi(-p)=-\psi(p)$,

$$(b^2+p^2)\psi(p)=\frac{c^2}{\pi}\int_{-\infty}^{\infty}\frac{a\psi(p')}{a^2+(p-p')^2}dp'.$$

Thus $\varphi_{n+1}(p)=\frac{1}{b^2+p^2}\frac{c^2}{\pi}\int_{-\infty}^{\infty}\frac{a\varphi_n(p')}{a^2+(p-p')^2}dp'$

and to a term $p/(g^2+p^2)$ in φ_n corresponds

$$\frac{c^2}{(a+g)^2-b^2}\left\{\frac{p}{b^2+p^2}-\frac{p}{(a+g)^2+p^2}\right\} \text{ in } \varphi_{n+1}.$$

Thus, taking $\varphi_0=p$, we get

$$\varphi_1=\frac{c^2p}{b^2+p^2}, \quad \varphi_2=\frac{c^4p}{(b^2+p^2)((a+b)^2+p^2)},$$

$$\varphi_3=\frac{c^6p(3a+2b)}{(b^2+p^2)((a+b)^2+p^2)((2a+b)^2+p^2)(a+2b)},$$

$$\varphi_4=\frac{c^8p\{19a^3+35a^2b+21ab^2+4b^3+ap^2\}}{(b^2+p^2)((a+b)^2+p^2)((2a+b)^2+p^2)((3a+b)^2+p^2)(a+2b)^2(a+b)},$$

$$\varphi_5=\frac{c^{10}p\{633a^5+1559a^4b+1525a^3b^2+736a^2b^3+174ab^4+16b^5+(65a^3+64a^2b+16ab^2)p^2+2ap^4\}}{(b^2+p^2)((a+b)^2+p^2)((2a+b)^2+p^2)((3a+b)^2+p^2)((4a+b)^2+p^2)(a+2b)^3(a+b)(3a+2b)},$$

and the successive approximations in excess to c^2 are ∞, ∞, ∞, $(a+2b)(2a+2b)$, $\frac{(a+2b)(3a+2b)}{2}$,

[3] The great simplification that can sometimes be obtained in this way has been pointed out by Fock, Zeits. f. Physik **98**, 145 (1936).

[4] Bethe and Bacher, Rev. Mod. Phys. **8**, 111 (1936).

$\frac{8(a+2b)(a+b)(2a+b)}{11a+10b}$, $\cdots$; and in defect (in each case the minimum is for $p=0$), b^2, $(a+b)^2$, $\frac{(a+2b)(2a+b)^2}{3a+2b}$, $\frac{(a+b)(a+2b)(3a+2b)(3a+b)^2}{19a^3+35a^2b+21ab^2+4b^3}$, $\frac{(a+2b)(3a+2b)(4a+b)^2(19a^3+35a^2b+21ab^2+4b^3)}{633a^5+1559a^4b+1525a^3b^2+736a^2b^3+174ab^4+16b^5}$,

Table I shows the convergence for $b=0$, $b=a$, $a=0$.

It is hoped to publish in the near future approximate solutions by this method of a number of problems for which approximations with known limits of error are not otherwise easy to obtain. The iteration for these problems has to be carried out numerically.

The author wishes to take this opportunity to thank Professor Bohr for the hospitality of his Institute last spring when he spent two months in Copenhagen. During that time the author's ideas about the above method took their present form.

TABLE I. *Convergence for $b=0$, $b=a$, $a=0$.*

$b=0$	$b=a$	$a=0$	REMARKS
$2\,a^2$	$12\,a^2$	$4\,b^2$	Approximations in excess
$1.5\,a^2$	$7.5\,a^2$	$2\,b^2$	
$1.454\,a^2$	$6.857\,a^2$	$1.6\,b^2$	
$1.4458\,a^2$	$6.592\,a^2$	b^2	Actual value[5]
$1.441\,a^2$	$6.380\,a^2$	b^2	Approximations in defect
$1.421\,a^2$	$6.077\,a^2$	b^2	
$1.333\,a^2$	$5.4\,a^2$	b^2	
a^2	$4\,a^2$	b^2	
0	a^2	b^2	

[5] Jahncke and Emde, *Funktiontafeln*, p. 238.

FEBRUARY 1, 1937 PHYSICAL REVIEW VOLUME 51

Nuclear Spins and Magnetic Moments in the Hartree Model

M. E. ROSE AND H. A. BETHE
Cornell University, Ithaca, N. Y.

(Received November 25, 1936)

From the results of Feenberg and Wigner for the wave function and term character of the ground state of light nuclei (mass number between 6 and 16), the nuclear spins are determined. For those nuclei which contain (or lack) a single proton (or neutron) and an even number (singlet state) of particles of the other kind the considerations of Inglis suffice to determine the spin. For those nuclei which contain a half-filled p shell in one kind of particle it is necessary to calculate the fine structure splitting explicitly. From the spins thus found and with the experimental values for the magnetic moments of the proton and neutron, the nuclear magnetic moments are calculated. The effects on the nuclear moment of the Heisenberg forces and of the motion of the $1s$ shell are considered. The moment of Li^7 which is of particular interest, is calculated to be 3.07 nuclear magnetons. This is in agreement with the measured value of 3.20 n. m.

1. INTRODUCTION

IT has been pointed out by Bethe and Bacher[1] that the individual particle model (Hartree model) affords one the opportunity to construct a rational theory of nuclear spins and magnetic moments for light nuclei. On the basis of this model, by assigning quantum states and individual wave functions[2] to each nuclear particle, one can calculate, in the same manner as in atomic spectra, the energy of the various terms which arise from any given configuration of neutrons and protons. From the spin and orbital momenta of the nucleus in the ground state found in this way and from considerations as to the coupling of these momenta the magnetic moment of the nucleus may be calculated. It is to be expected that the model will break down for all but light nuclei[3] and that even for these light nuclei one can obtain only roughly correct

[1] H. A. Bethe and R. F. Bacher, Rev. Mod. Phys. **8**, 82 (1936). In §36 these authors have treated the case of the Li^6 nucleus.

[2] These are determined by a suitable auxiliary central field which may be assumed to be the same for each particle. Following the usual procedure we shall take for this field an oscillator potential.

[3] The model may be expected to give relatively reliable results for nuclei up to O^{16} where the $2p$ shell is just completed.

TABLE I. *Ground states of light nuclei as given by Feenberg and Wigner.*

Nuclei	Ground State Term	Wave Function
He^6 C^{14}	^1S	
Li^6 N^{14}	^3S	
Li^7 *Be^7* N^{13} *C^{13}*	^2P	$C_1(^1D^2P)+C_2(^1S^2P)$
Li^8 *B^{12}*	^3P	$C_1(^3P^2P)+C_2(^3D^2P)$
Be^8 *C^{12}*	^1S	$C_1(^1S^2S)+C_2(^1D^2D)$
Be^9 B^9 B^{11} *C^{11}*	^2P	$C_1(^1S^2P)+C_2(^1D^2P)+C_3(^1D^2D)$
Be^{10}	^1S	$C_1(^1S^2S)+C_2(^1D^2D)$
B^{10}	^3S	$C_1(^3P^2P)+C_2(^3D^2D)$
N^{15} O^{15}	^2P	

quantitative results for the energy. Nevertheless, it is plausible that the order of the levels will be given correctly and it is only this feature of the results that need be used here.

The calculation of the term energies for nuclei of mass number between 6 and 16 has been given by Feenberg and Wigner.[4] On the assumption of Russell-Saunders coupling, which is almost certainly valid because the magnetic forces are very small compared to the nuclear forces, and neglecting Heisenberg forces,[5] in which case both the spins of the neutrons and protons are good quantum numbers, they find for the ground state the results given in Table I.

In the third column of the table the first term in the bracket gives the parent term of the neutrons and the second that of the protons except in the cases of the nuclei in italics for which neutrons and protons are to be interchanged. As is indicated, in most cases the wave function for the ground state is a mixture of wave functions arising from different parentages in the neutrons and protons. The coefficients C_1, C_2 and C_3 with which the various parent wave functions are multiplied depend, of course, on the specific nuclear forces though not very sensitively.[6] In addition, in the absence of Heisenberg forces between unlike particles, they are independent of the exchange properties of the forces between like particles.[7]

TABLE II. *Coefficients for the parent wave functions.*

Row	C_1	C_2	C_3
Li^7	0.681	0.732	
Li^8	0.785	0.619	
Be^9	0.731	−0.344	−0.589

For the unlike particle interaction we have (cf. reference 5)

$$V_{pn}=A_{pn}(1-g/2)e^{-r^2/a^2}P_M, \qquad (1)$$

P_M being the Majorana exchange operator, with $g=0.22$, $A_{pn}=37$ MV and $a=2.93\times10^{-13}$ cm.[8] For the like particle forces we take only

$$V_{pp}=V_{nn}=A_{nn}e^{-r^2/a^2}. \qquad (2)$$

with $A_{nn}=21$ MV. Then the coefficients are as given in Table II.

If the Heisenberg forces are not neglected the resultant spins of both the neutrons and protons will no longer be good quantum numbers. Thus the ^3P term of the p^2 configuration and the ^4S term of the p^3 configuration will interact with the other terms (i.e., ^1S, ^1D and ^2P, ^2D, respectively). Then the wave function for Li^7, e.g., has an additional parent wave function $C_3(^3P^2P)$. We shall consider the effect of this addition to the wave function in §4(a).

2. The Nuclear Spins

We now consider the total angular momentum J of the nucleus in the ground state. For the nuclei whose ground state is an S term we can, of course, obtain J at once from Table I. However for the nuclei whose ground state term is ^2P, i.e., those with odd mass number, and for Li^8 and B^{12} whose ground state term is ^3P, we have to consider the spin-orbit forces which split the levels of the multiplet.

In the case of Li^7 the fine structure splitting is due to the single p proton, the two p neutrons entering in a singlet state. Here we can apply

[4] E. Feenberg and E. Wigner, Phys. Rev. **51**, 95 (1937).

[5] The Heisenberg operator can be written as $P_H=\frac{1}{2}P_M(1+\boldsymbol{\sigma}_1\cdot\boldsymbol{\sigma}_2)$ where P_M is the Majorana operator and $\boldsymbol{\sigma}_1$ and $\boldsymbol{\sigma}_2$ are the spin operators referring to the two particles. The part $\frac{1}{2}P_M$ can be incorporated into the Majorana operator and the part $\frac{1}{2}P_M(\boldsymbol{\sigma}_1\cdot\boldsymbol{\sigma}_2)$ neglected.

[6] See §2 reference 12 below.

[7] See appendix.

[8] This range of the forces has been chosen by Feenberg and Wigner (reference 4), somewhat larger than that deduced from the theory of binding energies of H^2, H^3 and He^4 (namely, $a=2.3\times10^{-13}$ cm) in an attempt to compensate for the correlation forces between the particles which the present model fails to take into account. The particular value chosen for a makes the calculated energy of O^{16} agree with experiment.

the considerations of Inglis[9] who has pointed out that the Thomas part of the spin-orbit interaction will preponderate over the magnetic interaction. This is due to the fact that the Thomas term comes from the specifically nuclear forces while the magnetic interaction is due to the weak electrostatic forces. The nuclear forces being attractive, this leads to an inverted doublet for Li^7 and therefore a spin of 3/2.

In the absence of magnetic forces there is complete symmetry between neutrons and protons. Therefore the spins will be the same for any pair of isobars which may be obtained from each other by the interchange of neutrons and protons. Thus the doublet in Be^7 is inverted ($J=3/2$) with the same fine structure splitting as for the Li^7 doublet. Because of the opposite signs of the magnetic moments of the proton and neutron, the magnetic forces will slightly enhance the splitting in Li^7 as compared to that in Be^7.

The nuclei N^{13} and C^{13} are the images of Li^7 and Be^7 with respect to the half-closed shell of neutrons *and* protons; that is, the p shell for the former nuclei lack the particles which are contained in the latter nuclei. Moreover, just as in atomic spectra, the spin-orbit energy for the completely filled p shell is zero. Therefore the splitting for N^{13} and C^{13} is of opposite sign to that of Li^7 and Be^7. These nuclei should then have a regular doublet and spin $\frac{1}{2}$. Obviously O^{15} and N^{15}, lacking a single p particle, should also have regular doublets and spin $\frac{1}{2}$.

For Li^8, beside the single p proton, it is necessary to consider the contribution to the splitting of the half filled shell of neutrons. The Thomas part of the spin-orbit interaction may be written as

$$U=-\frac{\hbar^2}{2M^2c^2}\sum_i\left(\frac{1}{r}\frac{\partial V}{\partial r}\right)_i(\mathbf{l}_i\cdot\mathbf{s}_i), \tag{3}$$

in which $\mathbf{l}_i$ and $\mathbf{s}_i$ are the orbital and spin momenta (in units of $\hbar$) of the ith particle.

We must calculate the matrix element of this interaction with the ground state wave function for Li^8.

$$\Psi(^3P)=C_1\psi_1(^2P^2P)+C_2\psi_2(^2D^2P). \tag{4}$$

[9] D. R. Inglis, Phys. Rev. **50**, 783 (1936).

The P wave functions compounded from neutron and proton wave functions with the magnetic quantum number[10] $M_L=M_L^n+M_L^p=1$ for any multiplicities are

for $L_p=1$, $L_n=1$:

$$\psi_1=2^{-\frac{1}{2}}\{(P^0P^1)-(P^1P^0)\}, \tag{5.1}$$

for $L_p=2$, $L_n=1$:

$$\psi_2=10^{-\frac{1}{2}}\{6^{\frac{1}{2}}(D^2P^{-1})+3^{\frac{1}{2}}(D^1P^0)-(D^0P^1)\}, \tag{5.2}$$

writing the M_L for each kind of particle, M_L^n and M_L^p, as a superscript. For reference we give the wave functions in the m_lm_s scheme. For the three-neutron wave functions with $M_S^n=\frac{1}{2}$ one obtains[11]

$$\begin{aligned}
&^2P^1=2^{-\frac{1}{2}}[(1^+0^+0^-)-(1^+1^--1^+)],\\
&^2P^0=2^{-\frac{1}{2}}[(1^-0^+-1^+)-(1^+0^+-1^-)],\\
&^2P^{-1}=2^{-\frac{1}{2}}[(0^+0^--1^+)-(1^+-1^+-1^-)],
\end{aligned} \tag{6.1}$$

$$\begin{aligned}
&^2D^2=(1^+1^-0^+),\\
&^2D^1=-2^{-\frac{1}{2}}[(1^+1^--1^+)+(1^+0^+0^-)],\\
&^2D^0=6^{-\frac{1}{2}}[(1^+0^+-1^-)\\
&\qquad+(1^-0^+-1^+)-2(1^+0^--1^+)].
\end{aligned} \tag{6.2}$$

In (6) the numbers in the round bracket give the value of m_l for each neutron and the symbols + and − refer to the sign of the spin component in a given direction z. Each round bracket, of course, is a normalized antisymmetrical (determinantal) wave function and orthogonal to all the others. If we take for the proton wave function (m_l^+), the wave function (4) as given obviously refers to the substate $M=2$, $J=2$. The coefficients C_1 and C_2 may be taken from Table II.[12]

In the calculation of the spin-orbit energy it will be sufficient for our purposes to assume that the particles in the p shell move in a central field. For any central field (one-particle inter-

[10] $M_L^p=\sum_{\text{protons}} m_l$, $M_L^n=\sum_{\text{neutrons}} m_l$.

[11] For notation see Condon and Shortley, *Theory of Complex Spectra* (Cambridge Press), p. 169. The angular part of the single particle wave function for $m_l=1$, 0 and −1 contains $2^{-\frac{1}{2}}(x+iy)$, z and $2^{-\frac{1}{2}}(x-iy)$, respectively.

[12] In calculating these coefficients the wave functions (5) and (6) with the interactions (1) and (2) are used. As an example of the insensitivity of the coefficients with regard to the magnitude of the force constants it may be mentioned that if we take $A_{np}=A_{nn}$ we obtain $C_1=0.791$ and $C_2=0.612$.

action) the matrix elements of (3) are simply proportional to the matrix elements of

$$-\sum_i \mathbf{l}_i\cdot\mathbf{s}_i=-(\mathbf{l}_\pi\cdot\mathbf{s}_\pi+\sum_{\text{neutrons}}\mathbf{l}_\nu\cdot\mathbf{s}_\nu).$$

For the single proton, of course, only the diagonal terms $(\psi_1|\mathbf{l}_\pi\cdot\mathbf{s}_\pi|\psi_1)$ and $(\psi_2|\mathbf{l}_\pi\cdot\mathbf{s}_\pi|\psi_2)$ give a nonvanishing result. We find

$$\begin{aligned}(\Psi|\mathbf{l}_\pi\cdot\mathbf{s}_\pi|\Psi)&=\tfrac{1}{2}C_1^2(1|\mathbf{l}_\pi\cdot\mathbf{s}_\pi|1)\\&+\frac{1}{10}C_2^2\{6(-1|\mathbf{l}_\pi\cdot\mathbf{s}_\pi|-1)+(1|\mathbf{l}_\pi\cdot\mathbf{s}_\pi|1)\}\\&=\tfrac{1}{4}(C_1^2-C_2^2)=0.058.\end{aligned}\tag{7}$$

The numbers in the matrix element refer to the value of M_L.[12]

For the three neutrons we may transform the neutron wave functions to the JM scheme according to[13]

$$\begin{aligned}\psi(L,S,M,M_S=\tfrac{1}{2})&=\left(\frac{L+M+\frac{1}{2}}{2L+1}\right)^{\frac{1}{2}}\varphi(^2L^M{}_{L+\frac{1}{2}})\\&-\left(\frac{L-M+\frac{1}{2}}{2L+1}\right)^{\frac{1}{2}}\varphi(^2L^M{}_{L-\frac{1}{2}}),\end{aligned}\tag{8}$$

in which the subscripts in φ refer to the values of J and the superscript ν on the quantum numbers has been suppressed. For the neutrons we have $M=M_L+\frac{1}{2}$. We find that only the cross term gives a nonvanishing result.

$$\begin{aligned}(\Psi|\sum_\nu\mathbf{l}_\nu\cdot\mathbf{s}_\nu|\Psi)&=2C_1C_2(\psi_1|\sum_\nu\mathbf{l}_\nu\cdot\mathbf{s}_\nu|\psi_2)\\&=-2(20)^{-\frac{1}{2}}C_1C_2\{3^{\frac{1}{2}}(1|\sum_\nu\mathbf{l}_\nu\cdot\mathbf{s}_\nu|1)\\&+(0|\sum_\nu\mathbf{l}_\nu\cdot\mathbf{s}_\nu|0)\}.\end{aligned}\tag{9}$$

From (8) we have

$$(L=1,M_L|\sum_\nu\mathbf{l}_\nu\cdot\mathbf{s}_\nu|L=2,M_L)=-[(4-M_L^2)/15]^{\frac{1}{2}}(^2P_{3/2}|\sum_\nu\mathbf{l}_\nu\cdot\mathbf{s}_\nu|^2D_{3/2})\tag{10}$$

and taking the value for the matrix element from Condon and Shortley[14] this becomes

$$(1,M_L|\sum_\nu\mathbf{l}_\nu\cdot\mathbf{s}_\nu|2,M_L)=-\tfrac{1}{2}[(4-M_L^2)/3]^{\frac{1}{2}}.\tag{11}$$

Thus we obtain

$$(\Psi|\sum_\nu\mathbf{l}_\nu\cdot\mathbf{s}_\nu|\Psi)=\tfrac{1}{2}(5/3)^{\frac{1}{2}}C_1C_2=0.313.\tag{12}$$

Comparing (7) and (12) we see that the contribution to the spin-orbit energy of the three neutrons is of the same sign as the contribution of the single proton.[15] Thus with a positive value for the matrix element of $\sum_i\mathbf{l}_i\cdot\mathbf{s}_i$ it follows from (3) that the spin-orbit displacement of the level $J=2$ is negative. Therefore the multiplet is inverted and the lowest state of Li^8 has total angular momentum $J=2$.

Neglecting magnetic forces, the spin-orbit energy of a half-filled shell of protons is also given by (12). (Moreover, the magnetic forces give a contribution with the same sign as that of the half-filled shell.) Thus in B^{12} the main contribution to the spin-orbit energy will arise from the half-filled shell. The contribution of the five p neutrons, although of opposite sign, is much smaller (cf. (7) and (12)) and will not reverse the order of the levels. Therefore we have again an inverted multiplet with ground state $J=2$.[16]

For Be^9, B^9, B^{11} and C^{11} we have to consider only the spin-orbit energy of a half-filled shell in one kind of particle, the other kind of particle entering in a singlet state. A calculation similar to that given above leads to the result that these nuclei should have inverted doublets, ground state $J=3/2$.

It may be noted that the attribution of the major part of the spin-orbit interaction to the nuclear forces leads to the conclusion that the members of the isobaric pairs Be^7 Li^7, C^{11} B^{11},

[12] The phases are chosen so that the nondiagonal matrix elements of L_x are positive. Cf. Condon and Shortley, reference 11, p. 66 and §14.

[14] Reference 11, p. 268. We set $\xi(r)$ (their notation) $=1$ and therefore $\zeta_p=1$.

[15] We are indebted to Professor Wigner for pointing out an error previously made in this calculation.

[16] Although it is true that the central field model used here is somewhat crude it ought certainly to give the correct sign for each contribution to the spin-orbit energy. Furthermore, in view of the result that the contribution to the energy of the half-filled shell is about five times as large as that of a single particle, it seems safe to conclude that the sign of the spin-orbit splitting obtained here is correct.

N^{13} C^{13} and O^{15} N^{15} are completely analogous in the sense that they have the same ground state J. If only magnetic forces were considered one must conclude that the doublet of one member of the isobaric pair would be regular and that of the other member inverted. Therefore, in the β transformations between the two members of the pair, one would expect a spin change $\Delta J=0$ in the former case and $\Delta J=1$ in the latter. The former value is in agreement with the known fact that the observed β transformations (the last three pairs mentioned) belong to the first Sargent curve.[17]

The Russell-Saunders coupling, which has been assumed in our considerations, leads for many nuclei to a fairly narrow doublet of which the lower level is the ground state. Experimental evidence for this has been obtained by Rumbaugh and Hafstad[18] who observed a doublet fine structure in the proton group from $Li^6+H^2=Li^7+H^1$. The intensity ratio of the two groups was about 1 : 2, that is, the ratio of the statistical weights of the two levels of the doublet in Li^7. It may be suggested that similar fine structure may be observable in the proton groups from the reactions

$$B^{10}+H^2=B^{11}+H^1,$$
$$C^{12}+H^2=C^{13}+H^1,$$
$$N^{14}+H^2=N^{15}+H^1,$$

if thin targets are used. The best studied of these is the carbon reaction for which the range curve for the 14 cm protons has been given by Cockcroft and Lewis.[19] These authors also gave for comparison the range curve for the protons from the D–D reaction at the same deuteron energy (560 kv). The straggling of the D–D protons might be expected to be larger than that of the C–D protons for two reasons. Firstly, for the D–D protons there is a greater variation in energy with angle, the recoil of H^3 being larger than that of C^{13}. Secondly, the excitation function for the D–D reaction is flatter (smaller potential barrier) so that deuterons of a larger range of energies would be effective. Actually the straggling is somewhat less for the D–D protons. This might be taken as a rather weak argument for the existence in the C–D reaction of two proton groups superimposed on each other with an appreciable difference in range, say of the order of one cm.

[17] H. A. Bethe and R. F. Bacher, reference 1, Table XV, p. 195.

[18] L. H. Rumbaugh and L. R. Hafstad, Phys. Rev. **50**, 681 (1936). See also L. A. Delsasso, W. A. Fowler and C. C. Lauritsen, Phys. Rev. **48**, 848 (1935).

[19] J. D. Cockcroft and W. B. Lewis, Proc. Roy. Soc. **A154**, 261 (1936).

3. The Nuclear Magnetic Moments

The magnetic moments of the nuclei in the ground state may now be calculated according to the following procedure. The neutrons and protons enter the wave function for the ground state, as given in Table I, in either a singlet or doublet state. The part of the magnetic moment μ_S which is due to the spin of the neutrons and protons will then be

(1) 0 if both kinds of particles are in a singlet state,
(2) μ_π the proton moment, or μ_ν the neutron moment, if the protons, or neutrons, are in a doublet state,
(3) $\mu_\pi+\mu_\nu$ if both kinds of particles are in a doublet state and the nucleus is in a triplet state.

We shall take $\mu_\pi=2.85$, in units $e\hbar/2Mc$, and $\mu_\nu=-2.00$.

In addition to μ_S there is the contribution to the moment of the orbital motion of the protons. This is given by

$$\mu_L=C_1^2\mu_L^{(1)}+C_2^2\mu_L^{(2)}+\cdots, \qquad (13)$$

where

$$\mu_L^{(i)}=\frac{\mathbf{l}_\pi^{(i)}\cdot\mathbf{L}}{\mathbf{L}^2}L$$
$$=\frac{L(L+1)+l_\pi^{(i)}(l_\pi^{(i)}+1)-l_\nu^{(i)}(l_\nu^{(i)}+1)}{2(L+1)}, \qquad (14)$$

$\mathbf{l}_\nu^{(i)}$ and $\mathbf{l}_\pi^{(i)}$ are the neutron and proton orbital momenta (units of $\hbar$) in the ith parent wave function. The total orbital momentum $\mathbf{L}$ is their sum.

The total magnetic moment μ is obtained by adding the projections of $\boldsymbol{\mu}_S$ and $\boldsymbol{\mu}_L$ on the total angular momentum $\mathbf{J}=\mathbf{L}+\mathbf{S}$.

$$\boldsymbol{\mu}=\frac{g_S(\mathbf{S}\cdot\mathbf{J})+g_L(\mathbf{L}\cdot\mathbf{J})}{\mathbf{J}^2}\mathbf{J} \qquad (15)$$

or $$\mu=\tfrac{1}{2}(g_S+g_L)J$$
$$+(g_S-g_L)\frac{S(S+1)-L(L+1)}{2(J+1)}, \qquad (15.1)$$

where the g factors are defined by

$$g_S S=\mu_S, \quad g_L L=\mu_L. \tag{16}$$

For the nuclei with inverted multiplets the ground state $J=L+S$ and we obtain the obvious result

$$\mu=\mu_L+\mu_S. \tag{17}$$

For the nuclei with regular multiplets the ground state $J=L-S$ and (15.1) reduces to

$$\mu=(J/J+1)[(L+1)g_L-Sg_S]. \tag{18}$$

The nuclear magnetic moments, in units of the nuclear magneton $eh/2Mc$, calculated from the formulae (13), (14), (17) and (18) and the nuclear spins deduced in §2 are given in Table III.[20]

These values for the magnetic moment have not been corrected for the presence of Heisenberg forces. This correction will not pertain to those nuclei which have an S ground state (cf. §4(c)). In §4(a) we shall give the calculation of the effect of the Heisenberg forces on the moment of Li^7. We find there for the corrected value of the moment $\mu(Li^7)=3.07$.

Experimentally the following moments are known: $\mu(Li^6)=0.85$;[21] $\mu(Li^7)=3.20$ from atomic beam measurements[22] with neutral Li^7 and the use of the modified Goudsmit formula[23] and 3.28 from spectroscopic measurements of hyperfine structure for Li^7 II and the use of Breit and Doerman atomic wave functions.[24]

The agreement between the calculated and measured values of the Li^6 and Li^7 moments is quite gratifying since no empirical adjustment of constants has been made in the theory. A more decisive measure of the correctness of the theory can be obtained from the comparison of the ratio of the moments since this quantity is independent of atomic wave functions. The calculated value $\mu(Li^7)/\mu(Li^6)=3.61$ is in satisfactory agreement with the observed ratio 3.87 ± 0.03.[21] However, it must be admitted that the calculated ratio lies outside the limit of experimental error and cannot be changed sufficiently by any reasonable adjustment of the value of the proton (or deuteron) moment.[25] At the same time, the favorable comparison between the calculated and observed values of the magnitude of the moments is an indication that the atomic wave functions used for Li^7 are rather reasonable.

The general agreement obtained justifies the assumption, which is made in our calculation, that the magnetic moments of the proton and neutron are not affected appreciably when the particles are bound in the nucleus.

However, there is some experimental evidence that the magnetic moment of N^{14} is probably $\lesssim 0.2$.[26] It is difficult to reconcile the calculated moment with this value. In §4 we shall discuss the corrections caused by admixtures of other configurations due to Heisenberg forces.

4. Refinements to the Theory

(a) Heisenberg forces

We now wish to consider the effect on the magnetic moment of Heisenberg forces. To the unlike particle interaction (1) the interaction

$$gA_{rr}r^{-r^2/a^2}(P_H-\tfrac{1}{2}P_M) \tag{19}$$

is added (cf. reference 5). The values of a and A_{rr} are the same as in the Majorana interaction and $g=0.22$. In general the Heisenberg forces will yield only a small correction to the magnetic moment as calculated above and it will suffice to consider its effect only for the case of greatest interest, namely Li^7.[27]

The complete wave function for the ground state is

[20] The nuclei not listed in Table III have zero spin.

[21] J. H. Manley and S. Millman, Phys. Rev. **50**, 380 (1936).

[22] M. Fox and I. I. Rabi, Phys. Rev. **48**, 746 (1935).

[23] Using atomic wave functions due to James and Coolidge a value of 3.33 was calculated for $\mu(Li^7)$ by J. H. Bartlett, J. J. Gibbons and R. E. Watson, Phys. Rev. **50**, 315 (1936).

[24] L. P. Granath, Phys. Rev. **42**, 44 (1932). G. Breit and F. W. Doerman, Phys. Rev. **36**, 1262 (1930).

[25] The ratio of the Li^7 to Li^6 moments may be regarded as equal to the ratio of the proton to deuteron moments plus a small correction which is due mainly to the orbital motion of the protons in Li^7. The ratio μ_p/μ_D is known (J. M. B. Kellogg, I. I. Rabi and J. R. Zacharias, Phys. Rev. **50**, 472 (1936)) to be 3.35 with an error estimated to be 3 percent or less. The deuteron moment is given by the same authors, $\mu_D=0.85\pm0.03$. The computed ratio is $\mu(Li^7)/\mu(Li^6)=0.968\mu_p/\mu_D+0.306/\mu_D$. If we take the extreme values $\mu_p/\mu_D=3.45$ and $\mu_D=0.82$ we obtain $\mu(Li^7)/\mu(Li^6)=3.71$ in place of 3.61 given above.

[26] R. F. Bacher, Phys. Rev. **43**, 1001 (1933).

[27] Obviously in considering Li^7 we obtain at the same time the correction to the moments of Be^7, C^{13} and N^{13}.

TABLE III. *Calculated nuclear magnetic moments and spins.*

NUCLEUS	MAG. MOM.	SPIN	NUCLEUS	MAG. MOM.	SPIN
Li^6	0.85	1	B^{11}	3.50	3/2
Li^7	3.15	3/2	B^{12}	1.73	2
Li^8	0.97	2	C^{11}	−1.65	3/2
Be^7	−1.30	3/2	C^{13}	1.13	1/2
Be^9	−1.65	3/2	N^{13}	−0.75	1/2
B^9	3.50	3/2	N^{14}	0.85	1
B^{10}	0.85	1	N^{15}	−0.28	1/2
			O^{15}	0.67	1/2

$$\Psi(^2P)=C_1\psi_1(^1D\,^2P)+C_2\psi_2(^1S\,^2P)+C_3\psi_3(^3P\,^2P). \quad (20)$$

The wave functions ψ_1 and ψ_3 are given in (5.1) and (5.2) and for the same substate, namely $M=1$,

$$\psi_2(^1S\,^2P)=(^1S^0\,^2P^1). \quad (21)$$

The two-neutron wave functions are

$$^1D^2=(1\,1)\chi,$$

$$^1D^1=2^{-\frac{1}{2}}[(0\,1)+(1\,0)]\chi,$$

$$^1D^0=6^{-\frac{1}{2}}[2(0\,0)-(1\,-1)-(-1\,1)]\chi, \quad (22.1)$$

$$^1S_0=3^{-\frac{1}{2}}[(0\,0)+(1\,-1)+(-1\,1)]\chi, \quad (22.2)$$

$$^3P^1=2^{-\frac{1}{2}}[(1\,0)-(0\,1)]\alpha_1\alpha_2,$$

$$^3P^0=2^{-\frac{1}{2}}[(-1\,1)-(1\,-1)]\alpha_1\alpha_2, \quad (22.3)$$

$$\chi=2^{-\frac{1}{2}}(\alpha_1\beta_2-\alpha_2\beta_1), \quad (23)$$

and for the proton

$$^2P^{m_l}=(m_l)\alpha_3. \quad (24)$$

The indices 1 and 2 refer to the neutrons, 3 to the proton. α and β are spin wave functions corresponding to positive and negative spin component in the z direction.

With these wave functions the complete secular determinant of the interaction (1) plus (19) is calculated and the coefficient C_3 determined. We find, with the force constants as given above,

$$C_3=0.109. \quad (25)$$

The magnetic moment is given by

$$\mu=(1-C_3^2)\mu^{(12)}+C_3^2\mu^{(3)}, \quad (26)$$

where $\mu^{(12)}$ is the moment calculated without Heisenberg forces and $\mu^{(3)}$ is the moment associated with the state ψ_3.

$$\mu^{(3)}=\mu_S{}^{(3)}+\mu_L{}^{(3)}, \quad (27)$$

in which the moment due to spin $\mu_S{}^{(3)}$ is given by a formula analogous to (18)

$$\mu_S{}^{(3)}=\frac{g_p(S_p+1)-g_nS_n}{S_p-S_n+1}(S_p-S_n) \quad (28)$$

if $S_p>S_n$ and

$$\mu_S{}^{(3)}=\frac{g_n(S_n+1)-g_pS_p}{S_n-S_p+1}(S_n-S_p) \quad (28.1)$$

if $S_n>S_p$. g_p and g_n are the g factors for the neutron and proton, respectively, and the moment due to the orbital motion of the proton $\mu_L{}^{(3)}$ is given by (13). For Li^7 the correction to the moment is -0.075 and we obtain the corrected moment $\mu=3.07$. The corrected moments for Be^7, C^{13} and N^{13} are -1.33, 1.14 and -0.72, respectively.

(b) Motion of the 1*s* shell

In the foregoing we have omitted all consideration of the 1*s* shell. From naive considerations it might be thought that the orbital motion of the 1*s* shell, as well as that of the *p* particles, around their mutual center of gravity would give a contribution to the magnetic moment of the nucleus. It turns out that this is not the case. To show this we carry out the calculation of the orbital momentum of all the protons in the nucleus around the center of gravity of the whole nucleus. We introduce the coordinates of the center of gravity.

$$\mathbf{R}=\sum_i \mathbf{r}_i/N, \quad (29)$$

N being the total number of particles, and coordinates relative to that point

$$\boldsymbol{\rho}_i=\mathbf{r}_i-\mathbf{R}. \quad (30)$$

The orbital momentum operator is then given by

$$\mathbf{L}=\sum_{\text{protons}}\varrho_i\times\text{grad}_{\varrho_i} \tag{31}$$

and the corresponding magnetic moment by

$$\mu_L=eh/2Mc\sum_{\text{protons}}\varrho_i\times\text{grad}_{\varrho_i}. \tag{32}$$

The wave function $\Psi(\mathbf{r}_i)$ may be transformed into the coordinates (29) and (30) with the result[28]

$$\Psi(\mathbf{r}_i)=e^{-\gamma NR^2}\Psi(\varrho_i), \tag{33}$$

where γ is a constant characteristic of the oscillator potential.

In calculating the orbital momentum $(\Psi|\mathbf{L}|\Psi)$ we need only consider the proton part of the wave function. Further, since $\mathbf{L}$ is a one particle operator, any particular term in the expansion of the determinant in $\mathbf{L}\Psi$ combines only with that term of Ψ^* which is the same permutation of the particles. We may therefore consider only the principal diagonal term since all the terms give the same result. It is then readily seen that in the operator $\mathbf{L}$ only the p proton operators give a nonvanishing result, *the s shell wave functions being spherically symmetrical.* It follows that we get the same result for the orbital momentum as we would obtain if the absolute coordinates $\mathbf{r}_i$ were used; that is, the motion of the 1*s* shell does not affect the magnetic moment.

(c) Higher configurations for *S* state nuclei

In view of the discrepancy between the calculated and experimental magnetic moment of N^{14} it might be thought that the wave function of the ground state might contain an admixture of higher configurations and that these would give a different value for the moment. However, it is easily seen that all higher configurations which may mix with the ground state give the same value for the magnetic moment, namely $\mu_\pi+\mu_\nu$. For example, if we consider Majorana forces alone, the total spin of each kind of particle and the total L being good quantum numbers, the only terms of higher configurations which can interact with the ${}^3S({}^2P^2P)$ are other ${}^3S$ states which arise from two doublets. Such states yield only the deuteron moment, $\mu_\pi+\mu_\nu=0.85$. With Heisenberg forces we may obtain admixtures of ${}^3S$ states arising from combinations of either doublet and quartet states or two quartet states. In the former case we may have either ${}^3S({}^4L^2L)$ or ${}^3S({}^2L^4L)$. The moments for these two states are given by (28) and (28.1). This gives $\mu({}^4L^2L)=\frac{1}{2}(5\mu_\pi-\mu_\nu)$ and $\mu({}^2L^4L)=\frac{1}{2}(5\mu_\nu-\mu_\pi)$. These two states will presumably have about the same energy and therefore will appear with about the same coefficients in the ground state wave function. Thus the total moment μ' is obtained as the mean of these two values which gives again $\mu'=\mu_\pi=\mu_\nu$. In the case of the state ${}^3S({}^4L^4L)$ we have

$$\begin{aligned}\mu'({}^4L^4L)&=\frac{g_\pi(\mathbf{S}_\pi\cdot\mathbf{S})+g_\nu(\mathbf{S}_\nu\cdot\mathbf{S})}{S+1}\\&=\frac{S}{2}(g_\pi+g_\nu)=\mu_\pi+\mu_\nu.\end{aligned} \tag{34}$$

Note added in proof: Dr. Bacher has suggested to us that a rather large correction to the moment may be expected when the two states ${}^3S({}^4L^2L)$ and ${}^3S({}^2L^4L)$ differ in energy even though this energy difference is not large. If E_1 and E_2 are the energies of the two states, E_0 that of the ground state and V the matrix element of the Heisenberg forces between ground state and any of the two states, the correction to the moment is

$$\begin{aligned}\delta\mu&=\frac{3}{2}(\mu_\pi-\mu_\nu)\left(\frac{V}{E_0-E_1}-\frac{V}{E_0-E_2}\right)\\&\approx\frac{3}{2}(\mu_\pi-\mu_\nu)\frac{V(E_1-E_2)}{[\frac{1}{2}(E_1+E_2)-E_0]^2}.\end{aligned} \tag{35}$$

We may estimate $\frac{1}{2}(E_1+E_2)-E_0=5$ MV, $V=1$ MV, while E_1-E_2 may be expected to be of the order of the Coulomb energy for one proton which is about 1 MV for nitrogen. This gives

$$\delta\mu\approx 0.3 \tag{35.1}$$

which is of the same order of magnitude as the difference between the elementary theoretical and the experimental moments. It is satisfactory that this correction increases with increasing Coulomb energy and decreasing spacing between the levels arising from different configurations and is therefore to be expected to be much larger for N^{14} than for Li^6. Presumably the small moment of N^{14} is due to the joint action of this effect and others such as deviations from the Russell-Saunders coupling.

One of us (M. E. Rose) wishes to express his indebtedness to The American Philosophical Society for a grant.

[28] H. A. Bethe and M. E. Rose, Phys. Rev. (in press).

Appendix

Invariance of the coefficients with respect to the exchange properties of like particle forces

The most general model for the interaction between two like particles is a linear combination involving the Majorana operator P_M and a scalar (ordinary force). Heisenberg forces, because of antisymmetry of the wave function are equivalent to (repulsive) ordinary forces and, for the same reason, the Bartlett operator (exchange of spin coordinates) is equal to $-P_M$. The interaction involving the scalar product $\boldsymbol{\sigma}_1 \cdot \boldsymbol{\sigma}_2$ of the two spin operators referring to the two particles, which has also been proposed, is equivalent to $-(1+2P_M)$. We must choose the interaction which gives the correct energy for nuclei with symmetric space wave functions (H^2, H^3, He^3 and He^4).

This is
$$V(r)(bP_M+1-b), \tag{36}$$
in which $V(r)$ is a suitable function of the distance between the particles and b is an arbitrary constant (limited only by stability considerations). The difference between any two interactions for different values of b is obviously a multiple of $V(1-P_M)$. From this result we can show that the difference of the interaction energies of the like particles, using the various force models (36) is the same for all low terms of a p^n configuration.

For 2 or 4 particles the low terms are ^1S and ^1D. For these the space wave function is symmetrical. Therefore the operator $(1-P_M)$ gives a zero result in this case for both terms.

For 3 particles the low terms are ^2P and ^2D. Considering the particular substate $M=M_L+M_S=1$,[29] the wave functions are $\psi(^2P)=2^{-\frac{1}{2}}(\varphi_1-\varphi_2)$ and $\psi(^2D)=2^{-\frac{1}{2}}(\varphi_1+\varphi_2)$; $\varphi_1=(1^+0^+0^-)$ and $\varphi_2=(1^+1^--1^+)$. To prove the theorem for this case we have to show that $(\varphi_2|\,V(1-P_M)\,|\varphi_1)=0$. The only set of individual particle quantum numbers which match in φ_1 and φ_2 is the first, 1^+. Therefore it is clear from orthogonality considerations that only the interaction between particles corresponding to the last two sets of quantum numbers will contribute to the matrix element. If these particles are the ith and kth, the wave function φ_1 will contain z_iz_k as a factor and is therefore invariant with respect to the Majorana operator $P_M{}^{ik}$.

This shows that the difference between the matrix of the interaction energy for the various force models is a multiple of a unit matrix and this does not affect the values of the coefficients C_1C_2 and C_2.

Exceptions to the theorem

The invariance of the coefficients is no longer true if the high terms, ^2P and ^4S, of the p^n configurations are included. The like particle energy of the state ^2P will depend on the force model. The energy difference for the various force models is proportional to $(^2P|\,V(1-P_M)\,|^2P)=2(^2P|\,V|^2P)$, since the space part of the wave function is antisymmetrical, and this matrix element is not zero in contrast to the result for the singlet states. For the ^4S state, in the case of any two force models, the energy difference is twice that for the doublet states.[30]

Further, it is not sufficient for the truth of the theorem that the terms have the same multiplicity. In the configuration d^2 the terms ^3P and ^3F arise. In this case
$$(^3P|\,V(1-P_M)\,|^3P)=2(^3P|\,V|^3P)\neq 2(^3F|\,V|^3F),$$
so that the energy difference with the different force models depends on the L value of the term.

[29] We have omitted the superscript on the magnetic quantum numbers but, of course, they refer to a single kind of particle and should not be confused with the symbols used before to denote the magnetic quantum numbers of the whole nucleus.

[30] E. Feenberg and E. Wigner, reference 4, Table III.

Some Direct Evidence on the Magnetic Moment of the Neutron

J. G. HOFFMAN, M. STANLEY LIVINGSTON AND H. A. BETHE
Department of Physics, Cornell University, Ithaca, New York
(Received December 3, 1936)

An attempt has been made to observe the magnetic moment of the neutron through its selective scattering from magnetized iron. An experimental effect of 3.3 times the mean error has been observed. This effect agrees with that obtained from an evaluation of Bloch's theory.

INTRODUCTION

BLOCH[1] has suggested that the magnetic moment of the neutron might be observed through its interaction with the fields of ferromagnets. There should be a difference in the number of slow neutrons scattered by an iron atom according to whether the spin of the atom is parallel or antiparallel to that of the neutron. This can be observed by "polarizing" the neutron beam by passing it through a magnetized iron bar, and "analyzing" this polarized beam by a second iron bar. Then the number of transmitted neutrons should be larger if the magnetizations of polarizer and analyzer are parallel than if they are antiparallel.

EXPERIMENTAL PROCEDURE AND RESULTS

In the experimental arrangement these iron bars were made of transformer-core laminae of 0.9 cm total thickness for each bar, magnetized to approximately 15,000 gauss by electrical coils. The two iron bars reduced the slow neutron counts (neutrons absorbable in Cd) by a factor 3.18. A beam of slow neutrons from a Be-Rn source of approximately 500 mc strength located in a "howitzer" was collimated by apertures in Cd shields so as to traverse the two iron bars at right angles to the magnetization. (See Fig. 1.) The detecting apparatus consisted of a BF_3 ionization chamber in which the B disintegrations were registered, and a linear amplifier operating a thyratron "scale-of-eight" counter. The average solid angle subtended by the BF_3 chamber as viewed from a point midway between the iron bars was 0.14 radian.

In two runs with slightly differing geometrical arrangements the effects observed agreed within the rather large experimental error. The total counts were:

Fields parallel	218,868	
Fields antiparallel		216,695
Background (Cd penetrating neutrons)	96,580	96,580
Transmitted Intensity, I	122,288	120,115

The difference between the two directions of magnetization is 2173 counts. The mean error is the square root of the overall count of 435,563, or 660 counts. Expressed in percent the effect is therefore:

$$\frac{I(\text{parallel})-I(\text{antiparallel})}{I(\text{average})}=1.8\pm0.54 \text{ percent.}$$

THEORETICAL CALCULATIONS

If the incident neutron beam is perpendicular to the magnetization the cross sections for the two directions of neutron spin per unit solid angle are, according to Bloch:

$$\sigma=\sigma_\omega\pm\gamma_n\gamma_e\sigma_\omega^{\frac{1}{2}}(e^2/mc^2)\cos^2\tfrac{1}{2}\theta F(q). \quad (1)$$

Here γ_n is the magnetic moment of the neutron in nuclear magnetons (-2.0 as deduced from the moments of proton and deuteron); γ_e is

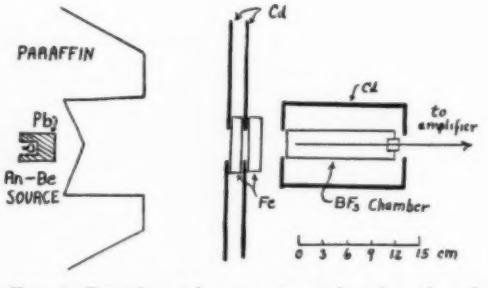

FIG. 1. Experimental arrangement for observing the magnetic moment of the neutron through its selective scattering in magnetized iron.

[1] F. Bloch, Phys. Rev. **50**, 259 (1936).

the average moment per atom in the iron (γ_e is equal to magnetization divided by 9800 gauss, which is 1.53 for our case); σ_ω is equal to[2] the total scattering cross section[3] divided by 4π, i.e.: $12.0\times10^{-24}/4\pi=0.96\times10^{-24}$ cm^2; θ is the angle of scattering of the neutron;

$$q=2\sin\tfrac{1}{2}\theta/\lambda \tag{2}$$

where λ is the de Broglie wave-length of the neutron divided by 2π; and $F(q)=\int e^{i(\mathbf{q}\cdot\mathbf{r})}g(\mathbf{r})d\tau$ is the form factor for the electrons responsible for the magnetic moment of the iron.

According to present ideas,[4] the electrons responsible for ferromagnetism are those in the 3*d* shell. The form factor for these electrons was calculated using the Hartree wave functions for Cu^+. It was found by numerical integration that the form factor could be represented fairly accurately by:

$$F(q)=(1+0.182a^2q^2)^{-1.5}, \tag{3}$$

where a is the Bohr radius. Since 3*d* shell is more contracted in Cu^+ than in Fe this form factor will be slightly too large, especially for large scattering angles. In order to take this effect roughly into account, we may multiply a in (3) by the ratio of the "effective nuclear charges" acting on the 3*d* electrons in Cu and Fe. From Hartree's paper, this ratio may be estimated to be about 917. Then we have for Fe:

$$F(q)=(1+0.30a^2q^2)^{-1}. \tag{3a}$$

Denoting the total scattering cross section for neutron spin parallel to the magnetization by $\sigma_0(1+p)$, we have by integrating (1):

$$p=\frac{\gamma_n\gamma_e}{\sigma_\omega^{\frac{1}{2}}}\frac{e^2}{mc^2}\frac{1}{2}\int\sin\theta d\theta\cos^2\tfrac{1}{2}\theta F(q) \tag{4}$$

$$=\frac{\gamma_n\gamma_e}{\sigma_\omega^{\frac{1}{2}}}\frac{e^2}{mc^2}\frac{1}{K^2}[K+1-(1+2K)^{\frac{1}{2}}],$$

where
$$K=2\times0.30a^2/\lambda^2. \tag{5}$$

For values of the wave-length λ in question the p is approximately proportional to λ. Therefore we insert for λ the average wave-length for neutrons of thermal velocities, which is the wave-length of a neutron of energy $\pi kT/4$. This gives $\lambda=3.2\times10^{-9}$ cm, and $K=1.64$. With the values of the constants given above we obtain:

$$p=0.178. \tag{6}$$

Let us assume that one of our iron bars reduces the intensity of a neutron beam to $e^{-\mu}$ if unmagnetized. Then the transmitted intensity will be $e^{-\mu(1+p)}$ for one direction of polarization and $e^{-\mu(1-p)}$ for the other direction. With parallel magnetization of the two bars the transmitted intensity will therefore be:

$$\tfrac{1}{2}e^{-2\mu(1+p)}+\tfrac{1}{2}e^{-2\mu(1-p)}\backsimeq e^{-2\mu}(1+2p^2\mu^2). \tag{7}$$

In the case of antiparallel magnetization the transmission will be simply: $e^{-2\mu}$. Thus the relative difference in transmission is:

$$\frac{I(\text{parallel})-I(\text{antiparallel})}{I(\text{average})}=2p^2\mu^2. \tag{8}$$

In our experiment the transmission coefficient was $e^{-2\mu}=1/3.18$ corresponding to $\mu=0.58$. With the value of p calculated in (6) this gives from (8):

$$\frac{I(\text{parallel})-I(\text{antiparallel})}{I(\text{average})}=2.3\text{ percent}.$$

This is in satisfactory agreement with the experimental results.

It is a pleasure to acknowledge the assistance of a grant in support of these investigations from the National Research Council through its Committee on Radiation.

[2] The measured cross section is an average of the scattering cross sections for the various iron isotopes. In calculating the ratio of the magnetic scattering (second term in (1)) to the nuclear scattering (first term) we should insert $(\sigma_\omega^{-\frac{1}{2}})_{av}$ rather than $(\sigma_{\omega av})^{-\frac{1}{2}}$ which will tend to increase the magnetic effect.

[3] Dunning, Pegram, Fink and Mitchell, Phys. Rev. **48**, 265 (1935).

[4] Slater, Phys. Rev. **49**, 537 (1936).

LETTERS TO THE EDITOR

Prompt publication of brief reports of important discoveries in physics may be secured by addressing them to this department. Closing dates for this department are, for the first issue of the month, the eighteenth of the preceding month; for the second issue, the third of the month. The Board of Editors does not hold itself responsible for the opinions expressed by the correspondents.

Communications should not in general exceed 600 words in length.

An Explanation for Directions of Easy Magnetization in Ferromagnetic Cubic Crystals

It is well known that in weak fields the stable direction of magnetization in iron is parallel to one or another of the cubic crystallographic axes [100], whereas in nickel it is equally inclined to these three axes, being parallel to [111]. This may be stated in another way: in the anisotropy equation for cubic crystals,

$$E = K_0 + K_1(S_2^2S_3^2 + S_3^2S_1^2 + S_1^2S_2^2) + \cdots,$$

K_1 is positive for iron but negative for nickel. In this equation, S_1, S_2 and S_3 are the direction cosines of the magnetization vector at any point with respect to the cubic axes, E is the magnetic potential energy density associated with this state, and K_0 and K_1 are constants independent of the direction cosines.

As far as we know there is no satisfactory explanation for the difference in sign of K_1 in different materials. A theory which ascribes the sign of K_1 to a particular crystalline lattice fails to explain changes of sign in K_1 in alloy series. A theory which ascribes K_1 to magnetostriction does not account for the difference in sign between iron and nickel.

The purpose of this note is to suggest an explanation for the sign and magnitude of the anisotropy in terms of the distribution of magnetic dipoles in the atoms of iron and of nickel.

If a dipole be placed at each lattice point in a crystal of iron or nickel it will not (in the absence of strain) contribute to K_1, this constant being different from zero only if there is a quadrupole or higher power term in the expression for the mutual potential energy of the dipoles. When the dipoles associated with each lattice point form a small magnet of finite length, calculations indicate that K_1 is negative in both cases; when they form a disk equivalent to a circular current loop, such calculations indicate a positive K_1. Thus one may say that the sign of K_1, and with it the direction of easy magnetization in a cubic crystal, may be determined by the distribution about the atom center of the spinning electrons (3d) that are associated with ferromagnetism; and that in iron, for which K_1 is positive, the distribution is nearer to that corresponding to a circular plate or oblate spheroid than to that corresponding to a bar magnet or prolate spheroid, the latter being approximated to in nickel. Distributions having these general features yield calculated anisotropies of the right signs and magnitudes. A choice between various possible distributions requires further study.

It must be remembered that the magnetic forces here discussed are small in comparison with the forces, due to electrostatic interaction, which maintain a large proportion of the disposable electron spins parallel throughout a domain. It is therefore realized that electrostatic anisotropy, at present ignored, may overweigh the magnetic anisotropy and so actually determine the degree of preference observed for certain directions. No method of calculating the electrostatic anisotropy is known at present, and there seems to be no reason for introducing such terms, since the magnetic forces are adequate to account for both the sign and magnitude of observed effects.

R. M. BOZORTH

Bell Telephone Laboratories,
New York, N. Y.

L. W. MCKEEHAN

Sloane Physics Laboratory,
Yale University,
New Haven, Connecticut,
January 8, 1937.